An Integrated Geophysical Study of the Northern Gulf of Mexico

---

A Thesis

Presented to the

Faculty of the Department of Earth and Atmospheric Sciences

University of Houston

In Partial Fulfillment

of the Requirements for the Degree

Master of Science

By

Eray Kocel

May 2012

An Integrated Geophysical Study of the Northern Gulf of Mexico

_____

Eray Kocel

APPROVED:

_____

Dr. Stuart Hall

_____

Dr. John F. Casey (Member)

_____

Dr. Dale Bird (Member)

Dr. Mark Smith

_____

Dean, College of Natural Sciences and Mathematics

ACKNOWLEDGEMENTS

This thesis would not have been possible without the help of my advisor Professor Stuart Hall. I specially thank him for his feedback and extensive critical comments during the study. I also want to thank the rest of my committee members, Dr. Dale Bird and Dr. John Casey who guided me since the beginning of my graduate studies in the University of Houston. I would like to express my deep gratitude for all their time and effort.

I am deeply thankful to my family. My parents for their unconditional love and help; without them I would not be here writing this thesis. At last but not the least, I really want to thank my dear beloved Sezen for her patience, understanding, support, and courage, keep on working besides the difficulties. I could not have finished any project without you.

An Integrated Geophysical Study of the Northern Gulf of Mexico

---

An Abstract of a Thesis

Presented to the

Faculty of the Department of Earth and Atmospheric Sciences

University of Houston

In Partial Fulfillment

of the Requirements for the Degree

Master of Science

By

Eray Kocel

May 2012

ABSTRACT

The end members of passive continental margins are characterized as non-volcanic or volcanic depending on the nature of the transition zone. Differences between these two types are usually reflected by the differences of the physical properties of the Ocean-Continent Transition (OCT).

Gravity, magnetic, and seismic data used to investigate the crustal structure of a portion of the northern Gulf of Mexico. Six 800-km long, crustal cross sections have been constructed across the study area with 70 km spacing. Two-dimensional crustal models, comprising 7 layers have been developed to simulate the observed Free-air gravity anomalies. The density of each layer has been kept constant and the geometry of the individual layers modified to obtain a good match to the gravity data. Where possible the gravity models have been constrained by available seismic and magnetic data.

Interpretations for the boundaries between different crustal types are delineated by modeling. The magnetic anomalies were used to define the extent of the transitional crust and interpreted as the effects of subaerial flood basalts. For this study OCT was defined as the region where the crustal thickness is greater than 9 km and less than 25 km. The average width of the OCT in the models is 250 km which is greater than that found in previous studies at other volcanic margins. To satisfy concerns that some

magnetic anomalies may be due to sea-floor spreading, an alternative model with a narrower transition was constructed which matched the data equally well.

In order to reconstruct the pre-extension position of Yucatan the stretched continental crust and transitional zone (restored back to 32 km thickness) across the northern margin, 15° of rotation about a pole south of Florida and 9° further rotation for southern Gulf of Mexico is required. Results from previous studies suggest that the Yucatan Block underwent an additional 20° of rotation due to sea-floor spreading along the restoration arc (total amount of 44° counterclockwise rotation).

The results of this thesis supports some previous studies that concluded: (1) the nature of the margin can be classified as being volcanic passive margin and (2) plate reconstructions require counterclockwise rotation for the opening of Gulf of Mexico.

TABLE OF CONTENTS

LIST of FIGURES and TABLES

LIST of ABBREVIATIONS

DNAG	Decade of North American Geology
GEODAS	Geophysical Data System Database
LCB	Lower Crustal Body
NGDC	National Geophysical Data Center
OCB	Ocean-Continent Boundary
OCT	Ocean-Continent Transition
SDRs	Seaward Dipping Reflector
VPM	Volcanic Passive Margin
NVPM	Non-volcanic Passive Margin
V.E.	Vertical Exaggeration

CHAPTER 1. INTRODUCTION

1.1 Motivation and Objectives

Rifting of continents and the generation of new oceanic crust involve a range of processes that include magmatic, tectonic and sedimentary processes *(Coffin et al., 2006).* Depending on the interaction between these processes, different types of margin styles can be produced (strong volcanic margins to non-volcanic margins). ''There are two end member types in the development of the passive margins. One end member responds by thinning of the continental crust'' (NVPM) and ''other end member responds by extrusion of large quantities of lava'' (VPM) *(White et al., 1987).* Volcanic passive margins can be identified by their seismic properties: (1) seaward dipping reflectors (SDRs) can be tracked on seismic data as strong reflections and (2) magmatic under plating layers with high ''P-wave velocities (>7.2 km/s) and high densities (~3100 g/cc)'' *(Stavar, 2007)*. It was observed for the volcanic margins that the transition zone is narrower when compared with those at non-volcanic margins. The physical properties of the ocean-continent transition (width, thickness, seismic velocity and structure, average density) can be used characterize the nature of the margin. Geophysical data best suited to determining these parameters include seismic refraction data and gravity anomaly data.

Although the Gulf of Mexico is one of the most studied ocean basins, researchers still lack detailed information about its crustal structure. The lack of detailed data has

caused a variety of hypotheses to be proposed about both tectonics (Figure 1.1) and geological development of the basin. Researchers have proposed that the formation of the Gulf is due to the movement of the Yucatan Block (clockwise, counterclockwise or drifting). The theories that require the rotation of the Yucatan block are also divided into some sub-groups, based on whether it's a volcanic or non-volcanic margin *(Buffler et al., 1980; Hall et al., 1982; Anderson and Schmidt, 1983; Pindell, 1985; Klitgord and Schouten 1988; Bird et al., 2005; Mickus et al., 2009)*. Another proposed model requires the activities of transform faults and shear zones for the evolution of Gulf of Mexico *(Thomas, 1991).*

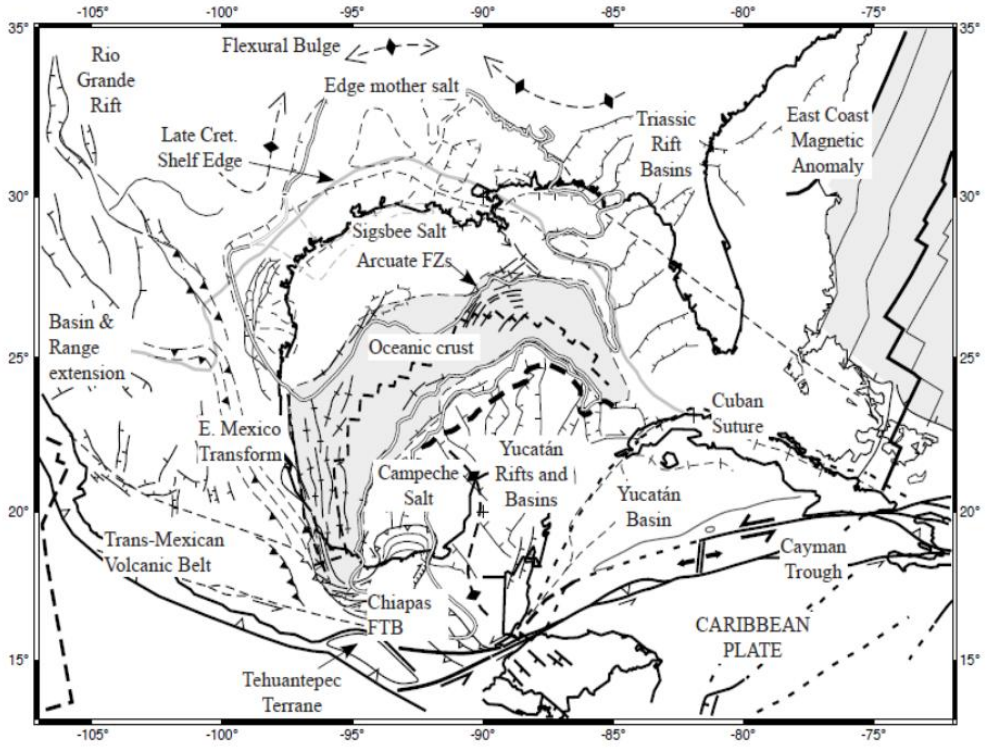

Figure 1.1 Tectonic map of Gulf of Mexico (Pindell and Kennan, 2009)

In order to evaluate the proposed models, the distribution of different crustal types as well as the structure of the crustal zones must be known. The ocean-continent boundary zone usually represents a small area in the regional scale. For the Gulf of Mexico region the boundary zone represents a significant portion of the Gulf area, and consequently any information from the boundary zone can actually provide information for whole Gulf area. Detailed studies over this zone may provide a large amount of both quantitative and qualitative data regarding the formation of the whole Gulf of Mexico. These data can be used for various needs (for example: crustal studies, geological development analysis and many more).

The data and interpretations presented here will contribute to studies of the geological development of Gulf of Mexico. In order to determine the tectonic events that played a critical role for the development of the basin, a detailed crustal structure study was completed. Although many quantitative crustal studies have been completed for the Gulf of Mexico, there are a limited number of integrated studies that have been completed over the northern Gulf of Mexico. Two-dimensional crustal models that were created using gravity, seismic, and magnetic data have helped to identify the boundaries of different crustal types and their properties for the northern Gulf of Mexico.

CHAPTER 2 PASSIVE MARGINS

2.1 General Concepts of Passive Margins

As the continents separate from each other in order to form ocean basins due to rifting, other oceans must close *(Bott, 1995).* The cycle of opening and closing of oceans is known as the Wilson Cycle, which can be divided roughly into 3 parts:

(1) Rifting of continents

(2) Sea-floor spreading and creation of ocean basins

(3) Continental collision and closure of ocean basin

General settings of passive margin are illustrated in Figure 2.1.

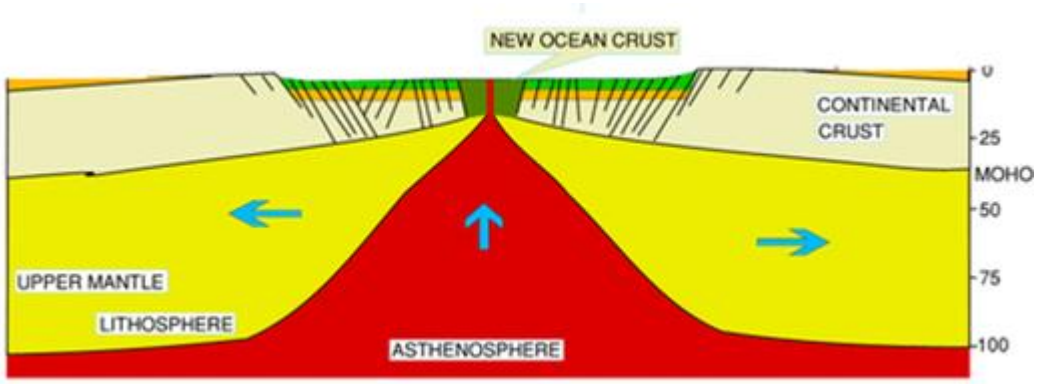

Figure 2.1 Illustration of passive margins (Olsen and Morgan, 1995)

2.2. Oceanic Crust and Continental Crust

The crust is generally classified of two different types. Oceanic crust is approximately 7 km thick *(Tarbuck et al., 2008)* whereas the continental crust averages 35 km. Oceanic crust is mainly composed of mafic igneous rocks (gabbros and basalts) whereas continental crust is composed of mostly metamorphic and felsic igneous rocks *(Tarbuck et al., 2008).*

Continental crust has an average density of 2.75 g/cc *(Tarbuck et al., 2008)* and characterized by its heterogeneous structure. For better understanding, it is commonly divided it into several layers, depending on the variation of the seismic velocities and composition. Layered crustal models suggest that the crust can be subdivided as upper and lower crust. In some areas where high quality and deep seismic data are available (better subsurface control), the crust can also be distinguished by having a middle layer.

Oceanic crust is mainly composed of mafic rock. It is denser than continental crust, (average density of 3.0 g/cc). The thickness of the oceanic crust is approximately 7 kilometers *(Tarbuck et al., 2008),* however the thickness of the oceanic crust may differ depending on the nature of the margin.

2.3. Formation of Passive Margins

Passive continental margins are formed after rifting processes. According to Kingston et al. (1983a), passive margins can be classified in four different ways:

1. Depending on their map-view formation geometry (rifted, sheared, and transtensional),
2. According to their nature of transitional crust (volcanic and non-volcanic),
3. Whether the transitional crust represents a continuous change from normal continental to normal oceanic crust (simple vs complex),
4. Depending on the type of sedimentation (e.g. carbonate-dominated, clastic-dominated)

- First Stage

In this stage continental rift is produced as a result of stretching or thermal expansion of the lithosphere. Crust and lithosphere may experience significant amounts of thinning at this stage *(Scrutton, 1982).*

- Second Stage

During the second stage sea-floor spreading leads to the generation of an oceanic basin. Beneath the rift zone, upwellings of magma occur in the mantle. As marine conditions are established, subsiding of the continental crust creates normal

faults (dipping basinward). Limited amount of sediment runoff towards the margin also starts at this stage. However, the existence of extensive salt is not present in all passive margins. Passive margin can also be dominated by clastic sediments (Shale, ex; South America). Crustal stretching and thinning are still active at this time. Depending on the nature of the margin, intrusions within the transition zone and sedimentary layers may occur.

- Third Stage

As crustal stretching decays and sea-floor spreading becomes established, conditions on the margin will become stable. As the margin becomes mature, high amount of sediment runoff starts to flow towards the margin causing thick sedimentary layers *(Scrutton, 1982).*

Initial results of rifting processes do not lead directly to the creation of oceanic crust *(Minshull, 2009).* An ocean–continent transition (OCT) zone exists between two types of crust (continental and oceanic). However the transition zone itself is also highly heterogeneous which can be sub divided into thick or thin transitional crust. Due to the complexity of the structure of the ocean-continent boundary, its composition and formation are still debated. Integrated geophysical studies (seismic reflection, seismic refraction, magnetism, gravimetry), (*Buffler and Sawyer, 1985; Mickus et al., 2009* and many more) have shown that the properties of the OCT zone are not the same as continental or oceanic crust.

2.4. Geophysical Properties of Passive Margins and Ocean-Continent Transition Zone

One of the common ways of characterizing continental crust is by using its seismic properties, e.g. ''low P wave velocity gradients (<0.05 /s) and low velocities in the lower crust (< 7.0 km/s)'' *(Mishull, 2009)*. Oceanic crust can be characterized easily by comparing the difference with continental crust in terms of its seismic properties, e.g. ''by having a velocity gradient in the upper crust of 0.1 /s and lower gradients (~0.01 /s) and velocities (6.8–7.2 km/s) in the lower crust'' (*Minshull, 2009).* A classical expectation for the boundary between oceanic and continental crust was to have an abrupt change in physical properties where different types of crust are positioned adjacent to each other. However, abrupt change in the physical properties within limited area doesn't seem logical. Geophysical studies have shown the existence of a transition zone (from tens of kilometers up to several hundreds of kilometer) between the two different types of crust *(White et al., 1987; Gladczenko et al., 1997; Bauer et al., 2000 and many more)*

Better characterization of the OCT requires better understanding of some geological terms, including normal oceanic, vs continental crust and thick vs thin transition zone. Previous studies have revealed different types of crusts and their estimated boundaries at the Gulf of Mexico (Figure 2.2) (*Buffler and Sawyer, 1985*).

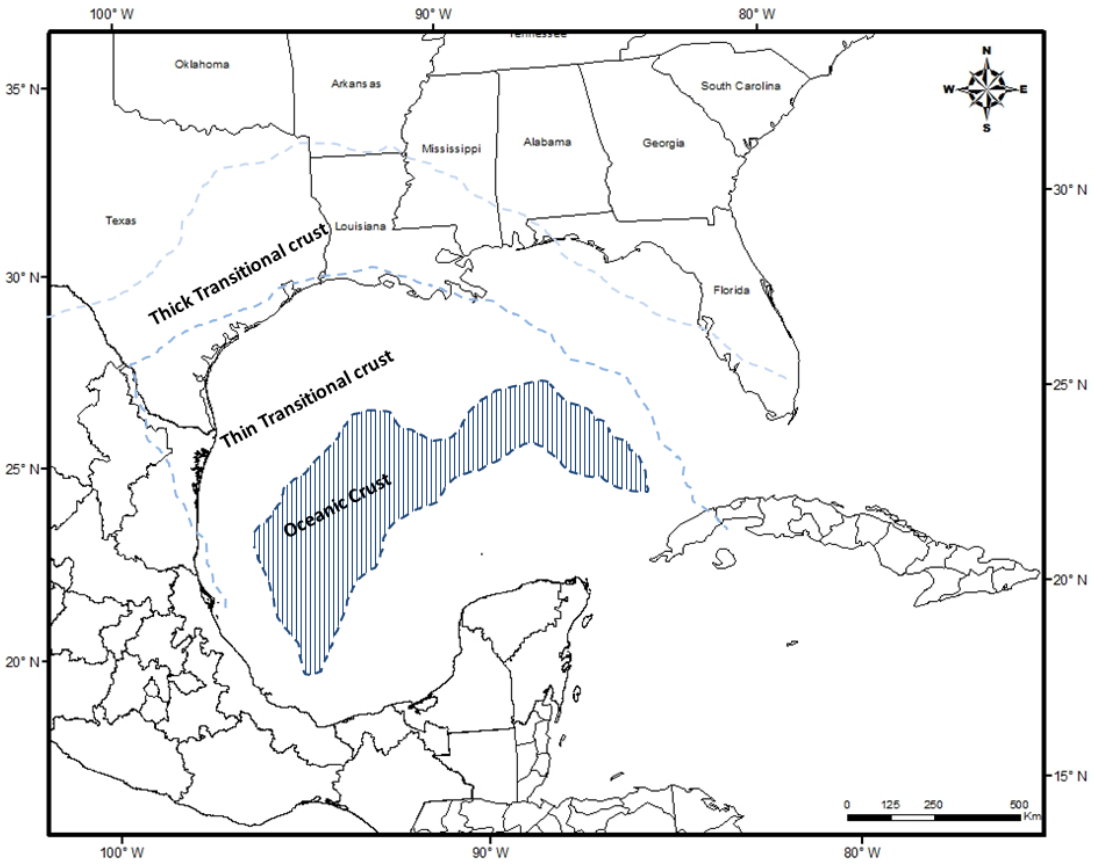

Figure 2.2 Distribution of crustal types (modified from Sawyer et al., 1991)

The boundary between thin transitional zone and normal oceanic crust can be defined by changes in the seismic reflection character and magnetic properties; the transitional zone has huge heterogeneity compared to normal oceanic crust. Although the areas of thick transition zone can easily be differentiated from thin transition zone, the boundary is hard to determine. Thick transition zone is characterized by having thicker crust *(Hales, 1973)* while having an average density closer to continental crust.

2.4.1. Classification of Passive Margins

Creation of a volcanic rifted margin requires a complete rifting process. When the rifting is completed a new ocean is formed above the asthenosphere (Figure 2.3) *(Minshull, 2009)*. In the case of rifting without the thermal perturbation, a non-volcanic margin is generated (Figure 2.3) (e.g. Iberia margin).

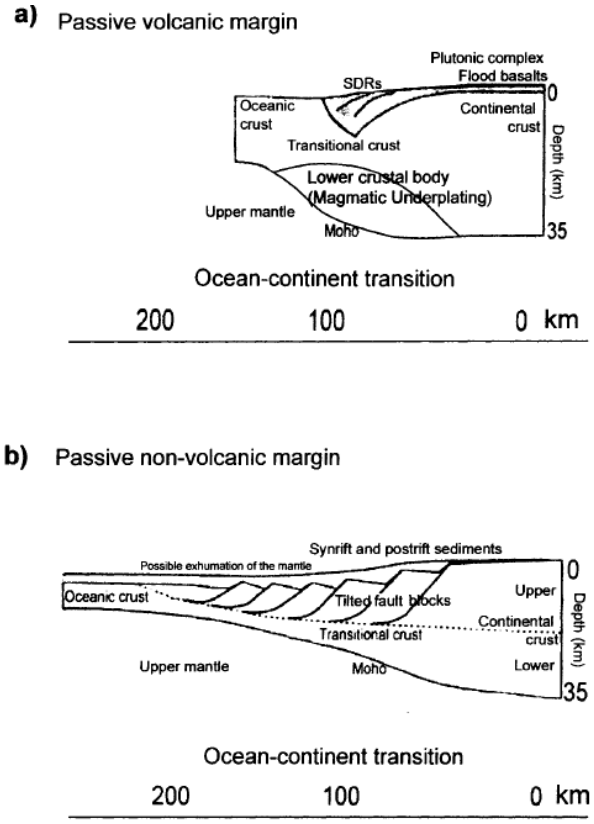

Figure 2.3 Characteristic features of volcanic margins and non-volcanic margins (Stavar, 2007)

2.4.1.1. Volcanic Margin General Concept

A large amount of basaltic volcanism is frequently associated with ''continental break up and the formation of volcanic rifted margins'' *(White and McKenzie, 1989)*. The classification of volcanic rifted margins generally refers to one with stretched lithospheric crust due to the active volcanism that took place during the formation. Volcanic passive margins are usually identified by the seaward dipping reflectors. These reflectors have high seismic P-wave velocities (>6.0 km/s) due to their densities (~2.5 g/cc -2.65 g/cc) *(Bauer et al., 2000; Mjelde et al., 2005)*

One of the main methods used in geophysical studies to characterize volcanic margins is gravity. The gravity response at the rifted volcanic margins is the result of processes that control rifted margins development, including extension (stretching of the crust), sedimentation, magmatic underplating, and flexure *(Watts and Fairhead, 1999).*

Gravity data are directly related to the subsurface mass/density distribution. Mechanical extension causes both crust and the lithosphere to be thinned. ''At the Moho there is a large density contrast between crust and mantle (~0.35 g/cc)'' *(Watts and Fairhead, 1999*).The gravity response of this sudden change is referred to as the free-air gravity edge effect.

The free-air gravity edge effect anomaly includes a gravity high (+25 to +50 mGals) which correlates with the outer shelf and a gravity low (- 25 to -50 mGals) associated with slope and rise regions *(Watts and Fairhead, 1999).*

According to Watts and Stewart (1998), the free-air gravity anomaly at volcanic margins is the result of contributions from:

- Increasing water depth seaward, representing a mass deficit (less dense water substitutes the denser oceanic crust) and a shallow effect (Figure 2.4b)

- Decreasing Moho depth and shallowing of mantle representing a mass excess (denser mantle material replacing less dense oceanic crust) and a deeper effect (gentle gradient). The sum of the water and mantle contributions described above were termed the rifting anomaly (*Watts, 2001b)* (Figure 2.4b)

- Sedimentation: The gravity variation directly due to the sedimentation represents the sum of the contribution from the sedimentary load (positive contribution) that substitutes for water and contributions from ''flexure of the basement and the underlying Moho (negative contributions)'' (*Watts and Stewart*, 1998). Highly sedimented rifted margins are associated with a gravity anomaly high located seaward of the hinge zone, at the shelf break *(Stewart et al., 2000)*

- Magmatic underplating: The gravity anomaly associated with magmatic under plating has two effects ,`` a low due to the low density underplated material and high due to the displacement of water by the uplift crust`` (*Watts and Fairhead, 1999).*

    - Margins where seismic data indicate large amounts of magmatic addition to the lower crust (North Atlantic, etc.) are associated with a free-air gravity edge effect anomaly that generally lacks a distinct offshore low.

In the case of lithospheric response to sediment loading by flexure, there are some simple models available for the rifted margins *(Watts and Marr, 1995; Watts, 2001a):*

- A short wavelength (~100 km), low amplitude (~50mgal) double gravity high associated with low rigidity , weak margin (Figure 2.4a)
- A long wavelength (~250km) high amplitude single gravity high (~100mgal) associated with high rigidity , strong margin (Figure 2.4a)

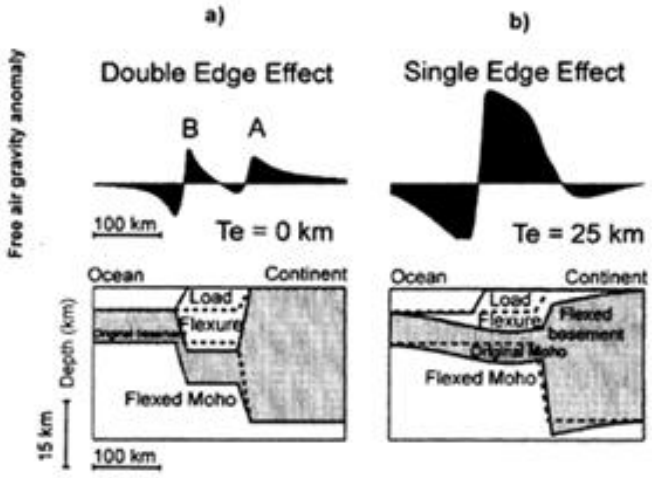

Figure 2.4a Free-air gravity edge effect at rifted margins (Watts, 2001b)

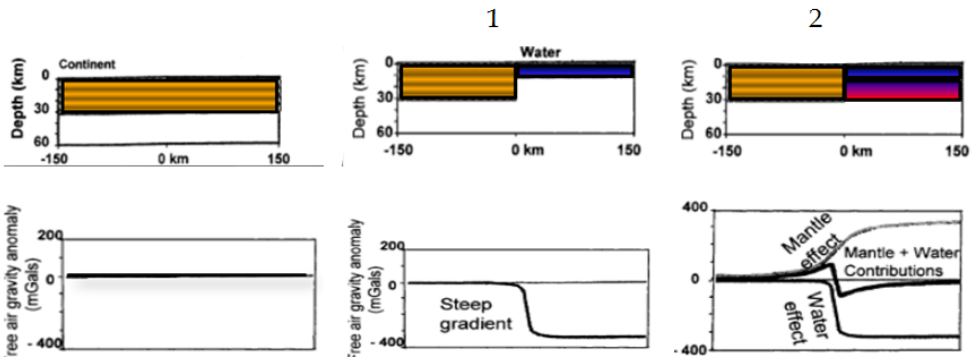

Figure 2.4b The water and mantle contributions at passive margins: 1) The water effect produces a negative density contrast and abrupt change in gravity; 2) The extra mantle beneath the oceanic crust generates a positive density contrast and a less abrupt change in gravity (Watts, 2001b)

Depending on the ability of lithosphere to support the loads for long periods of time, researchers characterize the margin as either weak or strong (Figure 2.5*, Watts and Marr, 1995*). If the sediment loads are mainly supported by the buoyancy of the underlying fluid substratum then these margins are called weak. If the sediment loads are supported by the strength of the lithosphere then these margins are referred to as strong.

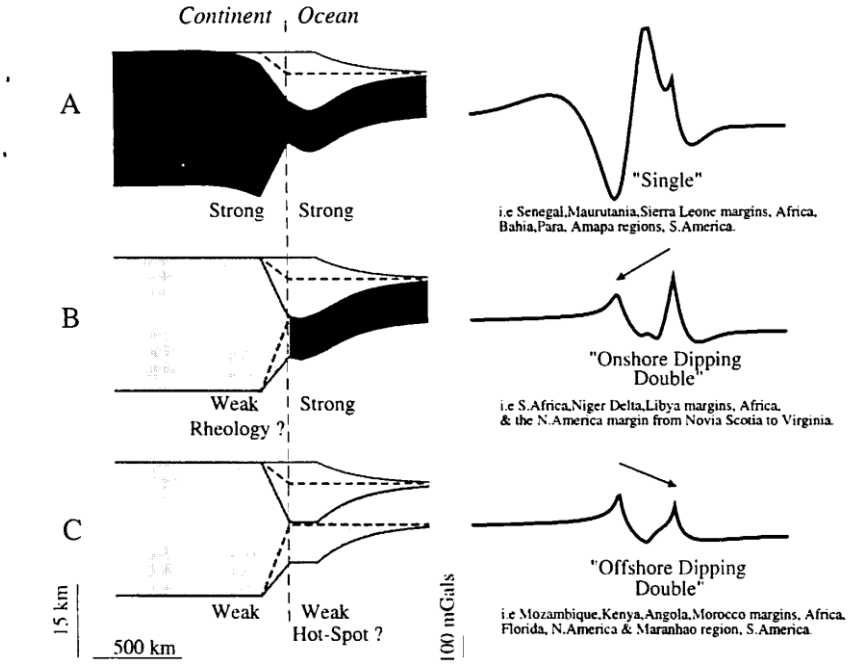

Figure 2.5 Types of rifted continental margins depending on the free-air gravity edge effect. (a) Single edge effect due to sediment loading of strong continental crust that abuts strong oceanic crust, (b) Onshore dipping double edge effect, (c) Offshore dipping double edge effect (corresponds to weak continental crust which abuts weak oceanic crust) (Watts and Marr, 1995)

2.4.1.1.1. Magnetic Properties

The total magnetic intensity response of any margin is associated with a material of high magnetization values; other properties (volume of material and depth of the material) of this magnetic material also control the magnetic response.

As volcanic passive margins have high amounts of magmatism during their formation, the magnetic response of these margins might be larger in terms of amplitude due to additional amount of igneous materials.

2.4.1.1.2. Seismic Properties

Volcanic passive margins are usually identified by seaward dipping reflectors (SDRs) (Figure 2.6) which are observed over the transition between continental and oceanic crust *(Eldholm et al., 1995).*

Hinz (1981) discovered that typical properties of SDRs on seismic profiles (Figure 2.7) were caused by thick extrusive basaltic flows. SDRs represent ''flood basalts that was rapidly extrude during earlier rifting, or during initial sea-floor spreading, formed by brief and voluminous extrusion'' *(Hinz, 1981).* It is generally accepted that the seaward dipping reflector sequences consists of a mixture of volcanic rocks, volcaniclastic and non-volcanic sedimentary rocks *(Menzies et al., 2002).*

According to the Jackson et al., (2000) the seismic character of SDRs is controlled by:

- volume and rate of magma production
- volcanic constructional environment
- relation to sea level
- syn- and post-volcanic deformation and subsidence

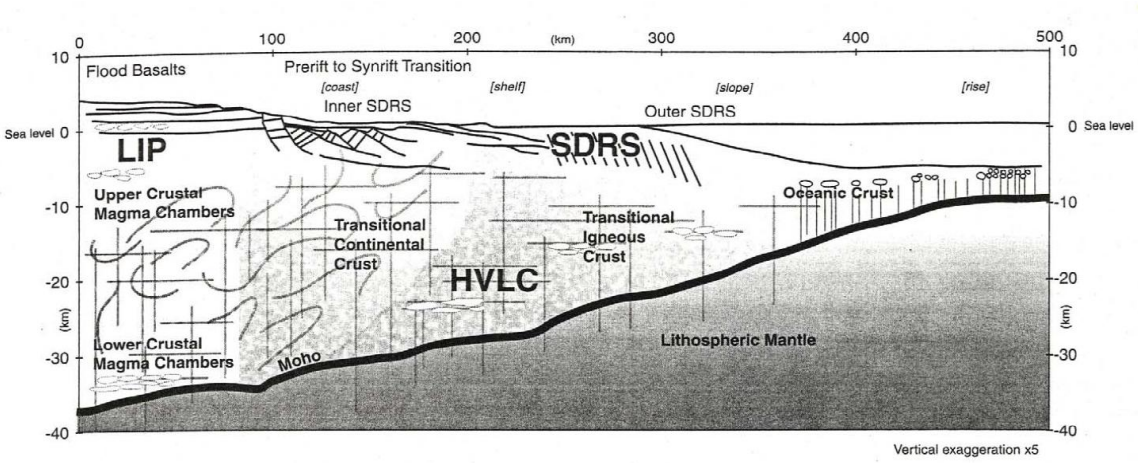

Figure 2.6 Illustration of SDRs within a wide angle profile (Menzies et al., 2002), HVLC: high velocity lower crustal body, SDR: Seaward dipping reflector, LIP: large igneous province

Seismic velocity measurements from wide angle profiles have confirmed that the dipping reflector units exhibit seismic velocities of volcanic rock that are too high for sedimentary deposits *(White and McKenzie, 1989).*

As it can be observed from the Figure 2.6, the dipping reflectors can easily represent 5 km of thickness within the transition zone; their velocities can vary from 3.5 to 6 km/s *(Hinz et al., 1999).*

Physical properties of SDRs usually differ depending of the characteristic of the specific magmatic margin. Here are the some published densities for seaward dipping reflectors:

- 2.55 – 2.67 g/cc, Norwegian margin *(Mjelde et al., 2005)*
- 2.6 g/cc, Norwegian margin (*Tsikilas et al., 2005)*
- 2.85 g/cc, East Coast of U.S. *(Holbrook et al., 1994)*

There are still debates about where and how SDR wedges occur. Some of the proposed models for SDR emplacement *(Talwani and Abreu, 2000; Franke et al., 2006)* include*;*

1. Models in which the SDRs are formed as thick subaerial oceanic crust i.e. ``the SDRs would be emplaced during continental break up, implying that a hotspot is not necessary for SDRs formation``. The SDRs would be emplaced as an initial oceanic crust subsiding due to addition of volcanic loading and forming symmetrical wedges in the conjugate margins *(Talwani and Abreu, 2000).*

2. Models in which the SDRs are erupted along transition zone (Referred as the rift model) suggest that the formation of SDR provinces may take place during the rift phase under the influence of a hotspot. In these models SDRs would be emplaced over an extended continental crust.
3. Models are also subdivided depending on where the SDRs are located within a given margin (Inner SDRs and Outer SDRs). Franke et al., (2006) report that beneath the shelf one or multiple Inner SDR wedges might be present. In the case of Argentina passive margin studies they note that the width of the Inner SDRs are around 100km. Outer SDRs were also observed far seaward.

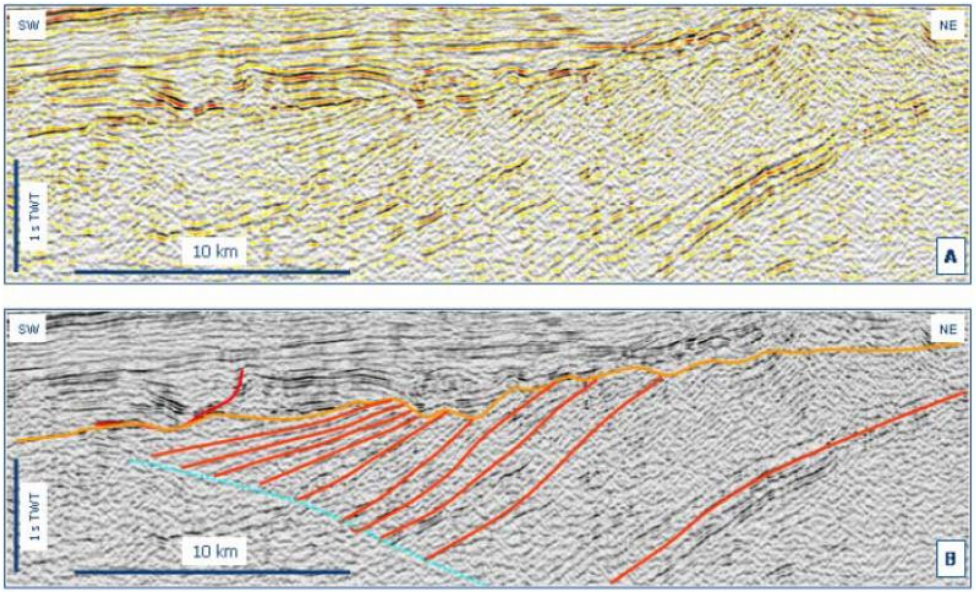

Figure 2.7 SDR reflections on seismic data in the eastern Gulf of Mexico (Imbert, 2005)

SDRs have often been used as indicators for the ocean – continent boundary extension. Different models make specific prediction for the location of the ocean – continent transition zone, depending on the extension of the SDRs *(Roberts et al., 1984).*

2.4.1.2. Non-volcanic Passive Margins (General Concepts)

Rifting without the additional thermal perturbation forms non-volcanic rifted margins. This type of margin is usually characterized by rotated fault blocks, a wide zone of deformation, with small (or none) amount of igneous intrusions *(White et al., 1987).*

NVPM differs from VPM due to lack of significant amount of volcanism during rifting. The amount of additional igneous materials on NVPM is limited *(White et al., 1987).* As a consequence the transition zone is composed of stretched (thinned) continental crust.

Non-volcanic passive margins are also identified by listric faults and continent ward dipping reflectors. As the NVPM lacks additional igneous materials, magmatic underplating and SDRs are not usually observed over these margins *(Manatschal and Bernoulli, 1999).*

2.4.2. Other Differences Between Volcanic and Non-volcanic Passive Margins

- The Width of the Transition Zone from Continental Crust to Oceanic Crust

Understanding the physical properties of the boundary zone is the key to defining the different types of passive margins. The classification of the passive margins also depends on the width of the transition zone. Studies have revealed that the transition from normal continental crust to normal oceanic crust is relatively narrow in VPM *(White and McKenzie, 1989).*

The difference in the width of the OCT is mainly due to high amount of igneous rocks for the volcanic margins. As the rifting starts these injected igneous rocks will cause the lithosphere to become weaker and weaker.

- The Thickness of the Transition Zone

The thickness of the crust in the transition zone also defines the different types of passive margins. Volcanic passive margins are usually characterized by having thicker crustal layers. Normal thickness for oceanic crust is expected to be 6.5 ±2 km *(White et al., 1992).* In the case of VPM the thickness varies a lot depending on the properties of that specific margin (this variation is mainly due to the amount of intrusive and extrusive igneous material). Generally the thickness is greater than 10 km.

- Magmatic Underplating

Magmatic underplating usually refers to the igneous material that can be found at or near the base of crust (Figure 2.8) *(Holbrook and Kelemen, 1993; Cox, 1980).* Seismic studies on volcanic passive margin have helped to better define the properties of the high velocity lower part of the crust.

Different ideas for the definition of magmatic underplating exist. According to White et al. (1987), magmatic underplating can be considered as the accumulation of additional igneous material which is derived below the continental crust. Talwani et al., (1995) argues that even the term (underplating) itself cannot be considered as appropriate due to requirement for extreme conditions for older crust to be underplated. They defined SDRs to represent the upper part of oceanic crust and underplating to represent the ''lower part of an initial oceanic crust'' *(Stavar, 2007).*

The discovery of an underplated zone is mainly due to the contrast in the physical properties of this area. P-wave velocity structure supports the view that this zone consists of magmatic material which has been underplated (7.1 to 7.6 km/sec). This same response is also supported from density of the specific-layer (2.9 g/cc to 3.1 g/cc) *(Watts, 2001a, 2001b; Gladczenko et al., 1998)*

- Thickness of the Oceanic Crust

Based on the thickness of the transitional crust, the two contrasting types of rifted margins (volcanic and non-volcanic) can be distinguished as the thick-crusted volcanic margins and thin-crusted non-volcanic margins. One characteristic of a volcanic rifted margin is the presence of thick igneous crust (>9 km) *(Menzies et al., 2002).* Studies at volcanic margins reveal that normal oceanic crust adjacent to the transition zone is thicker than that at non-volcanic margins *(Eldholm et al., 1995).*

2.5. Rifting Mechanisms

Early studies of lithosphere extension can be classified in two main rifting types *(Sengor and Burke, 1978)*.

- Active Rifting: Mantle convection and extension occurred as a result of uplift. This type of rifting is directly due to the stretching of the continental lithosphere as a result of a thermal process in the asthenosphere.

- Passive Rifting: Extension is considered to be the primary mechanism which usually takes place in wide zones. In this type of rifting the mechanical forces are winning.

Various models of rifting have been proposed. These models range from pure shear to simple shear model.

2.5.1. Pure Shear Rifting

The uniform stretching pure shear model *(McKenzie, 1978)* assumes that ''extension occurs by symmetric thinning of the crust and lithosphere'' *(Mjelde et al., 2007)* the crust and sub-crustal lithosphere are attenuated by an equal amount of stretching and the deformation is confined to the actual rift zone''. A major upwelling of the asthenosphere takes place beneath the center of the rift zone.

This model basically assumes that the extension amount is uniform with depth but varies depending on the position across the margin (Figure 2.9). Another assumption of this model suggests that any magmatic activity has minimal effect and accepts the uniform asthenospheric temperature at the base of the lithosphere

- Total subsidence: initial fault controlled subsidence due to crustal thinning, a thermal subsidence as the lithosphere cools and a gravity loading (subsidence to sediment load due to the density difference between water and replacing sediment) *(Allen and Allen, 2005)*.

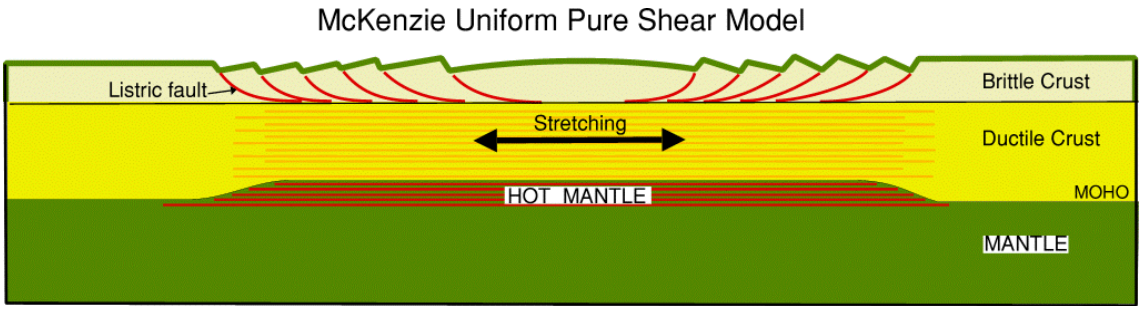

Figure 2.8 Illustration of pure shear model (Lister et al., 1986)

2.5.2. Simple Shear Rifting

In this model *(Wernicke, 1985)* the lithosphere extends asymmetrically and extension taking place by displacement on ‘’large scale due to a gently dipping shear zone that traverses the entire lithosphere’’ *(Wernicke, 1985).* Simple shear predicts an upper plate margin above a deeper detachment, with a rift-stage history of uplift and a lower plate margin comprising the footwall of the detachment. Melt generation and volcanism is probably minimal *(Latin and White, 1990).*

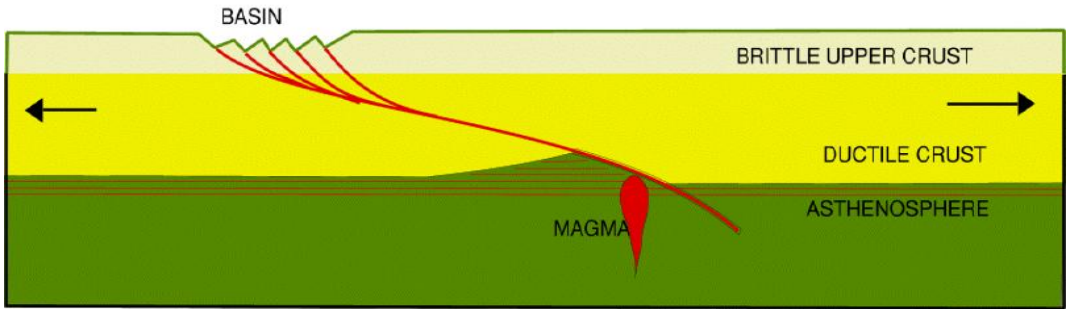

Figure 2.9 Illustration of simple shear rifting (Lister et al., 1986)

Symmetric extensional models failed to explain some features of continental margins such as: ‘’the asymmetry in the rift structures of some conjugate margins’’ *(Mjelde et al., 2007)*. Simple shear model were found to provide a better explanation for these features (Figure2.10). Various models for extension provided an explanation for structural and morphological features at passive margins.

Observations of significant asymmetries in conjugate margins suggest that many rifts may develop by a simple shear mechanism. The Brazil and West Africa margins are good examples of this view *(Mohriak et al., 2002).*

2.5.3. Composite Model

This model combine Wernicke-type simple shear in the upper crust with the McKenzie-type pure shear in the lower crust and mantle lithosphere (Figure 2.11) *(Barbier et al., 1986).* The simple shear model may be used to explain the early rifting stages, whereas the pure shear model is often used during the following stages of crustal extension.

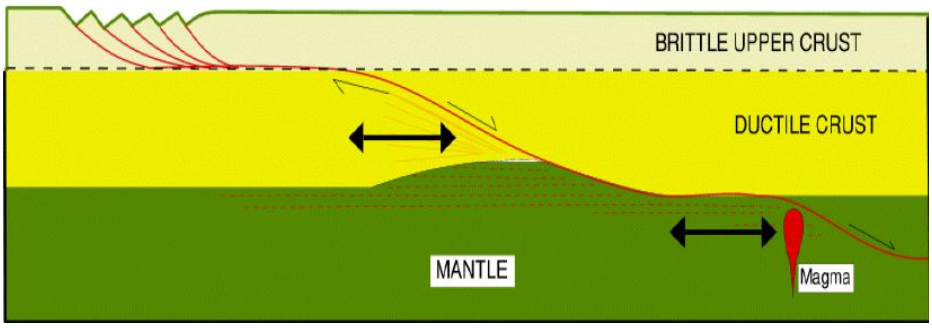

Figure 2.10 Illustration of composite model (Lister et al., 1986)

CHAPTER 3 GEOLOGICAL HISTORY of GULF OF MEXICO

3.1. Introduction

The Gulf of Mexico is a small ocean basin which has been characterized as having large amount of sedimentary deposits (thickness up to 18-20 km) *(Galloway, 2011).* The basin has supplied huge amount of hydrocarbons for more than 50 years.

Previous studies of the tectonic evolution of the Gulf of Mexico indicate several phases in its developments: (1) Late-Triassic-Early Jurassic phase associated with early rifting, (2) a mid- Jurassic phase of rifting which produced an area of transitional crust, (3) a late Jurassic period with oceanic crust formation in the center, and (4) a crustal subsidence modified by sediment depositions *(Sawyer et al., 1991).*

3.2. Late Triassic – Early Jurassic

This stage is mainly considered as a generation of rifting zones in brittle continental crust. ''Fault basins are usually characterized by half grabens bounded by listric normal faults'' *(Mancini et al., 2009).* They are filled with non-marine sediments and volcanics. During this stage similar rift basins are also thought to be occurring along

the east coast of North America, across northern Florida and southern Georgia, all along the Northern Gulf of Mexico and into the central Mexico. These rifts basins represent the initial rift stage (relative movement between Africa, North America) in the break-up of Pangea. The thickness of continental crust at the Gulf of Mexico region is assumed to have not thinned significantly *(Sawyer et al., 1991).*

3.3. Middle Jurassic

The main rifting and crustal attenuation took place during this stage. As a result of all these processes transitional crust was formed in the Gulf of Mexico region. However, not all parts of the region were affected. As a result of Yucatan Block rotation the continental crust in the outer periphery of the basin underwent moderate thinning and remained relatively thick, which ended up with thick transitional crust. The center of the basin underwent more crustal and lithospheric thinning and subsidence to form the large area of thin transitional crust *(Sawyer et al., 1991).* The thin transitional crust may be wide but it was formed from a piece of pre-rift continental crust that was narrow .Thick salt was deposited over the central area of thin crust as well as adjacent thicker crust due to the spilling of marine waters periodically *(Sawyer et al., 1991).*

3.4. Late Jurassic

This time is mainly characterized by the creation of oceanic crust *(Sawyer et al., 1991).* As the rotation of Yucatan block progressed the area of oceanic crust became much wider in the western part of the Gulf. As the sea-floor spreading continued the marine transgression into the basin was started. The transgression was accompanied by cooling and subsiding of the basin. Newly formed oceanic crust was covered with several kilometers of water. Gravity and sediment loading caused early basinward flow of salt tongues along the boundary of oceanic and thin transitional crust *(Sawyer et al., 1991).*

3.5. Rotation of the Yucatan Block

Many researchers agree that the rotation of the Yucatan Peninsula block involved a single ocean - continent transform boundary *(Bird et al., 2005)*. Although the details about the rotation itself may differ (e.g., total amount, role of sea-floor spreading vs crustal stretching), the rotation is interpreted to be counter clockwise *(Pindell, 1985; Salvador, 1987, 1991; Burke, 1988; Ross and Scotese, 1988; Christenson, 1990; Buffler and Thomas, 1994; Hall and Najmuddin, 1994; Marton and Buffler, 1994; Bird et al., 2005).*

Rifting Begins	Salt Deposition	Yucatan Rotation Begins	Sea-Floor Spreading Begins	Sea-Floor Spreading Ends	Source
Late Triassic to Early Jurassic	completed by Oxfordian, 160 Ma	late Middle Jurassic (Callovian)	Callovian, 166 Ma	Berriasian, 140 Ma	Marton and Buffler, 1994
Late Triassic, 200 Ma	Callovian (or earlier) to middle Oxfordian, by 160 Ma		early Oxfordian, 160 Ma	Berriasian, 137.85 Ma (M16)	Pindell, 1994
Late Triassic, 210 Ma	late Callovian, by 160 Ma		late Callovian, 160 Ma	Berriasian, 140 Ma	Pindell, 1985
Late Triassic to Early Jurassic	late Middle Jurassic to early Late Jurassic		latest Callovian or early Oxfordian	early Late Jurassic but not later than middle Oxfordian	Salvador, 1991
Late Triassic to end of Middle Jurassic	late Middle Jurassic		Late Jurassic	early part of Late Jurassic	Salvador, 1987
Late Triassic	Callovian, ~168–163 Ma		early Oxfordian, 160 Ma	Berriasian, 140 Ma	Winker and Buffler, 1988
Middle to Late Triassic, 230 Ma	late Callovian–early Oxfordian to Kimmeridgian, 160–150 Ma	late Callovian to early Oxfordian, 160 Ma	Kimmeridgian, 150 Ma	Berriasian, 140 Ma	this paper

Figure 3.1 Proposed formation events (Bird et al., 2005)

Investigation of the Gulf of Mexico formation is not only limited to its initial shape and/or properties but also to the driving mechanism which created the current Gulf of Mexico (Figure 3.1). Researchers have tried to explain the formation from many different perspectives, including rifting, sea-floor spreading, and the role of a possible mantle plume. One recent proposed idea suggests that a Late Jurassic mantle plume may have shaped the formation; Figure 3.2 shows the mantle plume associated anomalies *(Bird et al., 2005).*

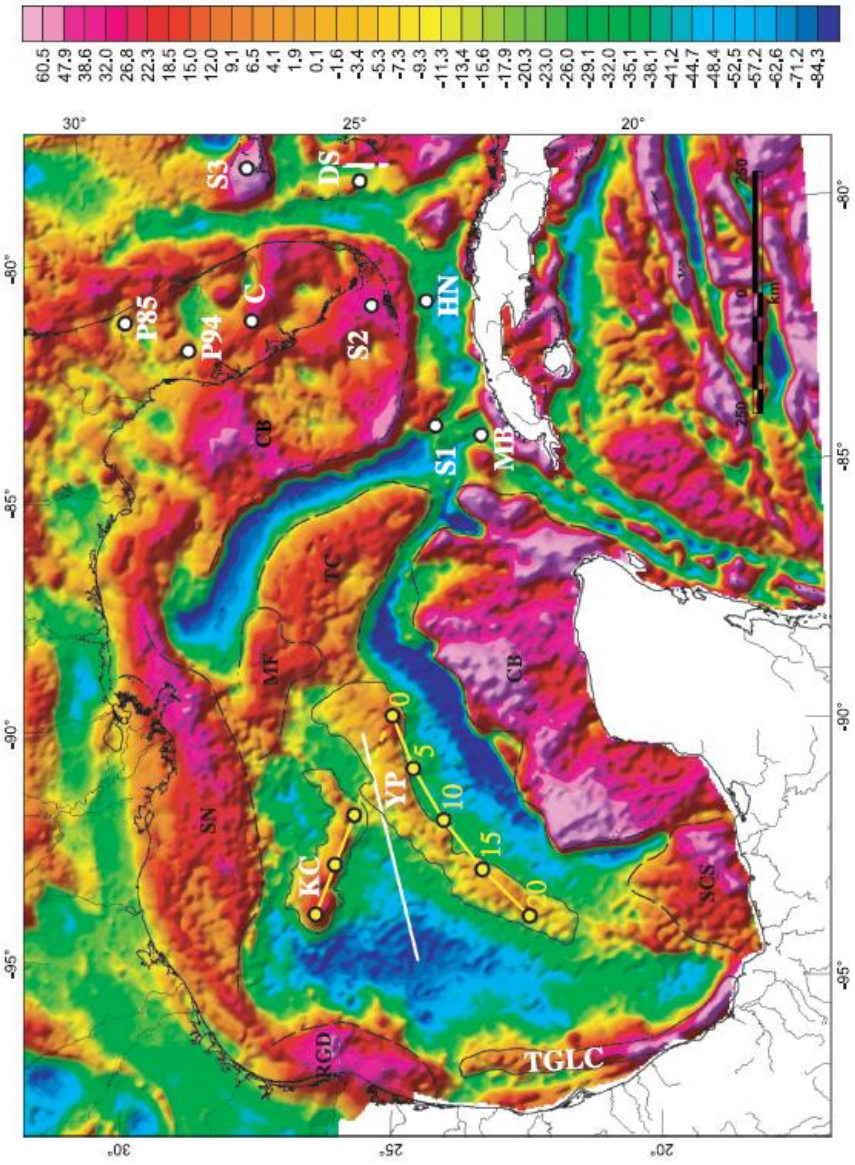

Figure 3.2 Mantle plume associated satellite derived free-air gravity anomalies (mGal) of Gulf of Mexico YC:Yucatan Peninsula KC: Keathly Canyon SN = Sisgbee nappe; MF =Mississippi fan; TC = thin crust; CB =carbonate buildups; SCS = south Campeche salt nappe; RGD = Rio Grande delta; TGLC = Tamaulipas–Golden Lane–Chiapas anomaly; YP =Yucatan parallel anomaly; KC = Keathley Canyon anomaly (Bird et al., 2005)

Another recent study from Mickus et al., (2009) also used potential field data for further investigation (Figure 3.3). The authors concluded that "Texas was strongly uplifted in Late Triassic time prior to rifting, and it is also consistent with Yucatan separating from Texas along this rift and the postulated fossil hotspot track in the western Gulf of Mexico'' *(Mickus et al., 2009).*

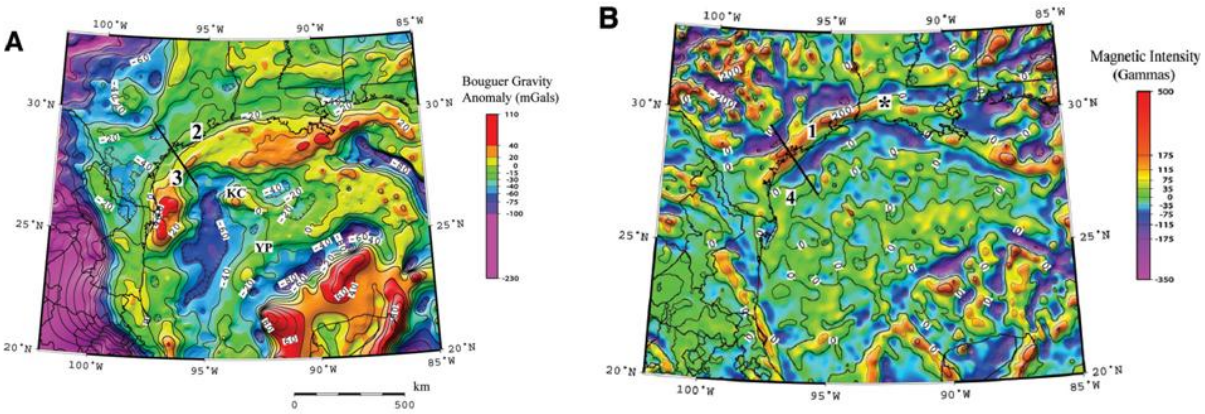

Figure 3.3 Gulf of Mexico and surrounding area free-air gravity anomalies, (a) total magnetic intensity, (b) and Texas Coastal Plain cross section, contour intervals are 10 mGal and 100 gammas, respectively KC, and YP Keathley Canyon, and Yucatan parallel gravity, respectively. Thick lines represent the crustal models (Mickus et al., 2009)

According to Bird et al. (2005), early stages in the formation can be summarized as follows (Figure 3.4): the initial position for the Yucatan Block is interpreted to be in the northern Gulf of Mexico. As continental extension progressed, the Yucatan block underwent a 20-22° counter clockwise rotation *(Hall and Najmuddin, 1994; Bird et al., 2005)*. Continental extension was followed by sea-floor spreading which caused another 20° counter clockwise rotation for the Yucatan block *(Bird et al., 2005)*. The present configuration of the formation was achieved by ~ 140 Ma (with the total rotation of 40-42° rotation)

In a different approach to the current problem Odegard (2010) has proposed that a large portion of the central Gulf of Mexico is underlain by proto oceanic crust.

According to the author, the development of passive margins requires 5 initial stages as follows: (1) Initial fracturing of the crust, (2) Extension of continental crust (3) Highly extended continental crust due to faster rifting (4) Formation of proto oceanic crust (5) development of the oceanic crust.

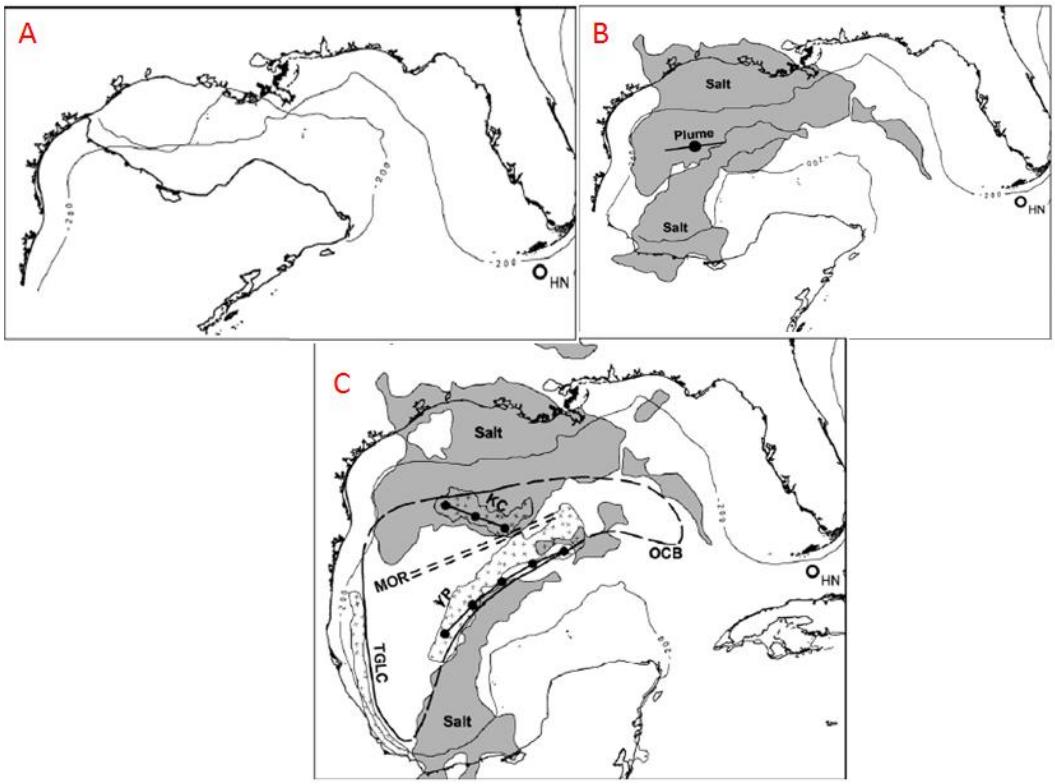

Figure 3.4 Reconstruction of Gulf of Mexico with three main stages, (a) Initial position (b) 22° of rotation and continental crust extension (about 150–152 Ma), (c) current configuration, 42° total rotation (20° by rotation of sea-floor spreading, Bird et al., 2005)

Odegard (2010) further explained the development of `proto-oceanic` crust and the true oceanic crust: ''Development of basin during the initial break up of continental plates is controlled by the zones of weakness in the continental crust''. ''Zones of weakness may not align exactly with the preferred direction of spreading and during rifting the interaction of continental plates cannot be well defined'' *(Odegard, 2010).*

The fourth stage occurs after rifting but prior to the drift phase. The continental crust on the fourth phase can be fragmented by volcanic materials that are produced by ridge system. The proto oceanic crust then undergoes some additional modifications that lead to the creation of true oceanic crust *(Dickson and Odegard, 2000)*.

The proto oceanic crust (Figure 3.5) is a zone with a mixture of volcanics, mantle material, and continental fragments. This zone shows spatially chaotic magnetic and sometimes gravimetric spreading anomalies.

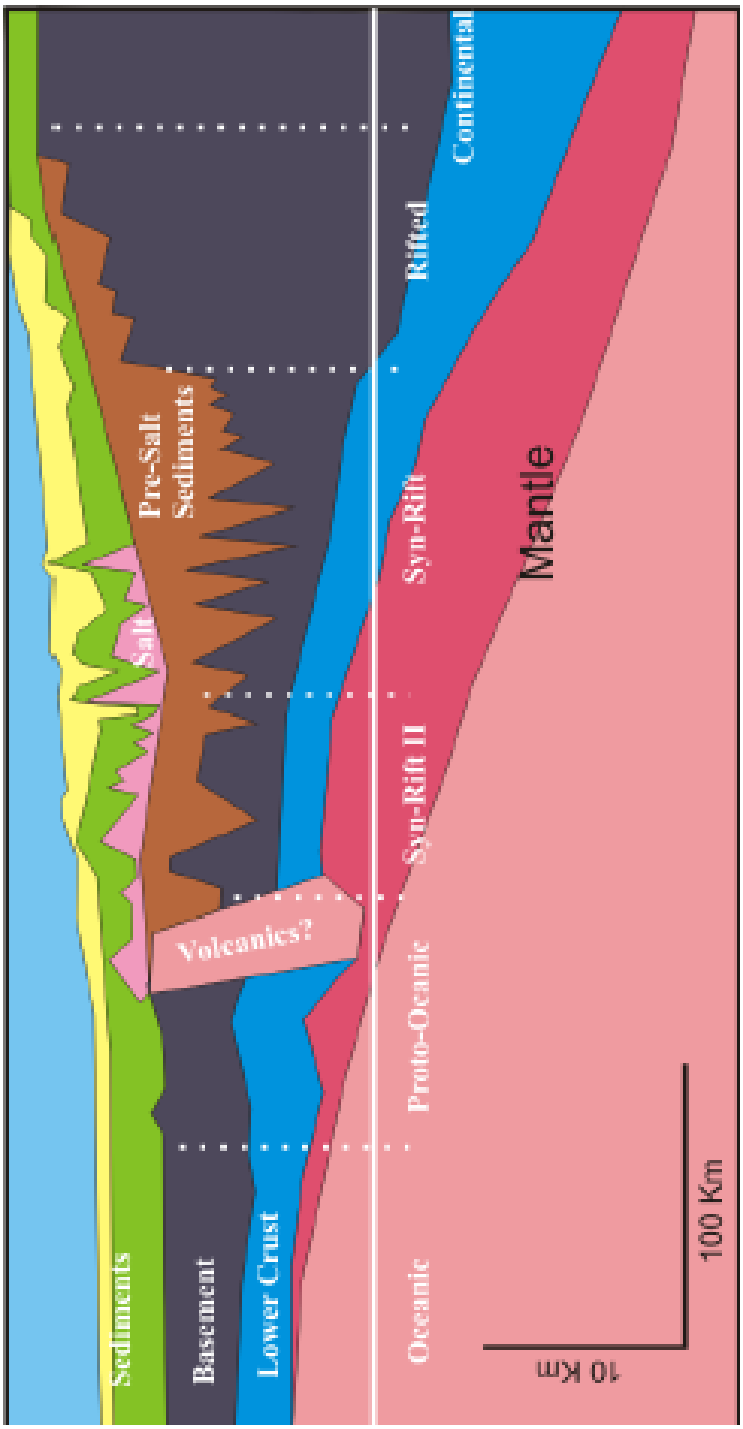

Figure 3.5 Typical proto oceanic crustal cross section (Odegard, 2010)

CHAPTER 4 DATA

4.1. Geophysical and Geological Data

Different types of data have been integrated during the modeling and interpretation of the gravity response of the northern Gulf of Mexico. These integrated data include onshore and offshore gravity, available seismic reflection and refraction, onshore and offshore magnetic data, available well information, and published geological maps and cross sections.

4.2. Gravity Data

4.2.1 Marine Ship Track Data (National Geophysical Data Center)

Ship track data from NGDC (Marine Trackline Geophysics Datasets, www. Ngdc.noaa.gov) were primarily used during the study.

The database GEODAS from NGDC was used to obtain digital data for the offshore part within the designated study area (W95° to W89°, N29.5° to N25.5°). Data extracted from GEODAS are mainly geophysical data including bathymetry data (Figure 4.1 and 4.2).

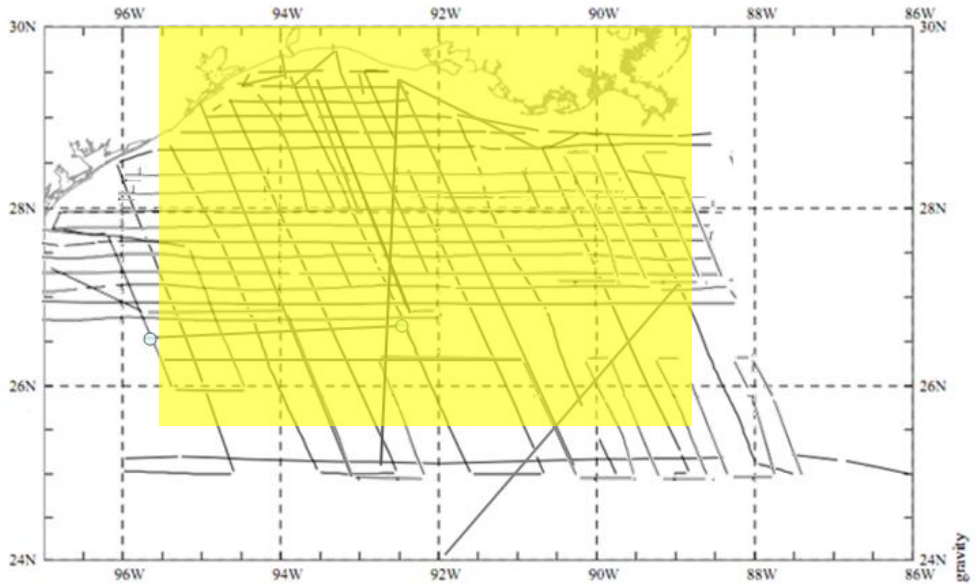

Figure 4.1 Available ship track data over the Northern Gulf of Mexico from GEODAS. Survey area highlighted

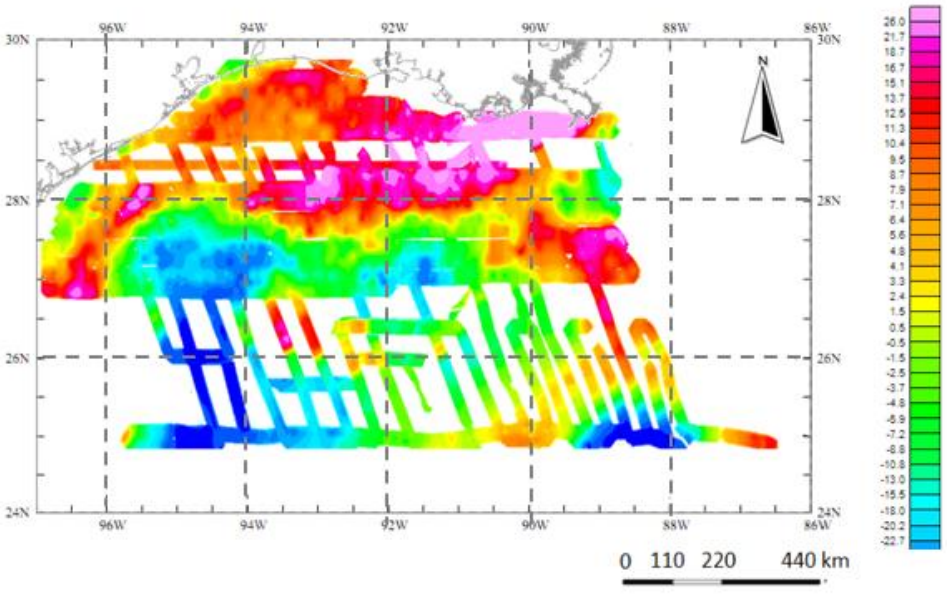

Figure 4.2 Free-air gravity (mGal) response from ship tracks (GEODAS)

4.2.2. Onshore Free-air Gravity Data (Texas and Louisiana State Surveys, USGS)

For onshore gravity data, USGS crustal studies and state surveys has been used. (http://crustal.usgs.gov/projects/namad/state_listing.html#texas

http://crustal.usgs.gov/projects/namad/state_listing.html#louisiana ,

Surveys over the area of interest have ±2 mGal resolution with 4–6 km of wavelength. The area of interest for the onshore part is limited between W95.5° to W91° and N33° to N30° (Figure 4.3 and 4.4).

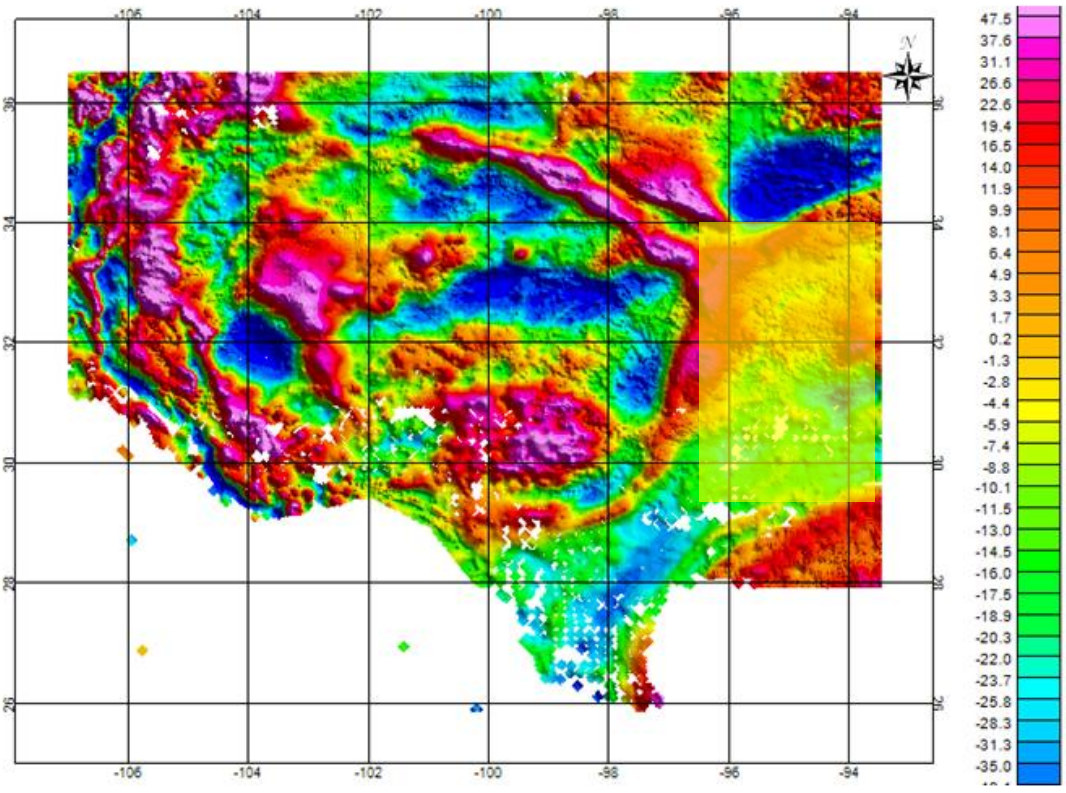

Figure 4.3 Free-air gravity (mGal) response of Texas (USGS) (Survey area highlighted)

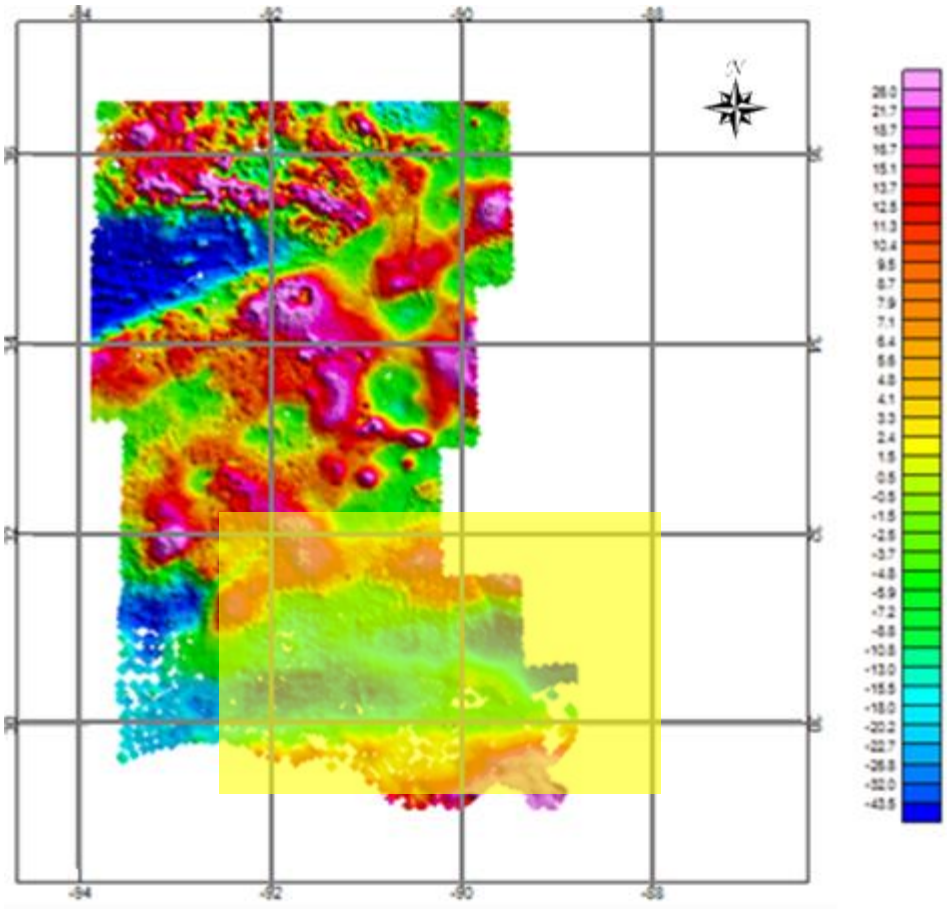

Figure 4.4 Free-air gravity (mGal) response of Louisiana (USGS) (Survey area highlighted)

4.3. Global Scale Studies

4.3.1. Global Crustal Model at 2x2 Degrees (Crust 2.0)

Crust 2.0 is a global crustal model that specifies density, and compressional and shear velocity on a 2x2° grid. A total of 360 different crustal profiles describe the variations in the 16200 cells of the 2x2° grid

(http://igppweb.ucsd.edu /~gabi/rem.dir/crust/rem.crust.html#crust2) (Figure 4.5 and 4.6).

''The 2x2 degree model is composed of 360 key 1D-Profiles. Each individual profile is a 7 layer 1D-model with'') (http://igppweb.ucsd.edu /~gabi/rem.dir/crust/rem.crust.html#crust2)

1. ice
2. water
3. soft sediments
4. hard sediments
5. upper crust
6. middle crust
7. lower crust

Parameters VP, VS, and density are given explicitly for these 7 layers as well as the mantle below the Moho.

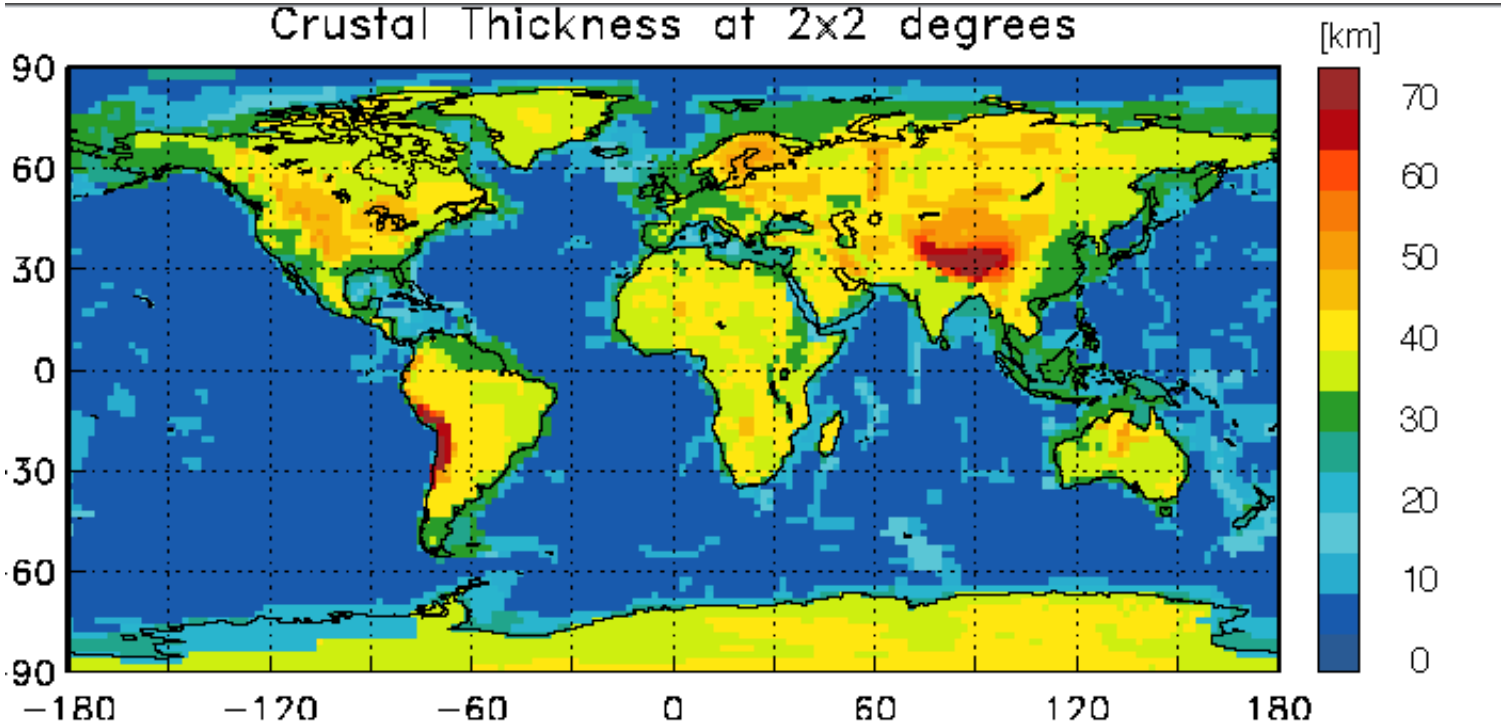

Figure 4.5 Generated world crustal thickness map, by Crust 2.0

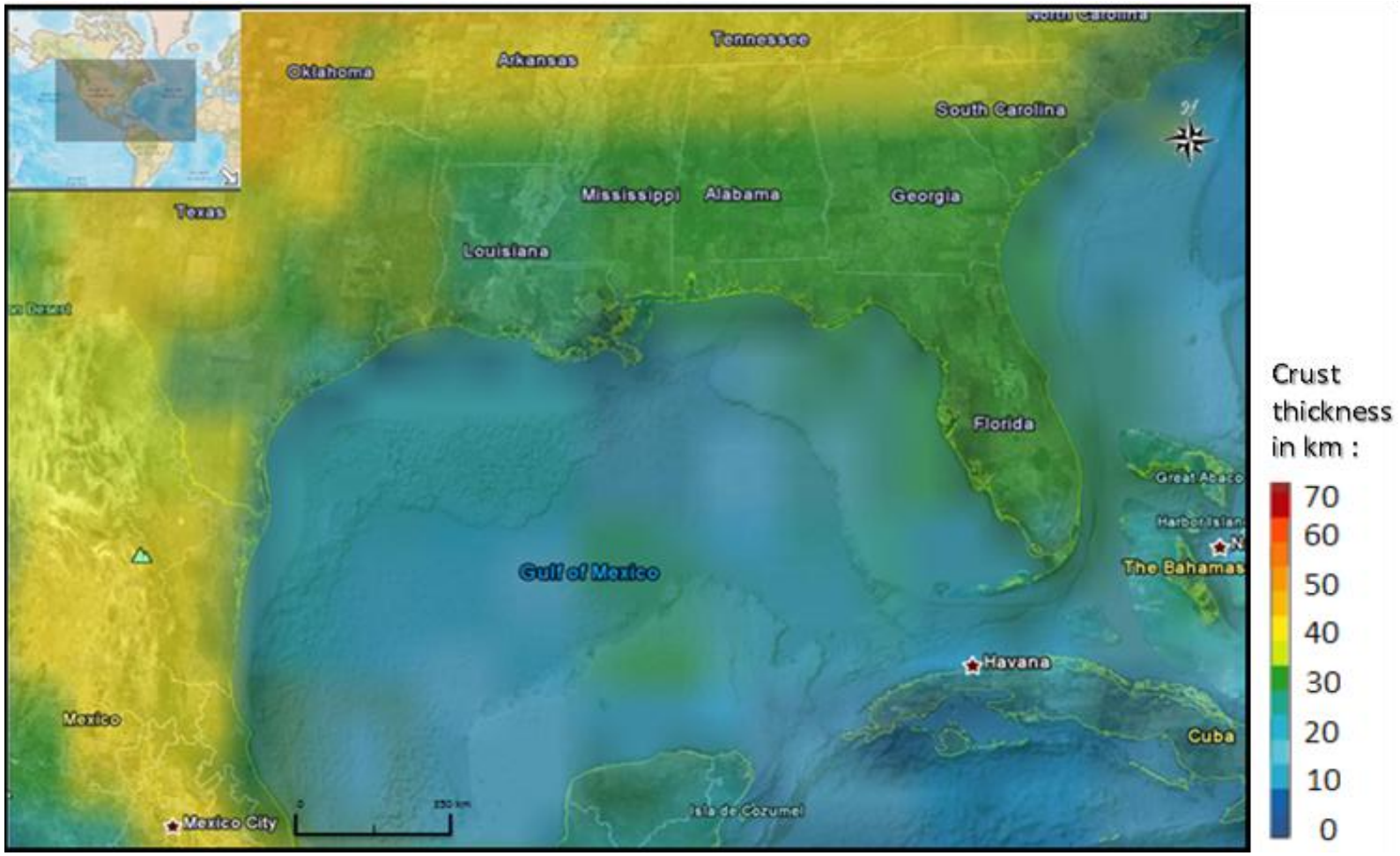

Figure 4.6 Generated (Crust 2.0) crustal thickness of the Gulf of Mexico and surrounding areas

4.3.2. Sediment Thickness Data

In order to generate accurate models, total sediment thicknesses as well as layer thickness (unconsolidated vs consolidated layers) are required. The sediment thickness along the Gulf area has been gathered from several different sources.

- Total Sediment Thickness of the World's Oceans and Marginal Seas

''A digital total-sediment-thickness database for the world's oceans and marginal seas has been compiled by the NOAA National Geophysical Data Center'' (NGDC) (http://www.ngdc.noaa.gov/mgg/sedthick/sedthick.html). ''The sediment thickness data were obtained from published source, ocean drilling results and seismic reflection Profiles archived at NGDC as well as seismic data and isopach maps'' (NGDC, ngdc.noaa.gov). The dataset that was obtained from NGDC was used to generate a sediment thickness map (Figure 4.7) of Gulf of Mexico region and used during crustal modeling.

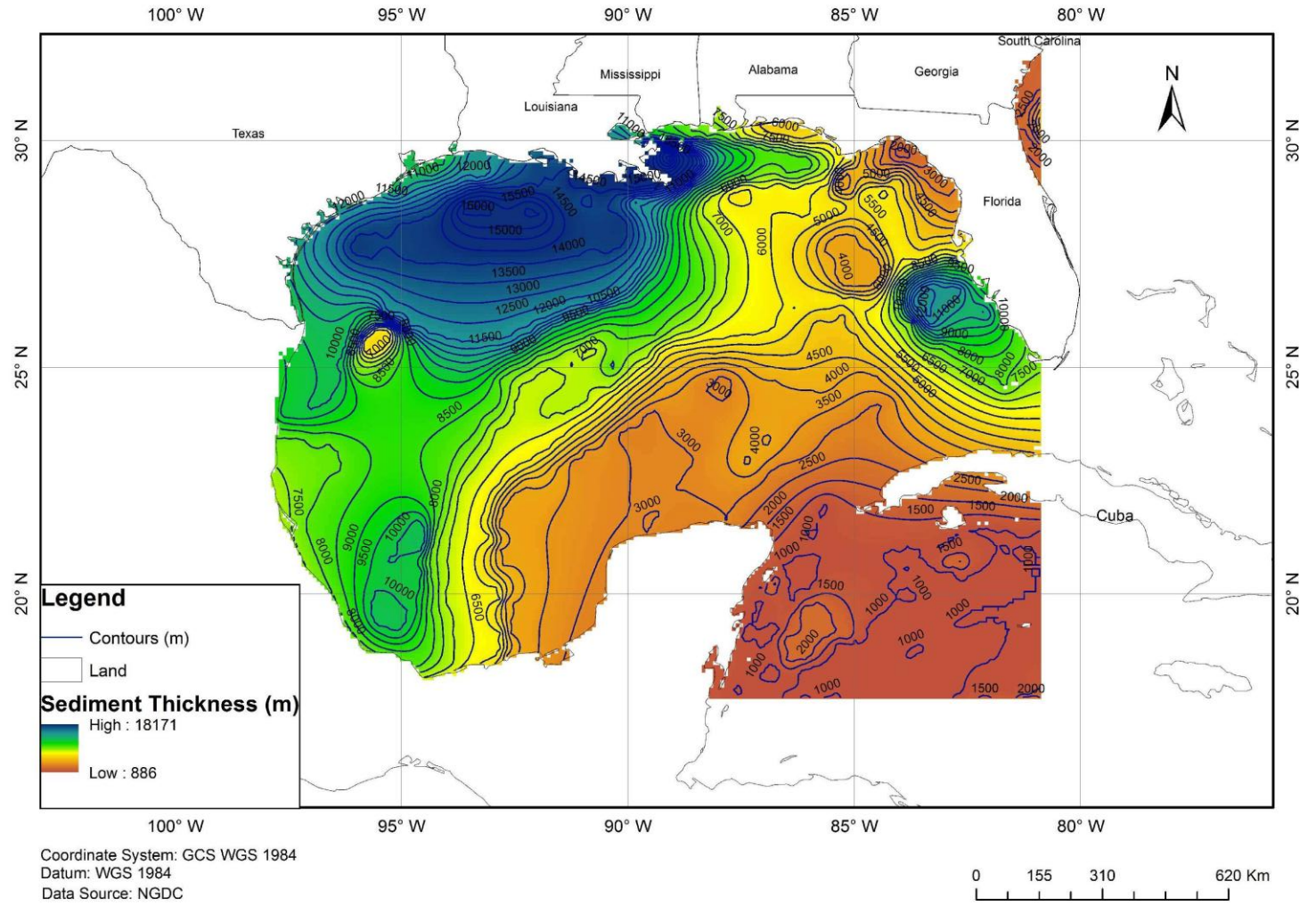

Figure 4.7 Generated total sediment thickness map for Gulf of Mexico

4.3.3. A Global Digital Map of Sediment Thickness

This global sediment map is ‘’digitized on a 1x1 degree grid’’(Figure 4.8). This dataset is basically the updated version of Crust 2.0 for the sediment thicknesses. (http://igppweb.ucsd.edu/~gabi/sediment.html)

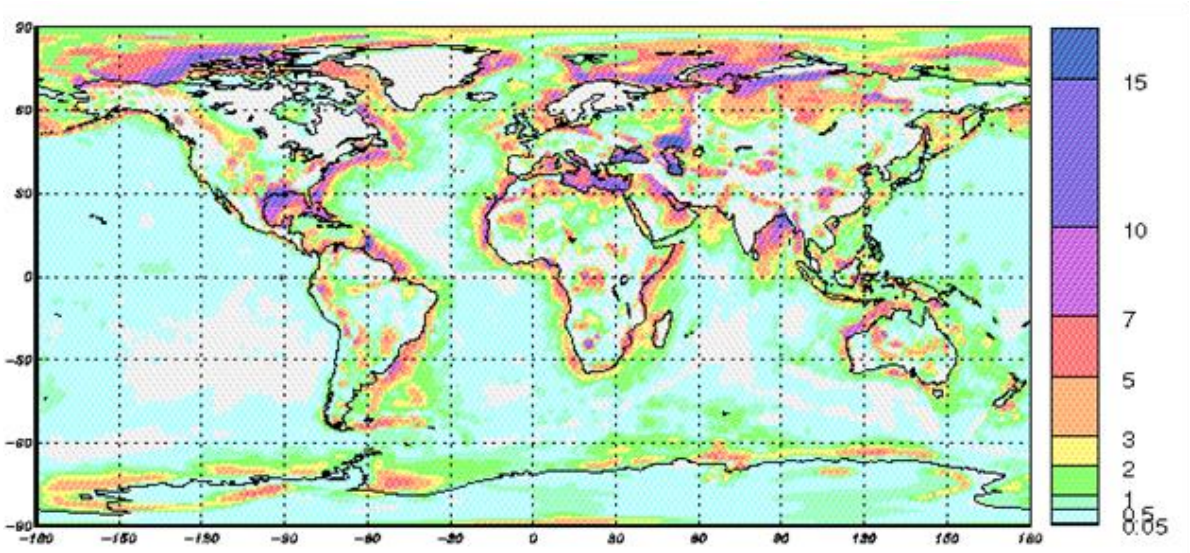

Figure 4.8 Generated sediment thickness map of the World (1°x1°)

4.4 Published Geophysical and Geological Data and Maps

In addition to digital data, various maps and other information from published sources were used;

4.4.1. Sediment Thickness Maps and Sediment Thickness Models

In the case of Gulf of Mexico region, it has been proposed that the sediment thickness can reach up to 18 km of thickness *(Galloway, 2011),* which makes sediments play a significant role in modeling studies. Physical properties of thick sediment piles will be one of the main elements that control the accuracy of the models. However, most of the seismic data are proprietary, and published data usually gives an idea for the relatively shallow subsurface (3-5 km depth from the sea-floor). Previously created models and maps were used to support the models. Structural and stratigraphic architectures of the northern basin are illustrated from many sources by regional transects (Figure 4.9 and 4.10). Maps and models are mainly taken from Galloway, (2011).

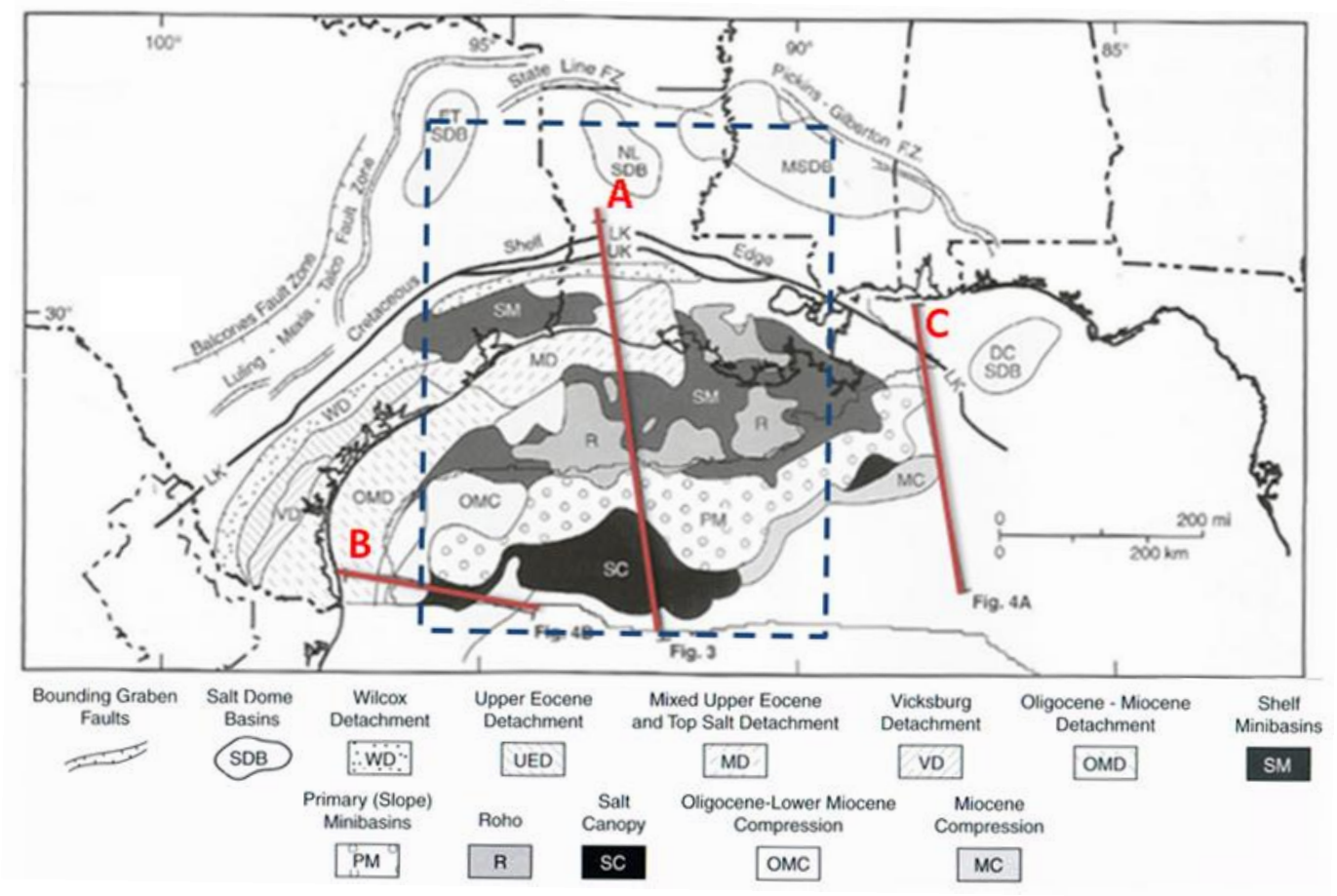

Figure 4.9 Structural domains of the Gulf of Mexico (available transects lines colored) (Galloway, 2011)

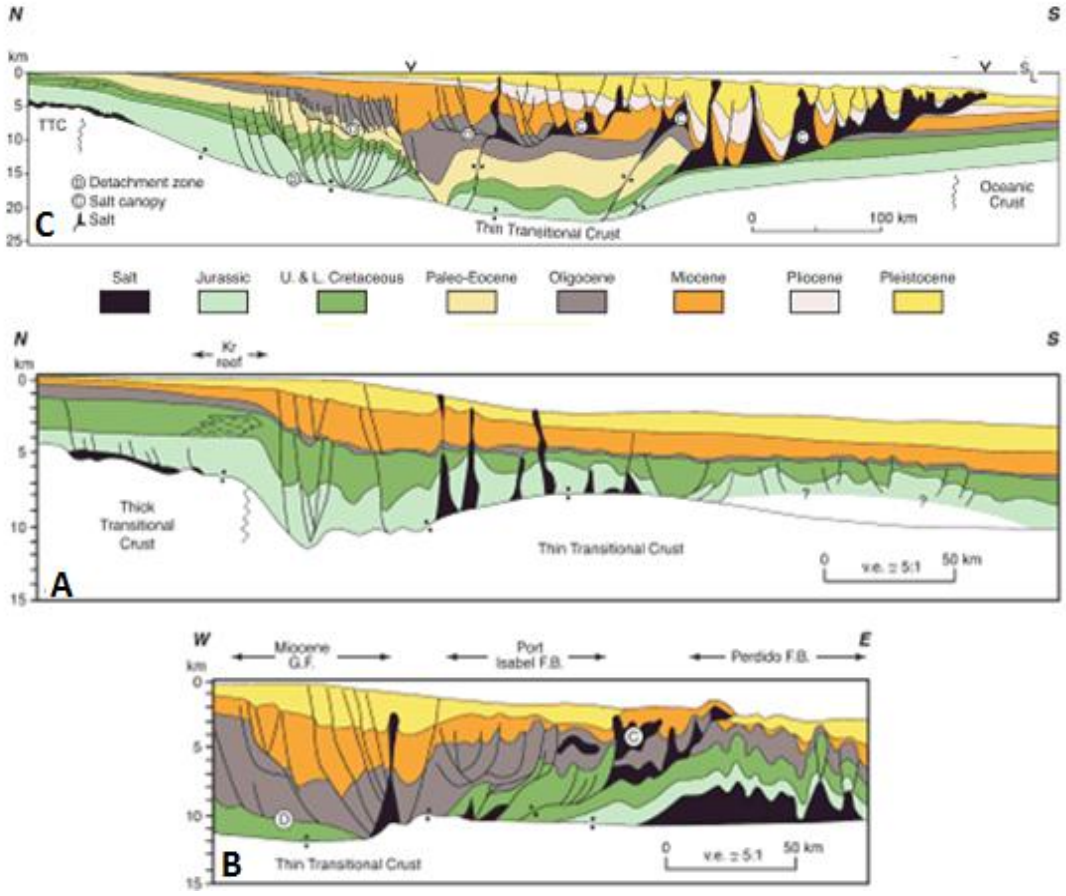

Figure 4.10 Cross sections through northern Gulf of Mexico showing crustal types and stratigraphy (locations on Figure 4.9, Galloway, 2011)

4.4.2. Total Tectonic Subsidence Analysis and Maps

In addition to the digital data (mainly used to create models), total tectonic subsidence maps are used to provide a rough estimates for the boundaries of different types of crust in the Gulf region. Crust extension analysis and maps and Moho depth estimates (Figure 4.11, 4.12, and 4.13) were taken from, Dunbar and Sawyer (1987) and Sawyer et al., (1991).

The total subsidence is the water depth plus the sediment thickness at certain point. Total tectonic subsidence (TTS) is the total subsidence less the loading effect of sediments. The amount of TTS due to crustal extension is proportional to the amount of crustal thinning *(LePichon et al., 1981*). TTS values also depend on the time since rifting. Zero TTS values described as zero extension (β=1) and Dunbar and Sawyer (1987) also assumed that when the β values ≥ 4.5 indicated oceanic crust.

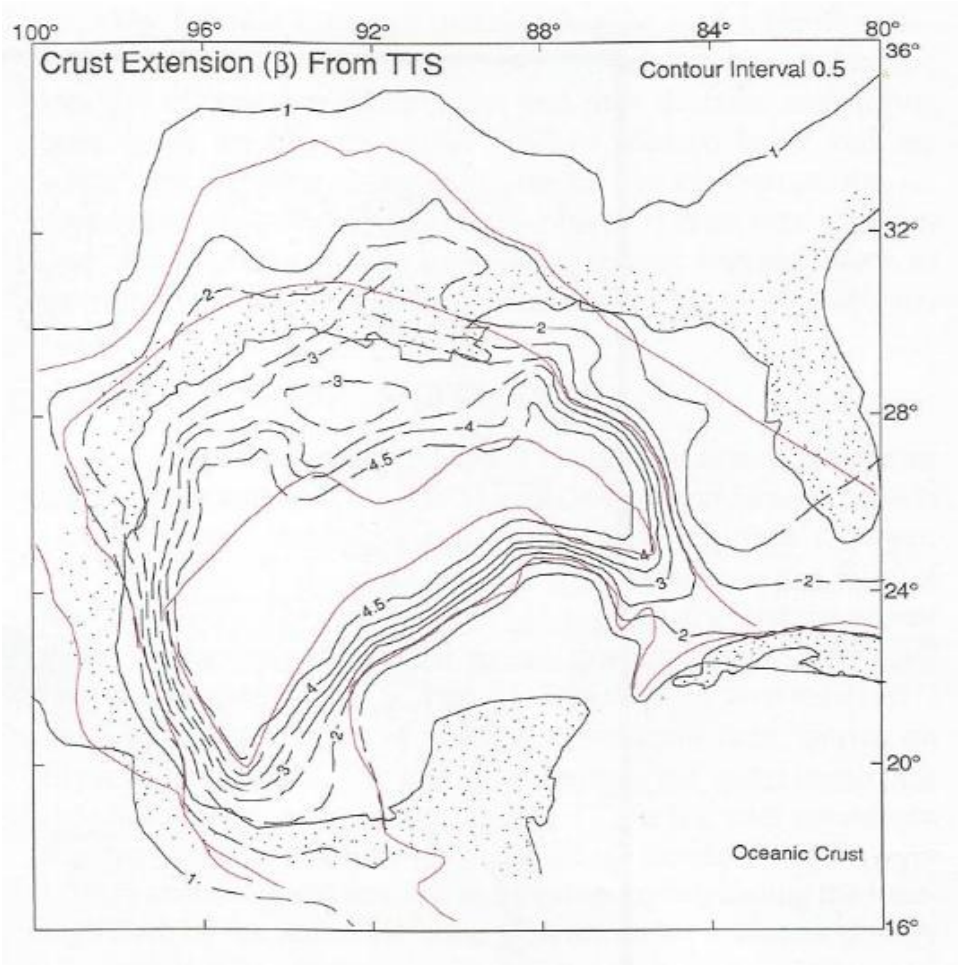

Figure 4.11 Map of crustal extension of Gulf of Mexico basin (Dunbar and Sawyer, 1987)

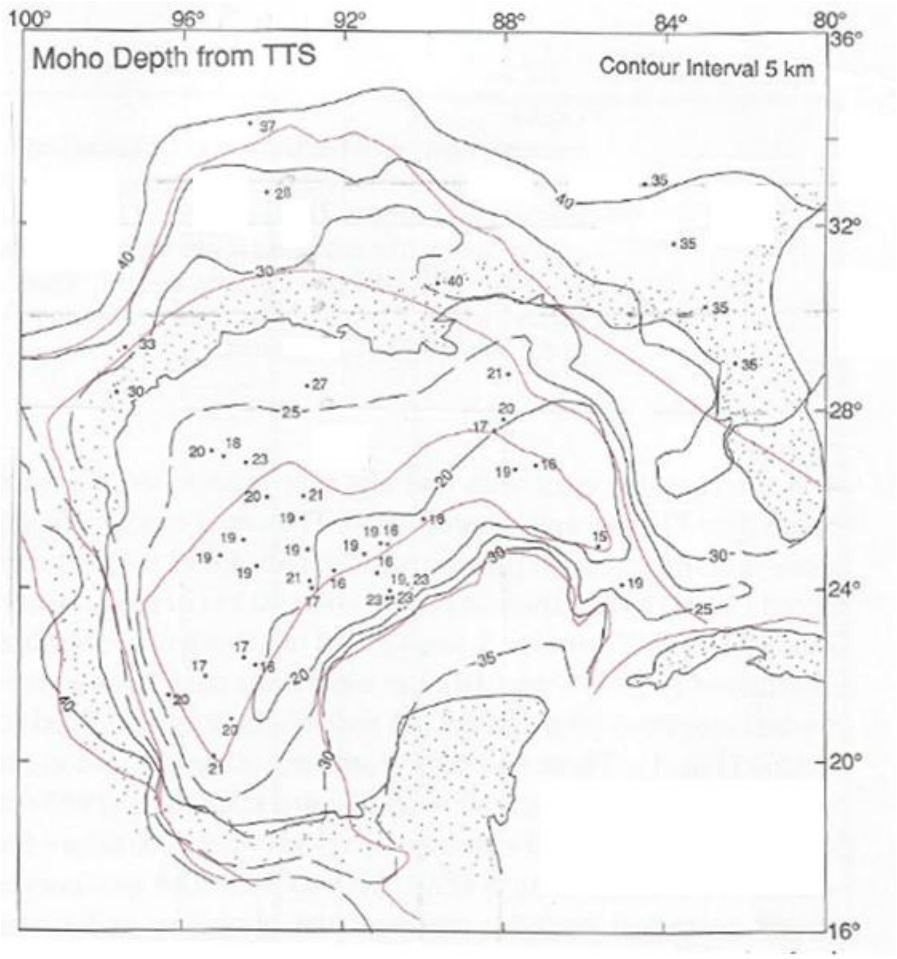

Figure 4.12 Map of estimated Moho depth in the Gulf of Mexico basin based on subsidence analysis (Sawyer et al., 1991)

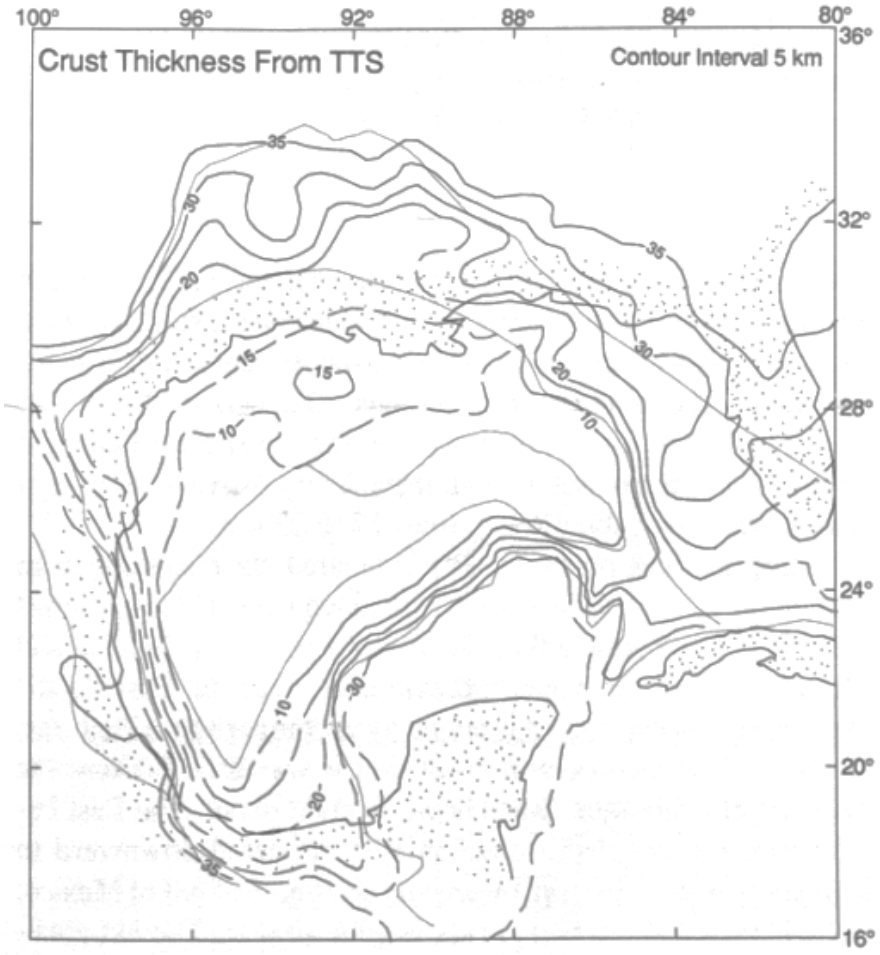

Figure 4.13 Map of estimated crust thickness in the Gulf of Mexico basin based on subsidence analysis (Sawyer et al., 1991)

4.4.3. Decades of North American Geology

Decade of North American Geology (DNAG) project represents ‘’the cooperative efforts of more than 1000 individuals from academia, state/federal agencies and industry to prepare syntheses that are as current as possible about the geology of the North American continent and adjacent oceanic regions’’ *(Sheridan et al., 1988).* These studies resulted in several maps and models that summarize the ‘’geology, tectonics, magnetic and gravity anomaly patterns, regional stress fields, thermal aspects, and seismicity of North America’’ (*Zietz, 1982*).

The issues that were presented for the Gulf of Mexico portion of the DNAG project mostly focus on basement depth, crustal types, and the geological history of Gulf of Mexico and surrounding areas. For this study, 3 regional transects are used (Figure 4.14. and 4.15).

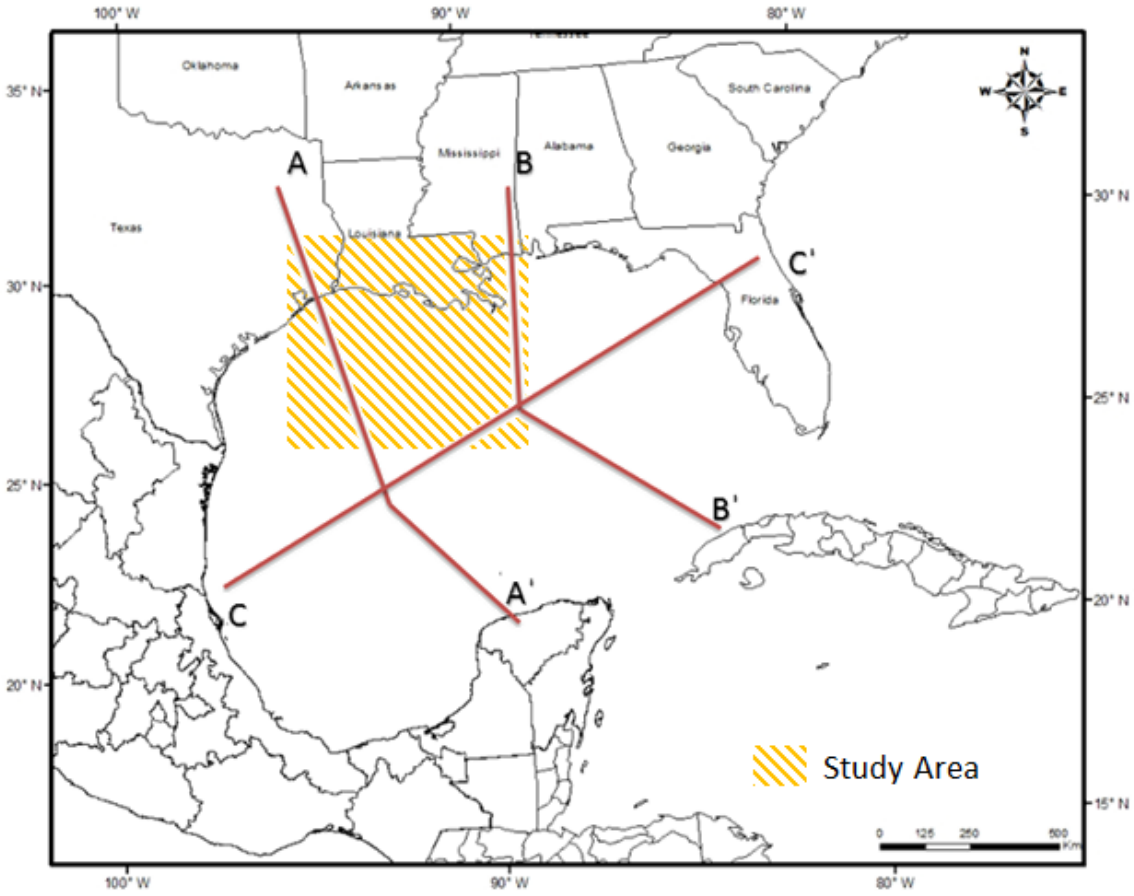

Figure 4.14 Location of cross sections from DNAG database, study are highlighted (Buffler and Sawyer, 1985)

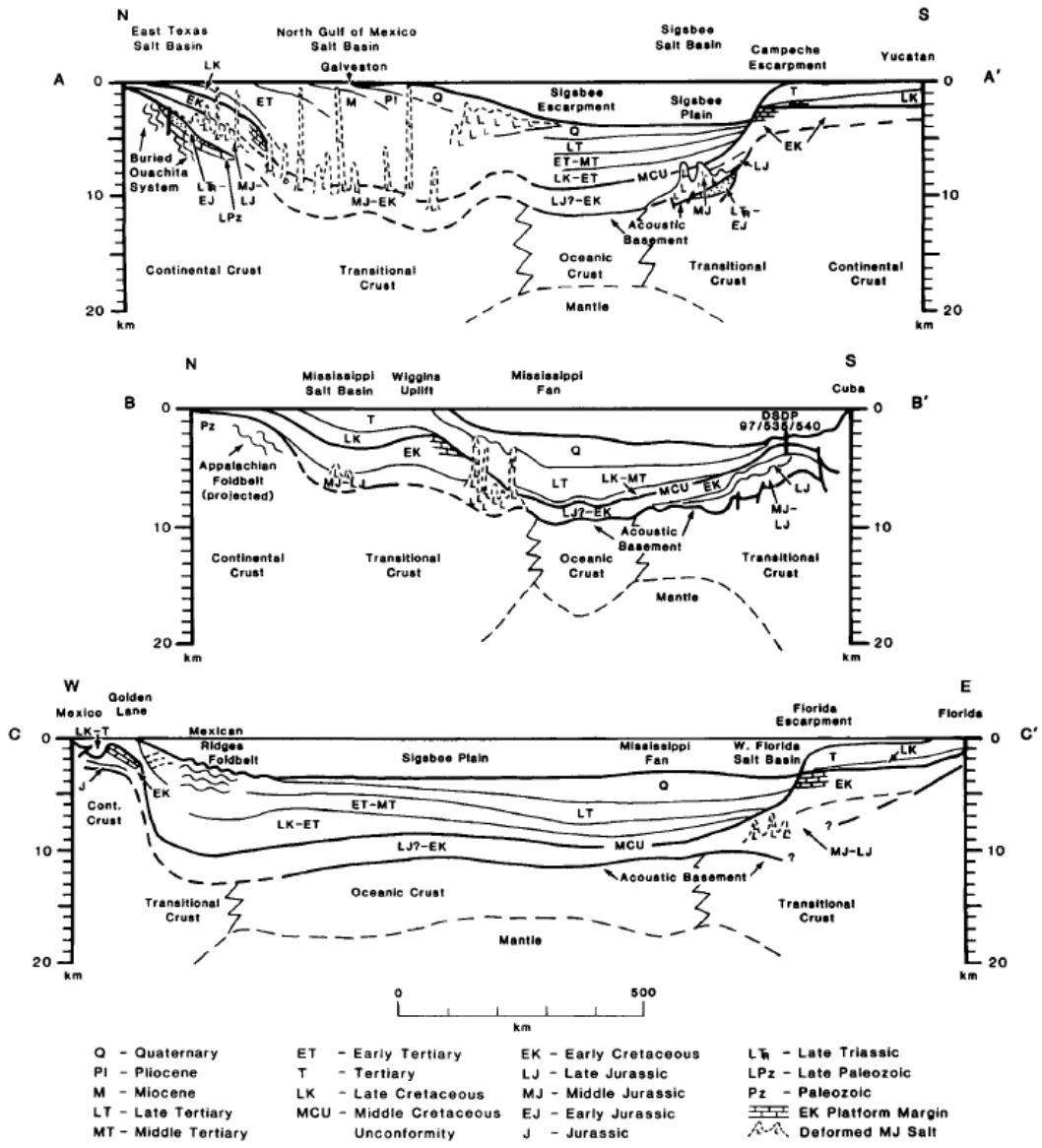

Figure 4.15 Schematic cross sections of Gulf of Mexico basin (see previous figure for locations) (Buffler and Sawyer, 1985)

The survey area for this study is surrounded by two regional transects (A and B). These transect and cross sections were used to provide additional information for the physical properties of the crust surrounding the Gulf of Mexico (boundaries, depth, and distribution).

Besides the DNAG transects there are some seismically generated crustal models available for the Gulf of Mexico which were used for the models. These are:

- Seismic cross sections from King (1969)

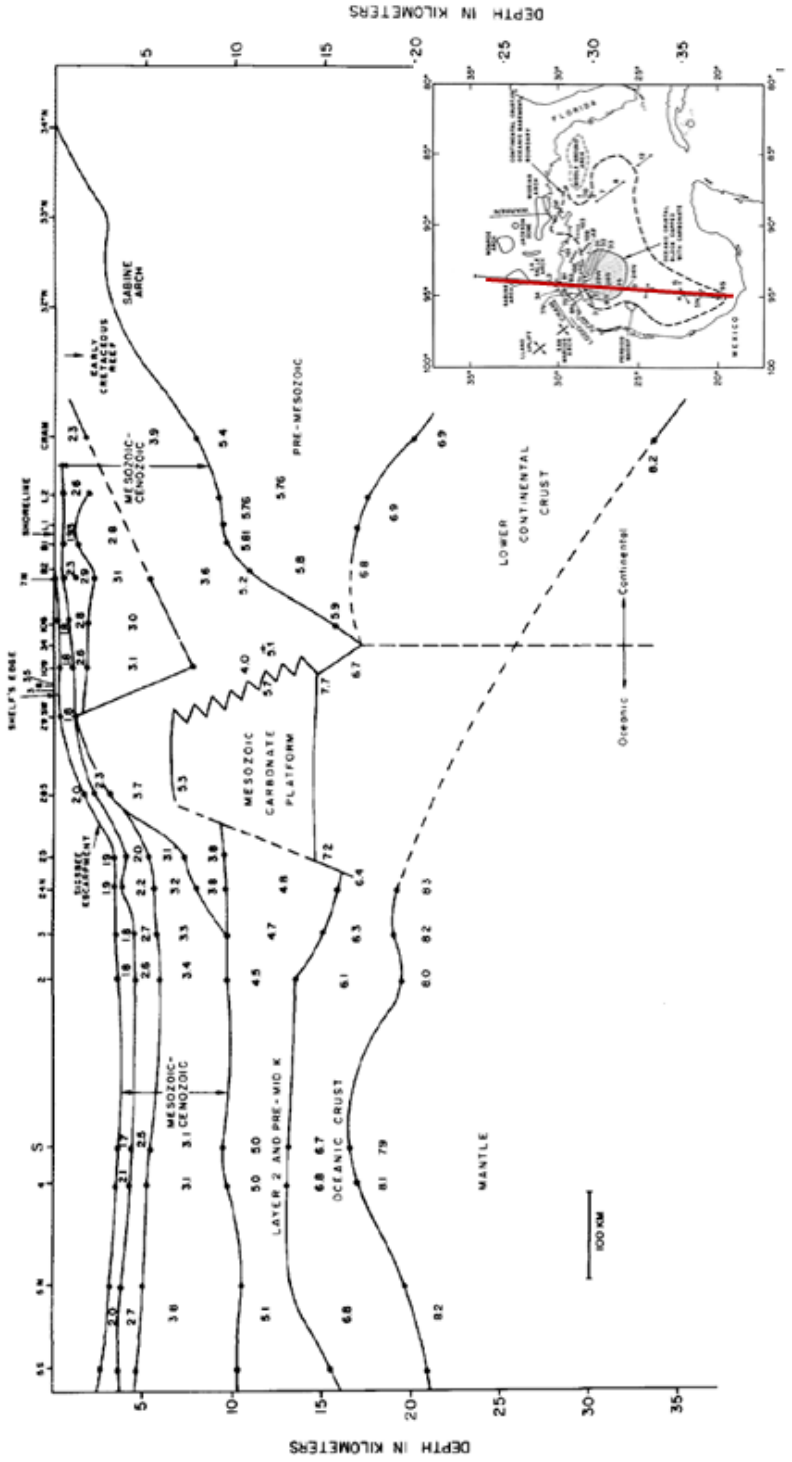

Figure 4.16 Seismic velocity (km/s) structure of Western Gulf of Mexico (Transect highlighted) (King, 1969)

- East Texas and Mississipi crustal cross section from Worzel and Watkins (1973)

  This transect is mainly generated by seismic reflection and refraction studies, and also extends for approximately 600 km.

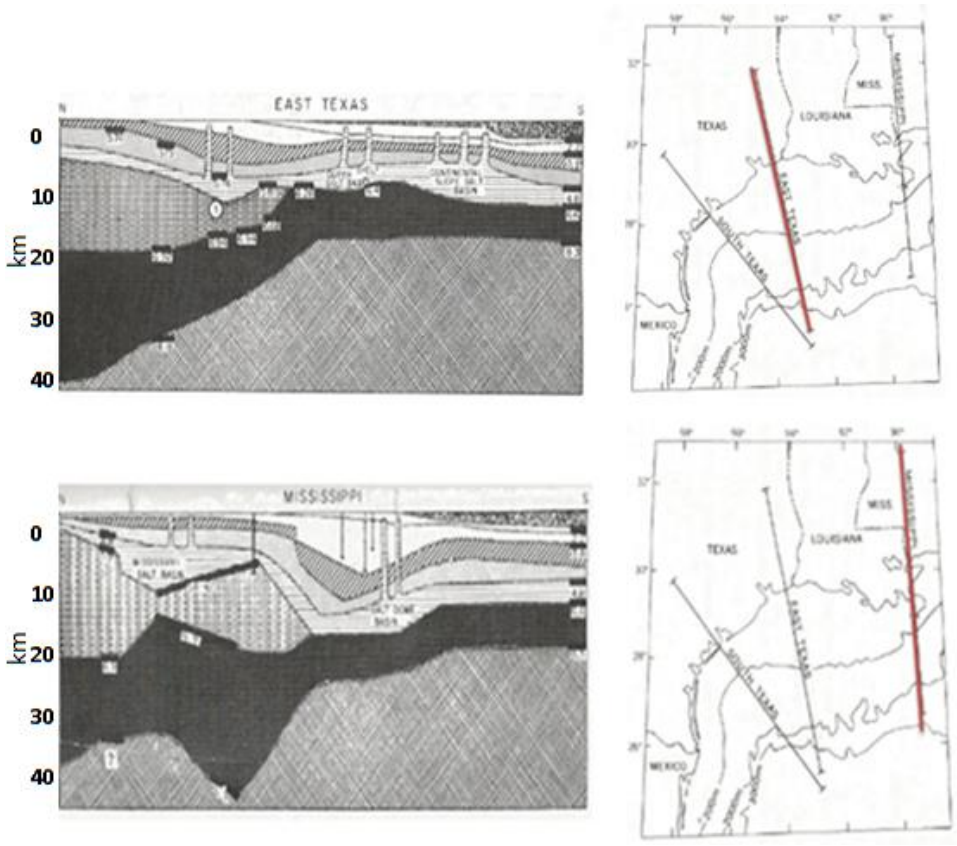

Figure 4.17 Crustal cross sections across continental margin, East Texas and Mississippi profile (Worzel and Watkins, 1973)

- Seismic Cross section at shelf edge from Ibrahim and Uchupi (1982)

  This section only provides thickness of the sediment layers. The location of this cross section crosses Profile 4 from this study.

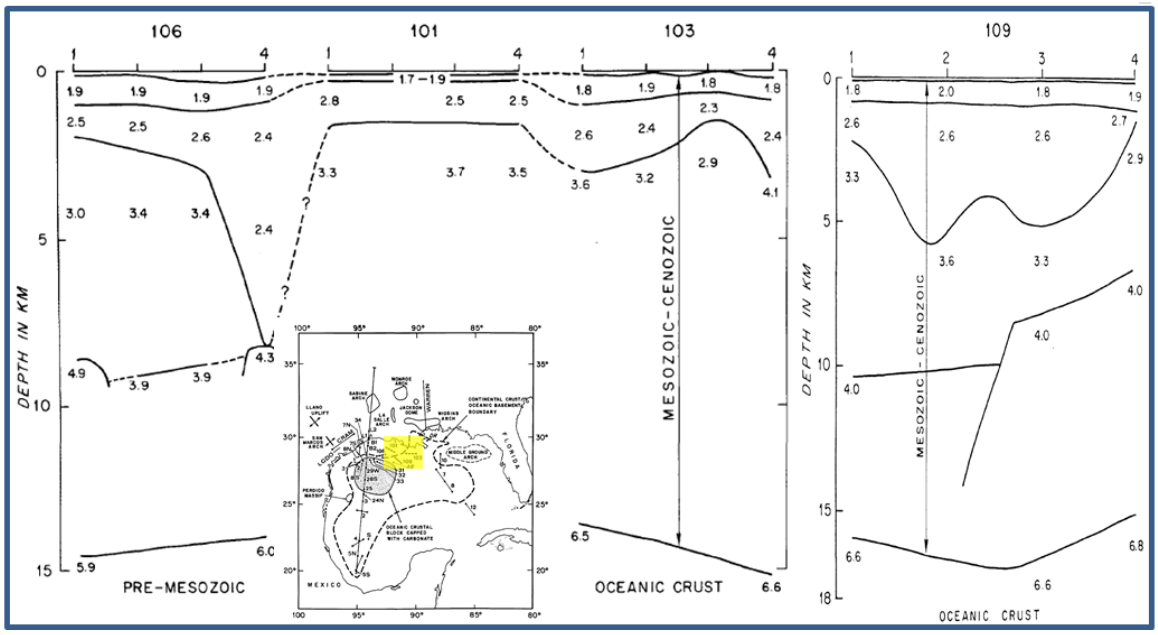

Figure 4.18 Seismic velocity (km/s) structure of East Texas shelf (Ibrahim and Uchupi, 1982)

4.5. Magnetic Data

4.5.1. Decades of North American Geology

The digital data grid for the magnetic anomaly map of North America is extracted from DNAG data base (http://pubs.usgs.gov/of/2002/ofr-02-414/), (Figure 4.19). These grids fully cover the Gulf of Mexico and the surrounding area as well. The magnetic anomaly map of North America was compiled and processed as part of the Geological Society of America's Decade of North American (DNAG) project. The grids are presented in Geosoft binary grid format. Onshore magnetic anomaly profile data used in this study were acquired mainly by aeromagnetic surveys. Offshore magnetic data were gathered along ship tracks over the Gulf of Mexico. These data were maintained by National Geophysical Data Center (NGDC) and kept in the Geophysical Data System (Geodas) database. DNAG data are gridded 1x1 km. Magnetic data from DNAG were actively used for the Profiles 1, 3 and 6.

Magnetic data were introduced into the models due to lack of seismic data from SDRs. Magnetic data have been used to interpret the properties of SDRs on many volcanic margins around the world (Norwegian margin, South America, etc.) *(White and McKenzie 1989; Yegorova and Goberenko, 2010)*

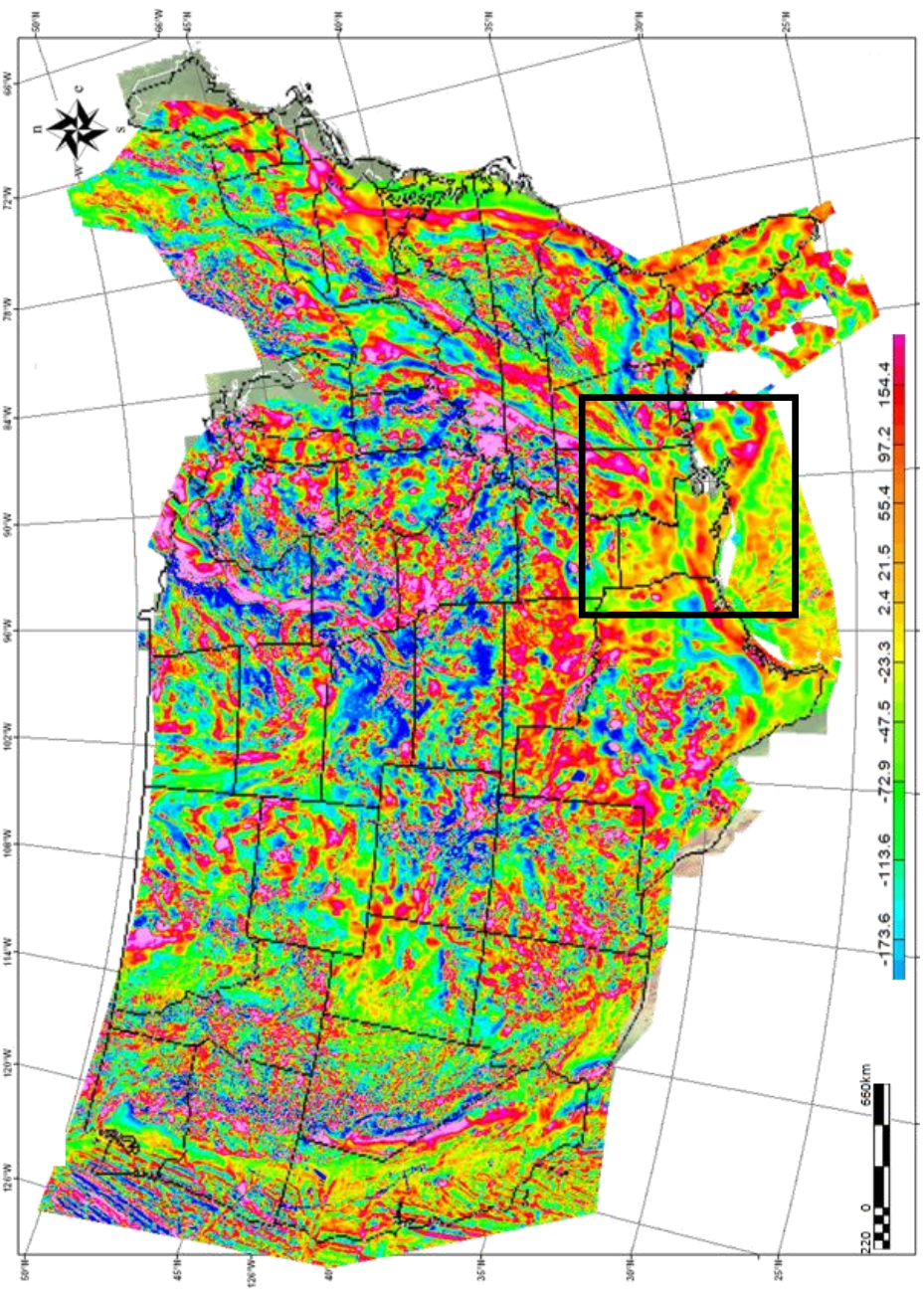

Figure 4.19 Total intensity magnetic anomaly map of USA, rectangle area represents study area (generated by DNAG database)

4.5.2. Previously Published Magnetic Studies

Data and maps were extracted from previous studies *(Hall and Najmuddin, 1994; Mickus et al., 2009)*. The aeromagnetic data from Hall and Najmuddin (1994) were used for the correlation between models. Profiles 4, 5, and 6 cross the aeromagnetic study area. Interpretations made by the authors were also used for plate reconstruction models.

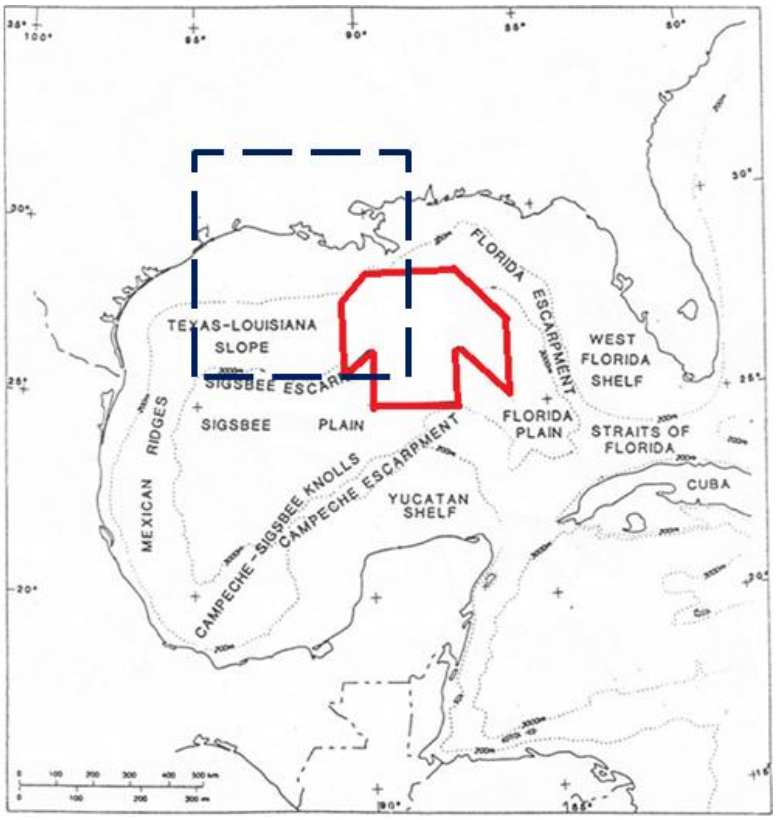

Figure 4.20 Location of the aeromagnetic survey (highlighted with red line) and study area (highlighted with dashed blue line) over Gulf of Mexico (Hall and Najmuddin, 1994)

CHAPTER 5 METHODOLOGY

5.1. Introduction and Selection of Profiles

Rift zones can often include complex structures. In order to analyze these features, some assumption and/or simplifications must be made. Rift zones are usually assumed to have changes in physical properties mostly on depth (Z axis) and offset (X axis). Change in the Y axis are often assumed to be invariant due to lack of data coverage and general geological rule of thumb (length > width). With the assumption of the y-axis as an invariant axis, the source of the anomalies can be assumed to be 2D.

I used 2-D forward gravity modeling in this study. Profiles have been chosen:

- To have maximum control points (available seismic reflection, seismic refraction and well data , proximity to previous studies)
- To be nearly perpendicular to the predicted ocean-continent boundary. The location and trend of the OCB of the northern Gulf of Mexico has been identified by several previous studies (trending approximately E-W direction)

A total of 6 profiles were used in this study. The separation between each of the Profiles is 60-80 km. The length of the profiles was designed so as to include different

types of crust (Continental crust, Transitional zone, Oceanic crust). As a result of this, selection length of profiles was chosen to be 800 km. Station spacing within each profiles (except for Profile 6) is 5 km, however this value varies at the Gulf coast (due to poor coverage) area. Profile 6 has the maximum seismic control points but it lacks dense gravity data coverage. As a result the station spacing was chosen as 15 km.

2D models are designed to have 8 different layers. These layers and their densities are as follows:

Water (1.03 g/cc)

Unconsolidated Sediments 2.30g/cc *(Warren et al., 1966; Christensen, 1989)*

Consolidated Sediments 2.50 g/cc *(Warren et al., 1966; Christensen, 1989)*

Seaward Dipping Reflectors 2.58 g/cc (chosen for this study)

Upper Crust 2.65 g/cc *(Ibrahim et al., 1982; Hales et al., 1970 and Hales 1973)*

Lower Crust 2.90 g/cc *(Ibrahim and Uchupi, 1982)*

Underplate 3.0g/cc (chosen for this study)

Upper Mantle 3.2g/cc *(Warren et al., 1966; Christensen, 1989)*

In the study area there is very little known about the middle crustal layer. As a result, the crust is considered to have 2 sections (Upper and Lower).

Calculation and construction of the models are based on the principle of forward modeling. In general, the observed data are put aside and depending on the geophysical data and geological knowledge, a rough approximation for the subsurface distribution is created. The gravity response for the initial model is calculated based upon the geometry and other physical properties assigned to the subsurface layers. Response from the initial model is compared with the observed data. However the match between the observed and calculated data is not only the factor that controls the accuracy of model. The difference between the observed data and the model response is minimized by modifying the initial model. Magnetic modeling is only done to test the presence of SDRs. Susceptibility value for the several layers:

Sedimentary layers: 0 cgs

SDR bodies: 0.0045cgs

Upper crust: 0.0004 cgs

Lower crust: 0 cgs

Underplating: 0 cgs

Upper Mantle: 0 cgs

As the materials reach the Curie point (~ 600°c), they will start to lose their magnetization. Geothermal gradient temperature increases as the depth through Earth's interior increase; near the surface it is usually 25–30°C per km of depth

(Buschow, 2001). Therefore any material that is below 20 km from the surface will have a temperature of more than 600°C. Upper mantle, underplating and lower crust materials are assumed to have zero susceptibility values as they have passed the Curie threshold because of their depth.

Magnetization of sediments is usually assumed to be low or zero due to their lack of highly magnetic materials *(Mickus et al. 2009; Yegarova et al., 2010* and many more)

Two-dimensional gravity and magnetic models were constructed using GMSYS software, developed by Northwest Geophysical Associates .This software uses a simple 2D earth model in order to calculate the gravity response for designated geometry and density (results are due to the variation in density in the X and Z direction).This software basically uses the method described by Talwani et al., (1959), and Talwani and Heirtzler (1964), to calculate the gravity and magnetic response.

During modeling, sediment layers are divided into 2 layers, mainly separated from each other because of a density variation.

Evaporite deposits play very a significant role for the formation of passive margins. Besides their economical values as a hydrocarbon trapping structure, they can also play significant role to characterize the margin .The density and the geometry of the salt bodies are quite variable *(Martin, 1975).* Salt can be treated in two different ways for generating regional crustal models. It can be assumed as a restricted body,

which would not have crustal significance or very long wavelength contributions to the regional field. The second is that salt can reach a point where it's completely mixed with silts and sands so that density variation within a body is on small scale and will not affect regional studies *(Martin, 1975).* As a result of these assumptions salt is included within the sediment layers and densities of these layers are re-arranged with the existence of salt. As the profiles pass over the Sigsbee Escarpment, the amount of salt in sediment layers is dramatically reduced. Because of the lack of significant salt, densities of the sedimentary layers were changed starting from the Sigsbee Escarpment (km 760 for Profile 1, km 750 for Profile 2, km 760 for Profile 3, km 700 for Profile 4 , km 600 for Profile 5 , km 520 for Profile 6).

Density values of sedimentary layers located southeast of the Sigsbee Escarpment:

Unconsolidated Sed. 2.35g/cc

Consolidated Sed. 2.55 g/cc

5.2. Two-dimensional Gravity Models

5.2.1. Profile 1

The westernmost profile is 800 km long (Profile 1) and oriented NW-SE, approximately orthogonal to the proposed ocean-continent boundary *(Schouten and Klitgord, 1994; Marton and Buffler, 1994; Salvador, 1991; Buffler and Sawyer, 1985).* The northern end of the profile starts from onshore Texas (32.0° N, 96.2°W) extends south eastward into the Northern Gulf of Mexico and ends up at 26.25° N, 93.15° W. Only 320 km (65 stations with 5 km separation) of Profile 1 are located onshore and the remaining 360 kms are over the offshore area (73 stations with the 5km separation). Profile 1 extends approximately 60 km southeastward beyond the Sigsbee Escarpment.

Seismic constraints are available along Profile 1. For the sediment layers, a global total sediment thickness dataset (NGDC) is used along with available seismic data *(Worzel and Watkins 1973; King 1969; Galloway, 2011).*The boundary between the consolidated-unconsolidated sediments is obtained from previously published models *(Galloway, 2011)* and digital sediment thickness 1°x1° (*Laske and Masters, 1997)* dataset. Sediment layer densities are adjusted for the existence of salt bodies as described earlier in the modeling section.

Water depth values are obtained directly from bathymetry data from ship trackline (NGDC). The boundary between upper and lower crustal layers are extracted from available refraction studies *(Hales et al., 1970; Worzel and Watkins, 1973; Ebeniro*

et al., 1988) at km 100, km 250, km 345, and km 500 with the approximate velocity of 6.3 km/s for the upper crustal layer and 7.1 km/s for the lower crustal layer. Due to the limited coverage of the upper-lower crustal boundary, the thickness of the crustal layers is mainly controlled by the effort of keeping their thickness ratio constant or similar (1:1). Moho depth values are extracted from various sources *(Ibrahim et al., 1981, Ibrahim and Uchupi, 1982; Worzel Watkins, 1973; Ebeniro et al., 1988 and Crust 2.0 database).* Refraction studies for Moho depth are available at km 100 km, 250, km 345, and km 615 with the mantle velocities between 8.0 km/s to 8.3 km/s. For the areas where refraction studies are limited Crust 2.0 was used to obtain the Moho depth.

Using the constraints explained above, initial Model 1 was constructed. Typical thickness for the continental crust was chosen at the northern section of the profile with the average thickness value of 32+ km (from beginning of the profile to km 120). Oceanic crust with less than 9 km thickness was chosen at the southern end of the (starting from km 520). Partially thinned and minimally intruded crust observed between km 120 to km 270 with the thickness value between 25 km to 32 km. An rms value of 2.34 mGal was obtained for the model shown in Figure 5.1.

As described in the methods section, SDRs can directly be identified by their seismic response (strong reflections). As we lack relatively shallow seismic data, magnetic data are used in order to test for the presence of SDRs. This is because the SDRs are interpreted as basaltic flows and sedimentary material and as such may be strongly magnetized. Since the SDRs are often used as an indication of the ocean-

continent boundary *(White and McKenzie, 1989)* magnetic data might provide additional support for the boundary geometries. SDRs have a distinct signature that can be observed on magnetic data *(Schreckenberger et al., 1997).* SDRs are associated with high amplitude magnetic anomalies over other passive margins around the world (ex; Norwegian margin, *Berndt et al., 2000).*

Magnetic data over Profile 1 show 3 distinctive anomalies (with amplitude values of ~150 nT). The first step of magnetic modeling is to check whether these anomalies can be explained by using uniform susceptibility within each individual layers (magnetic susceptibility values for individual layers were described at the beginning of this chapter) without any intrusion or extrusive SDR bodies. Results of such a magnetic model are shown in Figure 5.1. This model failed to explain the observed magnetic response. A new model was generated in which the anomalies are produced by SDR bodies (km 275, km 425, and km 555). When susceptibility values (0.0045 cgs) are assigned for SDR bodies, a better fit to the observed anomalies is obtained (Figure 5.2). Proposed SDR bodies provided a rough estimate of the extent of the transitional crust (SDRs are often located at the seaward and/or landward end of the ocean-continent transition (*White and Mcknezie, 1989).* When the SDRs are introduced to the model, the calculated gravity responses at corresponding areas have increased due to density variation. Surrounding sedimentary layers have density values of 2.50 g/cc whereas the SDR bodies have values of 2.58 g/cc. Overall rms (gravity error) value of the model was increased by 0.5 mGal. In order to improve the rms value the following steps were taken

(1) SDR shapes were adjusted, (2) the thickness of sedimentary layers between available constraints (for the areas between km 275 and km 550) was increased by .8 km (unconsolidated sedimentary layer thickness increased by .5 km and consolidated sedimentary layer thickened by .3 km). The final model (Figure 5.2) generated with the SDR bodies showed a 2.45 mGal rms value.

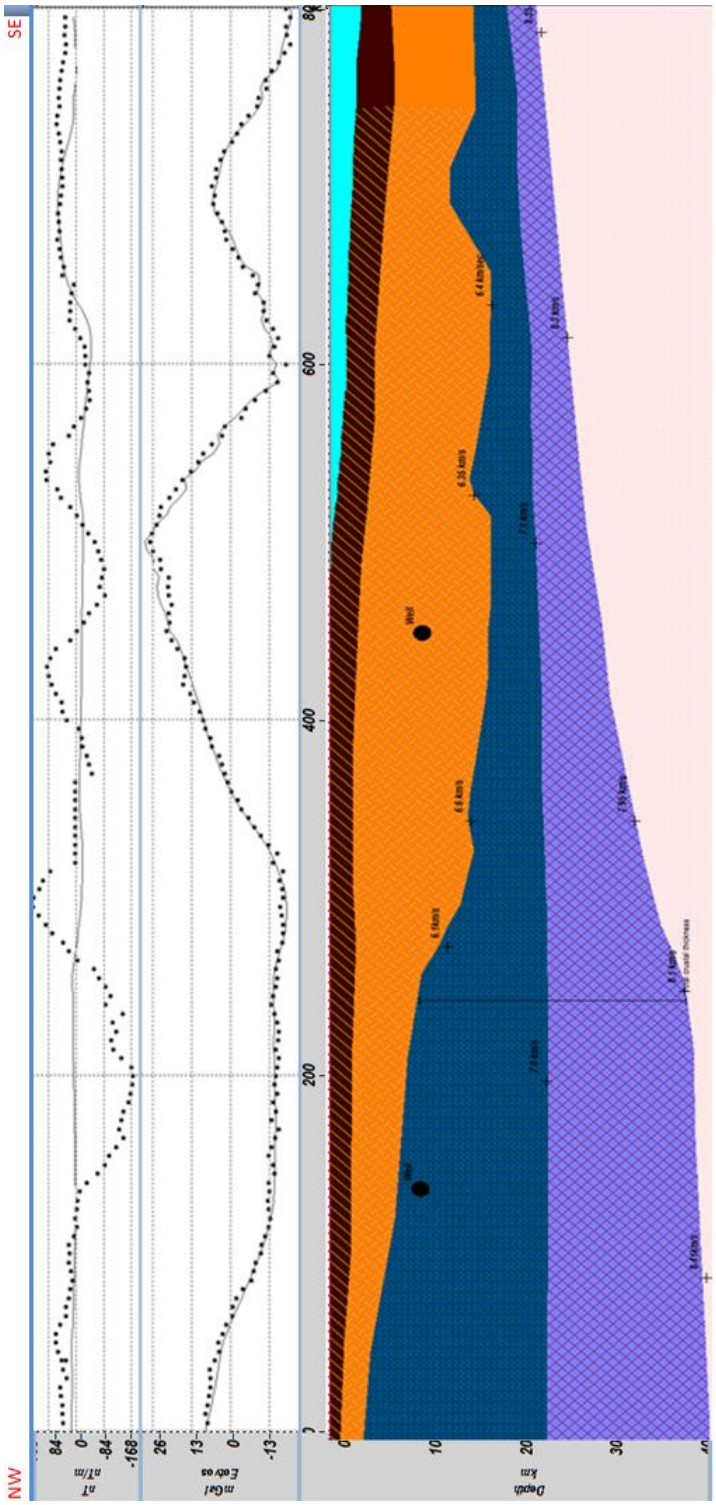

Figure 5.1 Initial model without SDRs for Profile 1 (v.e. 5)

Similar to the other profiles, seismic control for the magmatic underplating is not available. Although the magmatic underplating layer has never been drilled, one of the widely accepted idea is to have the high velocity lower crustal body coincide with the ocean-continent transition. By accepting this assumption a magmatic underplated body is introduced into the model between km 280 and km 515. The geometry of the underplating layer is mainly controlled by looking at the other passive margins around the world as well as the match between the observed and calculated gravity data. Average thickness value of 4 km and 235 km for width is found plausible for the many passive margins *(Wilson, 2002).* The gravity response between km 280 and km 515 is increased by 4 mGal due to density change on the new layer (2.85g/cc to 3.00 g/cc). In order to lower the calculated response of the model, total thickness of the sedimentary layer (average change of .5 km) and Moho depth changed (average change of 1km) between available seismic constraints (between km 280 and km 515).The base of the underplating layer is controlled by available constraints on Moho depth. Since there are no control points available for the top of the magmatic underplating layer, the top part of the layer is shaped to provide improvement in the fit of the calculated gravity response to the observed data. The final model (Figure 5.3) generated with the underplating showed a 2.64 mGal rms value.

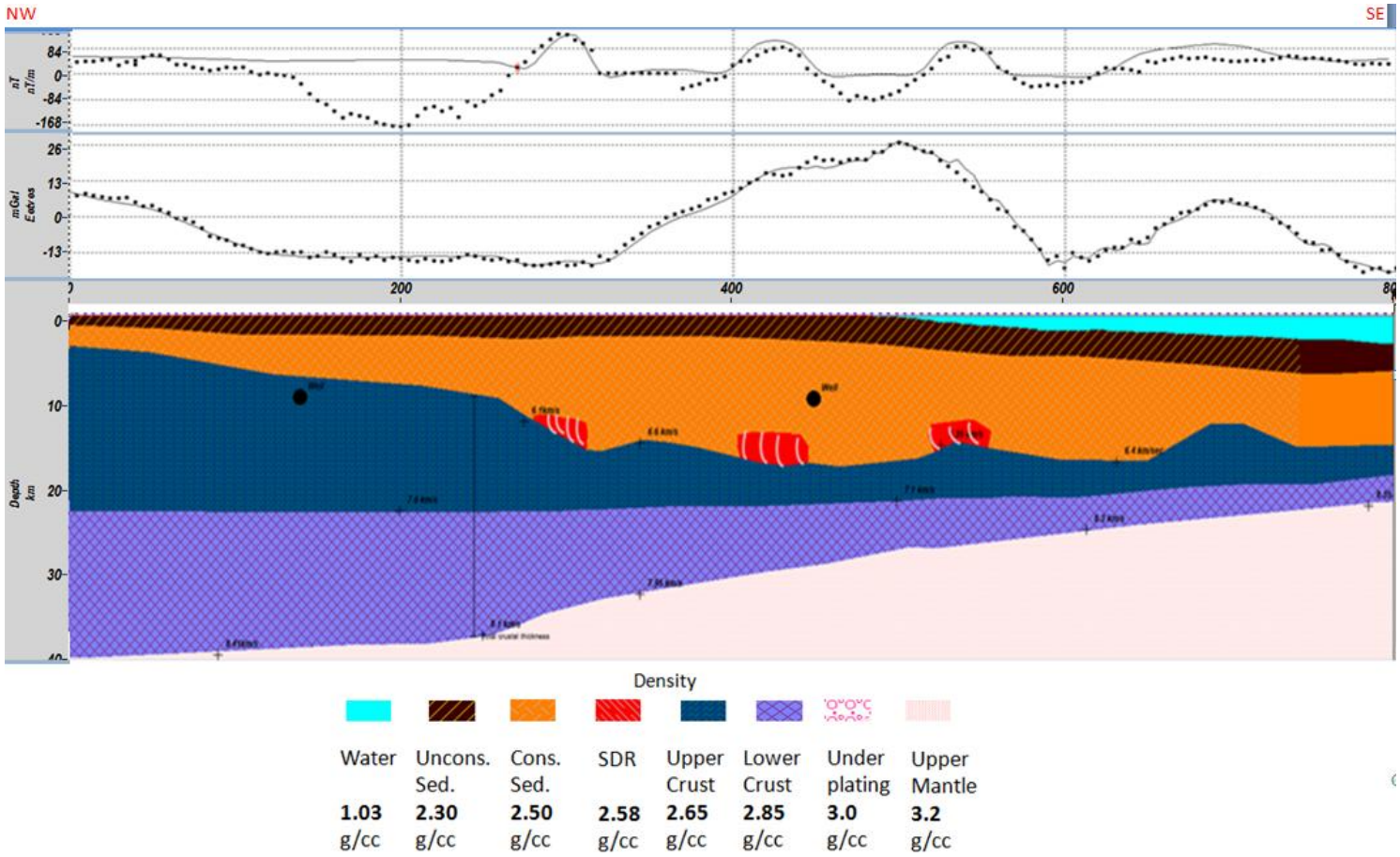

Figure 5.2 Gravity and magnetic response with SDRs for profile 1(v.e. 5)

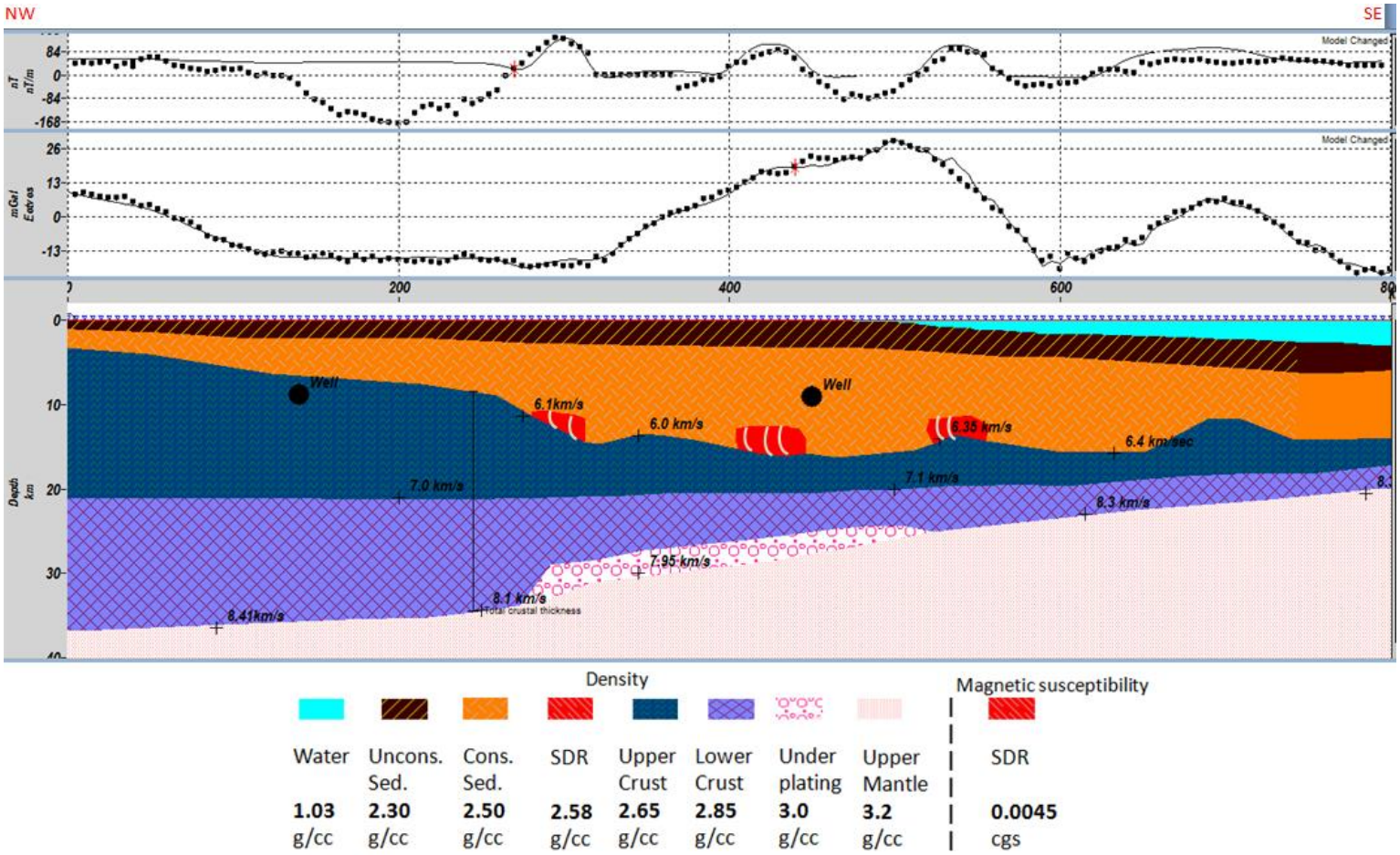

Figure 5.3 Final model for profile 1 (v.e. 5)

5.2.2. Profile 2

Profile 2 is 800 km long and oriented NW-SE, approximately orthogonal to the proposed ocean-continent boundaries proposed by Schouten and Klitgord (1994), Marton and Buffler (1994), Salvador (1991), Buffler and Sawyer (1985), and Hall and Najmuddin (1994). The northern end of Profile 2 starts from Texas (32.0° N, 95.30°W), extends southeastward into the northern Gulf of Mexico, and ends at 26.30°N 91.90°W. The major part of Profile 2 is offshore (285 km with 58 stations are located onshore, 415 km with 84 stations are located offshore). Profile 2 extends approximately 50 km southeastward from the Sigsbee Escarpment.

The overall shape of Model 2 is similar to Model 1. Various seismic constraints are available at several points along Profile 2. For the sediment layers, a global total sediment thickness dataset (NGDC) is used together with available seismic data *(Emery and Uchubi, 1984; Ebeniro et al., 1988; Sawyer et al., 1991; Ibrahim and Uchubi, 1982).* The boundary between the consolidated-unconsolidated sediments is obtained from previously published models *(Diegel et al., 1995),* and digital sediment thickness 1°x1°(*Laske and Masters, 1997)* dataset. As with other profiles, salt bodies are assumed within the sediment layers. As Profile 2 crosses over the Sigsbee Escarpment at km 750 there is a sudden reduction in the amount of salt present and consequently the properties of sediment layers have been changed.

Water depths values are obtained directly from ship track, bathymetry data (NGDC). There are no direct seismic refraction data available for the boundary between upper and lower crustal layers within Profile 2. As Profile 2 is located 70 km east of Profile 1 and 70 km west of Profile 3, an assumption was made to keep the boundaries between crustal layers similar to Profiles 1 and 3. Previously published seismic studies showed an approximate P wave velocity of 6.5 km/s for the upper crustal layer. Total crustal thickness information was obtained from TTS analyses (Dunbar and Sawyer, 1987). Various seismic control points for Moho depth are available with approximate P wave velocity of 8.0 km/s *(Sawyer et al., 1991; Hales et al., 1970; Kruger and Keller, 1983)*. For the areas where seismic control points are not available Crust 2.0 was used to obtain the Moho depth.

Typical thickness for the continental crust was chosen at the northern section of Profile 2 (i.e., $\geq$ 32 km) from beginning of the profile to km 100. Between km 100 and km 260 the crustal thickness varies between 32 km to 25 km. Typical thickness for oceanic crust observed at the southern end of Profile with thickness ≤ 9km extending from km 530 to the end of the line. Transition zone is chosen for the area between km 260 and km 530 with the crustal thickness range of 9 km to 25 km. There is a significant change in gravity response (approximately +20mGal) starting from km 650, variation on the gravity response at the southern end of the profile coincides with the Keathley Canyon concession area. The gravity anomaly over the Keathley Canyon concession area has

been interpreted to be due to a hot spot *(Bird et al., 2005).* An rms value of 2.04 mGal was obtained for the initial model shown in Figure 5.4.

Although there are no digitized magnetic data captured for Model 2, previously published magnetic maps are used to correlate features between profiles (shown in next section).

With the assumption of having underplated layer within the transition zone, *(Kelemen and Holbrook, 1995; Menzies et al., 2002)* magmatic underplating was introduced to the model between km 290 and km 520. The geometry of such a feature was kept similar to that used in Model 1 as we lack any direct control over it. The gravity response between km 290 and km 520 is increased by 4.3 mGal due to density change on the new layer (2.85 g/cc to 3.00 g/cc). In order to lower the calculated response of the model, total thickness of sedimentary layer was thickened by .7 km (between km 290 and km 520), Moho depth increased by .65 km (between km 290 and km 520) by keeping the available seismic constraints. The base of the underplating layer is controlled by available constraints on Moho depth. Since there are no control points available for the top of the magmatic underplating layer, the top part of the layer is shaped to provide improvement on the observed and calculated gravity response. The Final model (Figure 5.5) generated with the underplating showed a 2.53 mGal rms value.

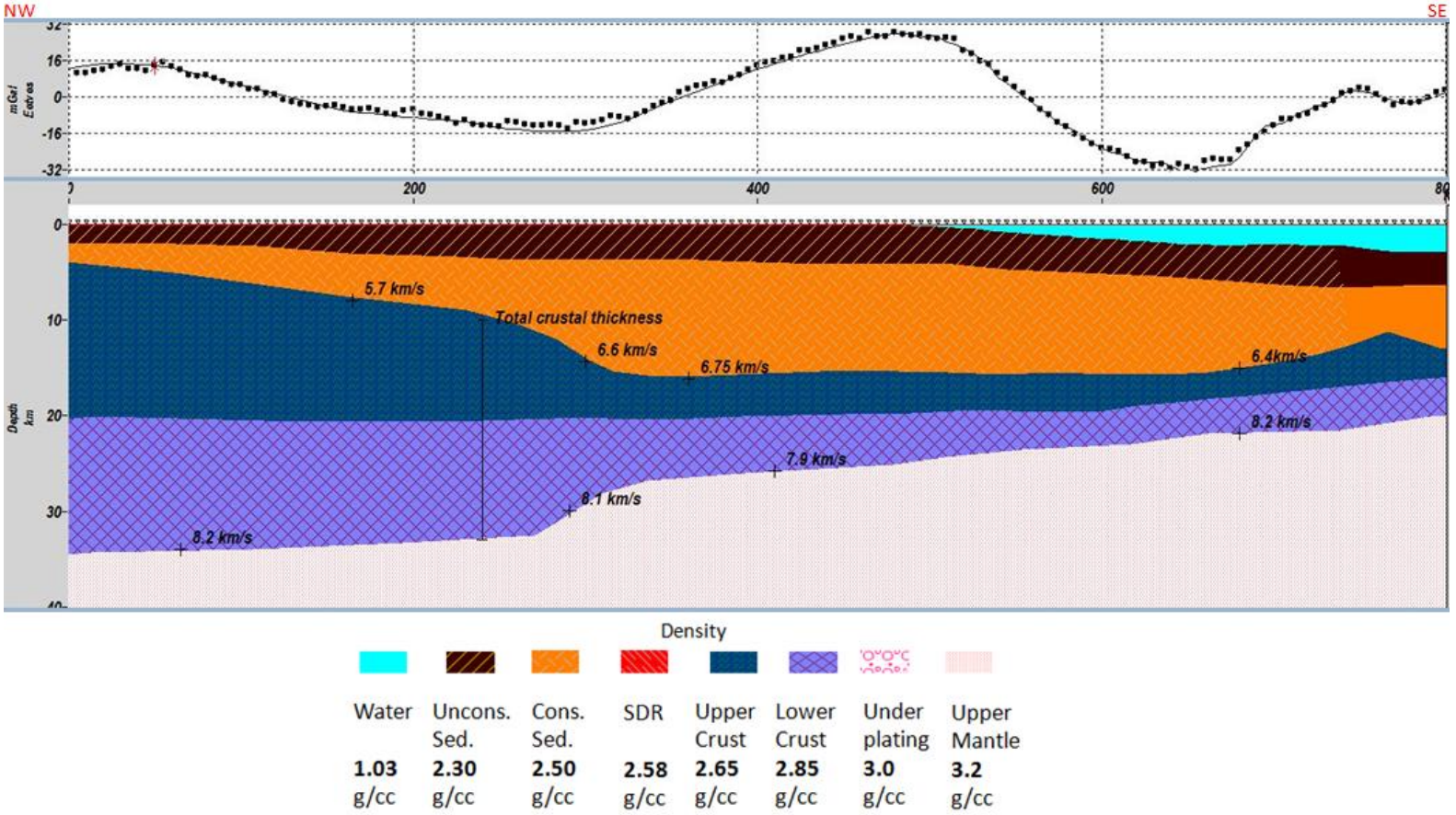

Figure 5.4 Initial model (without underplating) for profile 2 (v.e. 5)

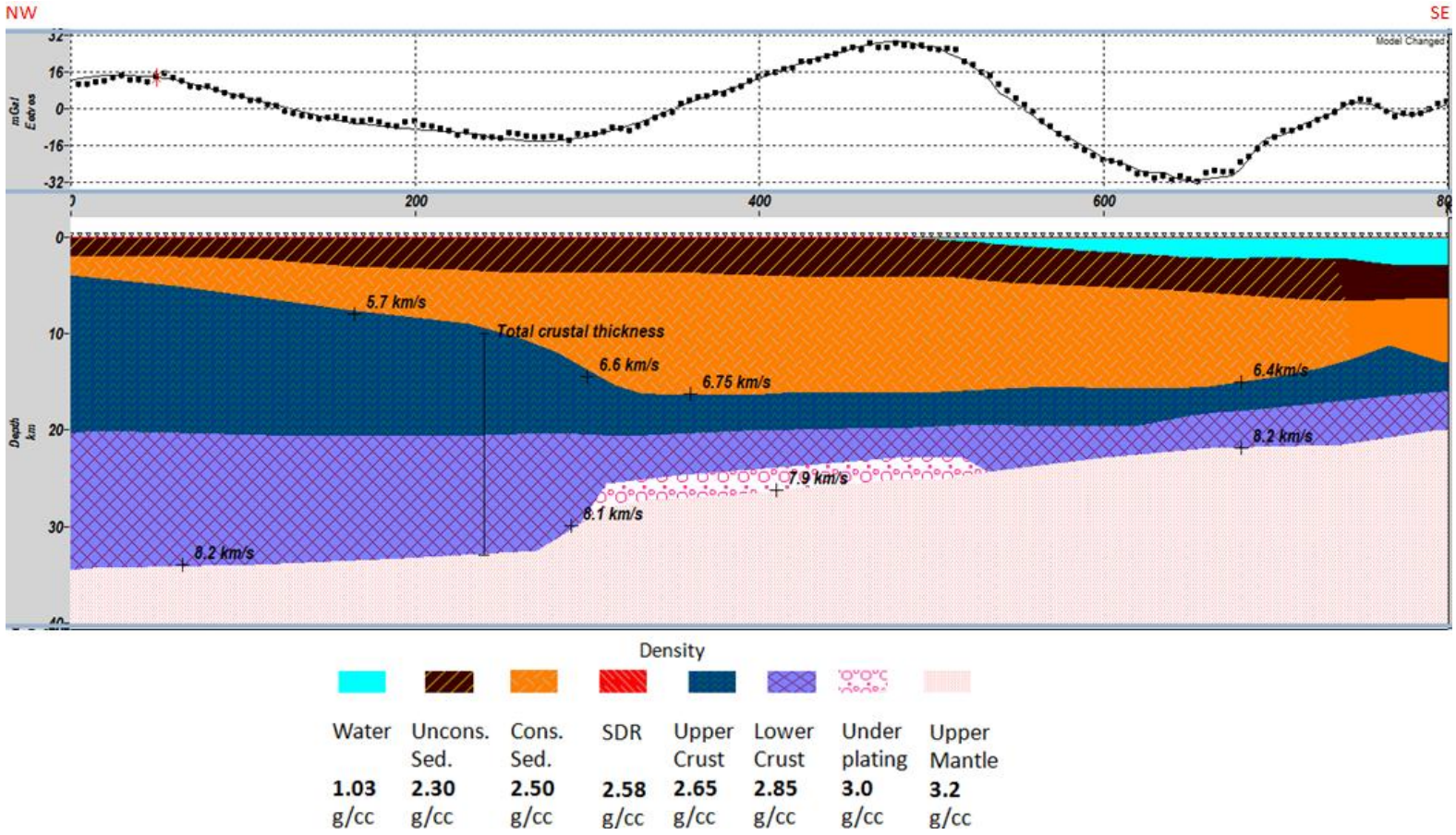

Figure 5.5 Final model for profile 2 (v.e. 5)

5.2.3. Profile 3

The length of this profile is 800km. The northern end of the profile begins at Texas Louisiana border (32.0 °N 94.35° W) and extends southeastward into the Northern Gulf of Mexico (25.5° N 91.8° W). Only 270 km of Profile 3 (55 stations with 5km spacing) is located on shore and the remaining 530 km (107 stations with 5 km spacing) is over the offshore. Profile 3 crosses the Sigsbee Escarpment at 25.85° N 92.0° W and extends southeastward for additional 45 km.

Seismic constraints are available at several points along Profile 3. Sediment boundaries are well constrained by previous studies and maps *(Galloway, 2011)* as well as seismic reflection/refraction studies (*Ibrahim and Uchupi, 1982; Emery and Uchupi, 1984; Dunbar and Sawyer, 1987)*. For the areas where direct seismic data are not available, total sediment thickness dataset (NGDC) and Sediment thickness 1°x1° (*Laske and Masters, 1997)* are used. Similar to other models, salt bodies are assumed within the sediment layers. The boundary between the consolidated-unconsolidated sediments is obtained from previously published models *(Galloway, 2011; Diegel et al., 1995)* and digital sediment thickness 1°x1° (*Laske and Masters, 1997)* dataset. As Profile 3 crosses over the Sigsbee Escarpment at km 760 there is a sudden reduction in the amount of salt present and consequently the properties of sediment layers have been changed.

Water depth values are directly obtained by bathymetry data from ship trackline, as the profile crosses the Sigsbee Escarpment a sudden increase in water depth is observed (approximately 1km increase in depth over a 20 km distance).

The boundary between crustal layers and Moho depth values are extracted from available refraction studies *(Ibrahim and Uchupi, 1982; Emery and Uchupi, 1984; Dunbar and Sawyer, 1987).* An average P-wave velocity value of 6 km/s for the upper crustal layer, 7.2 km/s for lower crustal layer and 8.0 km/s for upper mantle were observed on the seismic constraints. For the areas where refraction constraints are limited Crust 2.0 was used to obtain the depth and thickness values. Due to the limited coverage of the upper-lower crustal boundary, the thickness of the crustal layers is mainly controlled by the effort of keeping their thickness ratio constant or close to (1:1).

Normal crustal thickness for the continental crust (i.e., $\geq$ 32 km) was chosen at the northern section of the Profile starting from the northern end of the profile to the km 160. The area between km 160 to km 245 has the crustal thicknesses between 25 km to 32 km. These values are smaller than those for typical continental crust but thicker than for transition zone. Typical oceanic crust with a thickness ≤ 9km extends from km 530 to the end of the line. As a result, the transition zone assigned for the area between km 245 and km 530 (295 km in width). It was also observed that the overall width of the transition zone is slightly longer than the other profiles. An rms value of 2.3 mGal was obtained for the model shown in Figure 5.6.

Magnetic data were available for Profile 3. It has been shown from many authors that heavily intruded transitional crust ''covered with flood-basalts and tuffs'' (SDRs) can generate positive distinct anomalies which can be tracked on magnetic data *(Geoffroy, 2005*). As I lack seismic control over SDRs, magnetic data are used to test for the presence of SDRs.

Although no magnetic data were captured between km 290 and km 360, previously published airborne magnetic maps were investigated for any anomalous response within 70 km area. No anomalous response was detected and magnetic readings were assigned a value of 0 nT. Three distinctive anomalies are observed on the magnetic data with roughly 150 nT total variation near km 250, km 410, and km 530. An initial model was generated with the assumption of using uniform susceptibility within each individual layers (magnetic susceptibility values for individual layers were described at the beginning of this chapter) (Figure 5.6). This model failed to explain the variation in the magnetic response. A new model was generated in which the anomalies are produced by SDR bodies (inner SDR at km 250, outer SDR at km 530). When susceptibility values (0.0045 cgs) are assigned for SDR bodies, a better fit over the anomalous area is obtained. As it can be observed from Model 3, SDRs are often located at the seaward and/or landward end of the ocean-continent transition *(White and McKenzie, 1989).* When the SDRs are introduced to the model, the overall error value for gravity response is increased by .45 mGal due to density variation (Surrounding sedimentary layers with 2.50 g/cc density values whereas the SDR bodies with 2.58

g/cc). In order to fit the data, the thickness of sedimentary layers as well as the Moho depth between available constraints (for the areas between km 250 and km 530) was increased by approximately 1 km and the boundary between upper and lower crustal layers were lowered by 0.5km between km 250 and km 530. The final model (Figure 5.2) generated with the SDR bodies showed a 2.5 mGal rms value.

With the assumption of having underplated layer within the transition zone, *(Kelemen and Holbrook, 1995; Menzies et al., 2002)* a magmatic underplating was introduced to the model (between km 280 and 515) The gravity response between km 280 and km 510 is increased by 4.2 mGal due to density change on the new layer (2.85 g/cc to 3.00 g/cc). In order to lower the calculated response, the model was modified in the following ways (1) sedimentary layers were thickened (0.5 km) by keeping the available seismic constraints (2) mid crustal boundary was lowered (0.5 km), and (3) Moho depths were deepened (0.5 km) between constraints (between km 280 and km 510). There are no control points available for the top of the magmatic underplating layer, the top part of the layer is shaped to provide improvement on the observed and calculated gravity response. Final model (Figure 5.8) generated with the underplating showed a 2.92 mGal rms value.

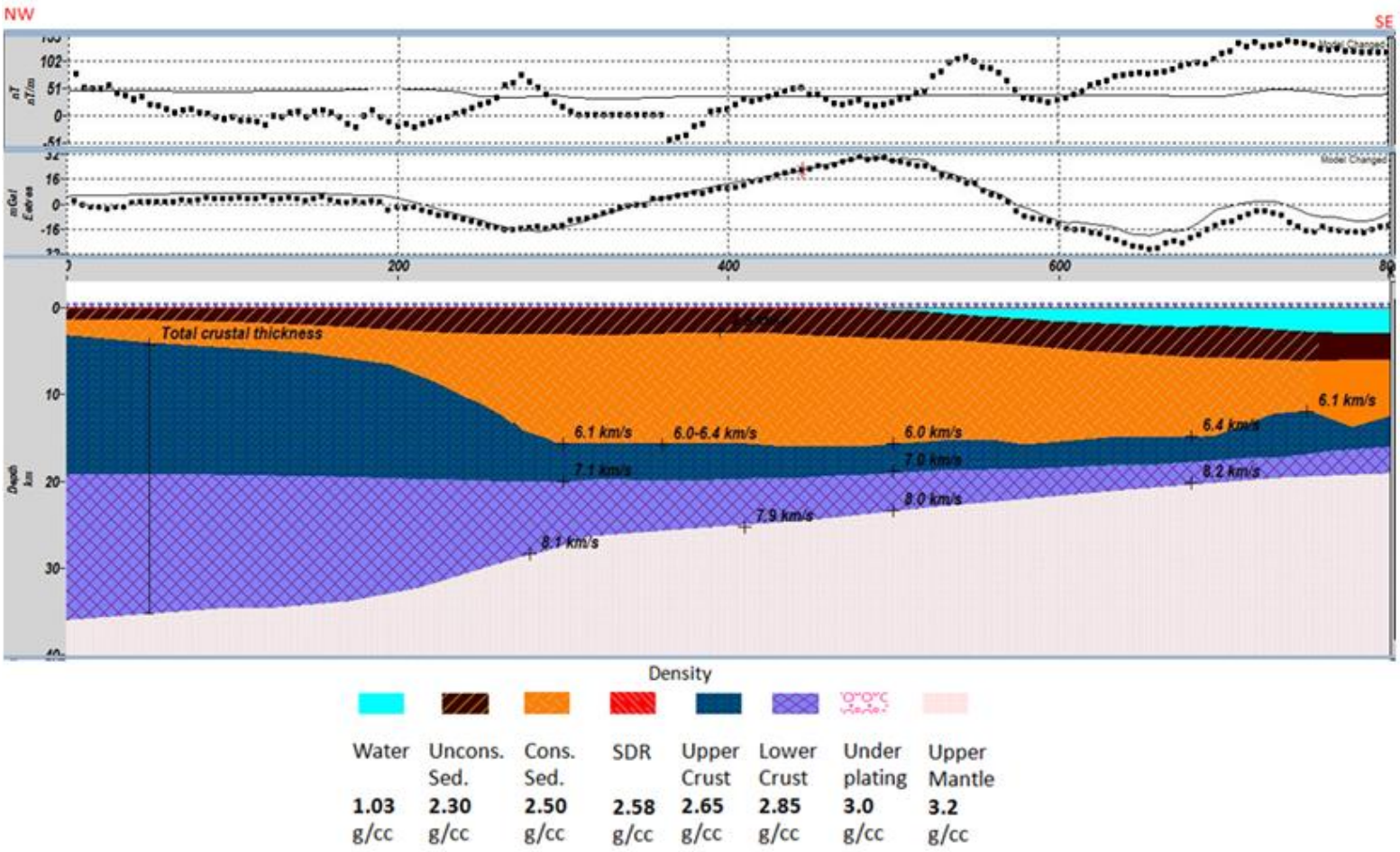

Figure 5.6 Initial model (without SDRs) for profile 3 (v.e. 5)

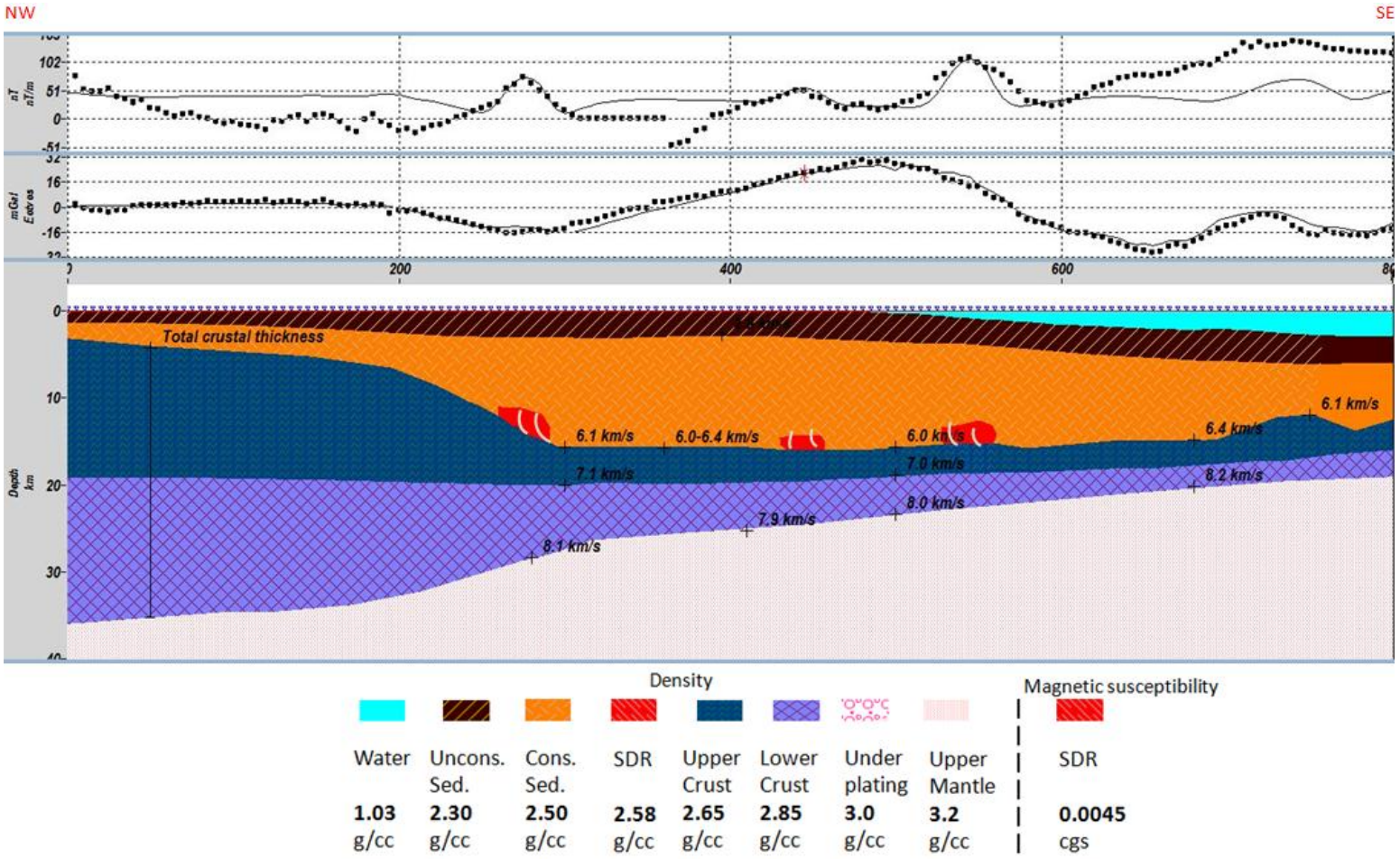

Figure 5.7 Initial model (with SDRs) for profile 3 (v.e. 5)

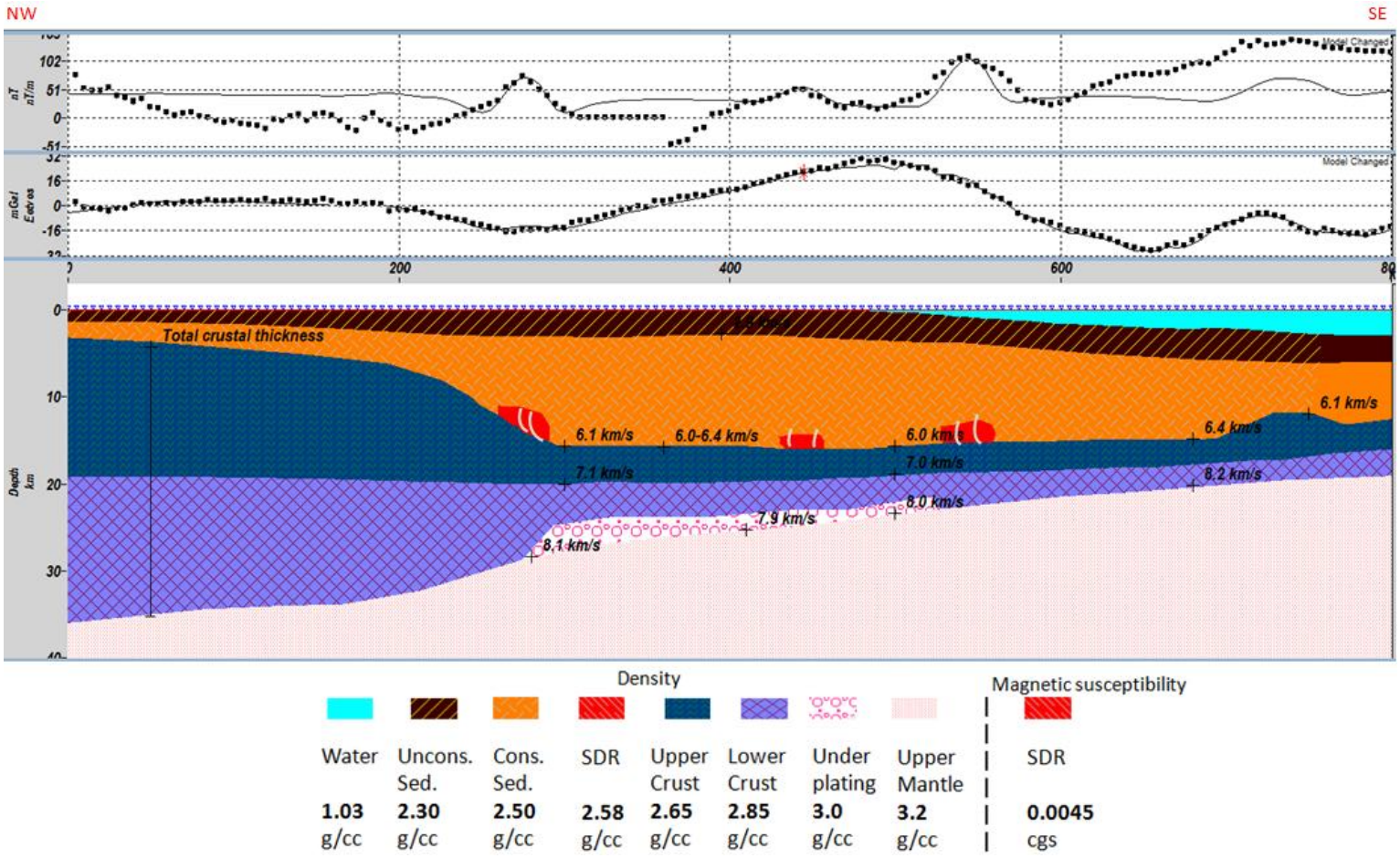

Figure 5.8 Final model for profile 3 (v.e. 5)

5.2.4. Profile 4

Profile 4 is 800 km long and oriented NW-SE. The northern end of the profile starts from on shore Louisiana (32.0° N, 93.3° W) extends south eastward into the northern Gulf of Mexico and ends at 25.5° N 90.0 °W. Profile 4 crosses the Sigsbee Escarpment and continues southeastward for 100 km. 300 km (61 stations with 5 km spacing) of the Profile 4 are located onshore and remaining 500 km (101 stations with 5 km spacing) are located offshore.

There are few seismic control points available for this profile. For the sediment layers, the constructed model mostly depends on the Total sediment thickness data (NGDC), previously published maps *(Galloway, 2011; Marton and Buffler, 1994; Harry et al., 2004)* and few available seismic control points. The boundary between the consolidated-unconsolidated sediments is obtained from digital sediment thickness 1°x1° (*Laske and Masters, 1997)* dataset.

Water depth values are extracted from ship track, bathymetric data (NGDC). Moho depth values are extracted from available sources (*Ibrahim et al., 1981; Hooton, 1992; Marton and Buffler, 1994).* For the area where refraction studies are limited Crust 2.0 was used to obtain the Moho depth.

Although there are no digitized magnetic data captured for Model 4, previously published magnetic maps are used to correlate between profiles.

As I have very limited seismic control points for this Profile, overall properties of the model were kept similar to the closest well constrained model (Model 3). Typical thickness for continental crust (i.e., $\geq$ 32 km) was chosen at the northern section of the Profile from the beginning of the Profile to the km 150. Between km 150 and km 270 the crust has a thickness between 32 km and 25 km. Typical oceanic crust with a thickness ≤9km was observed at the southern end of the Profile extending from km 540 to the end of the Profile. A transitional crust observed between km 270 and km 540. Crustal thickness within the transition zone varies between 25 km and 9km. An Initial model was generated with 2.3 mGal rms value (Figure 5.9).

Seismic data to determine the presence of magmatic underplating are not available for any Profiles. With the assumption of having underplated layer within the transition zone, *(Kelemen and Holbrook, 1995; Menzies et al., 2002)* a magmatic underplating introduced to the model (between km 285 and 515). The gravity response between km 285 and km 515 is increased by 4 mGal due to density change on the new layer (2.85g/cc to 3.00 g/cc). In order to lower the calculated response, the model was modified in the following ways: (1) total thickness of sedimentary layers thickened (≤ 1km), (2) Moho depths were deepened (by 0.7 km) between seismic constraints (for the area between km 285 and km 515). There are no control points available for the top of the magmatic underplating layer, the top part of the layer is shaped to provide improvement on the observed and calculated gravity response. The final model (Figure 5.10) generated with the underplating showed a 2.75 mGal rms value.

Although there is no direct seismic control, by keeping the physical properties of a feature similar to other examples around the world, magmatic underplating has been added to Model 4 (total width of 230 km and 4 km average thickness).

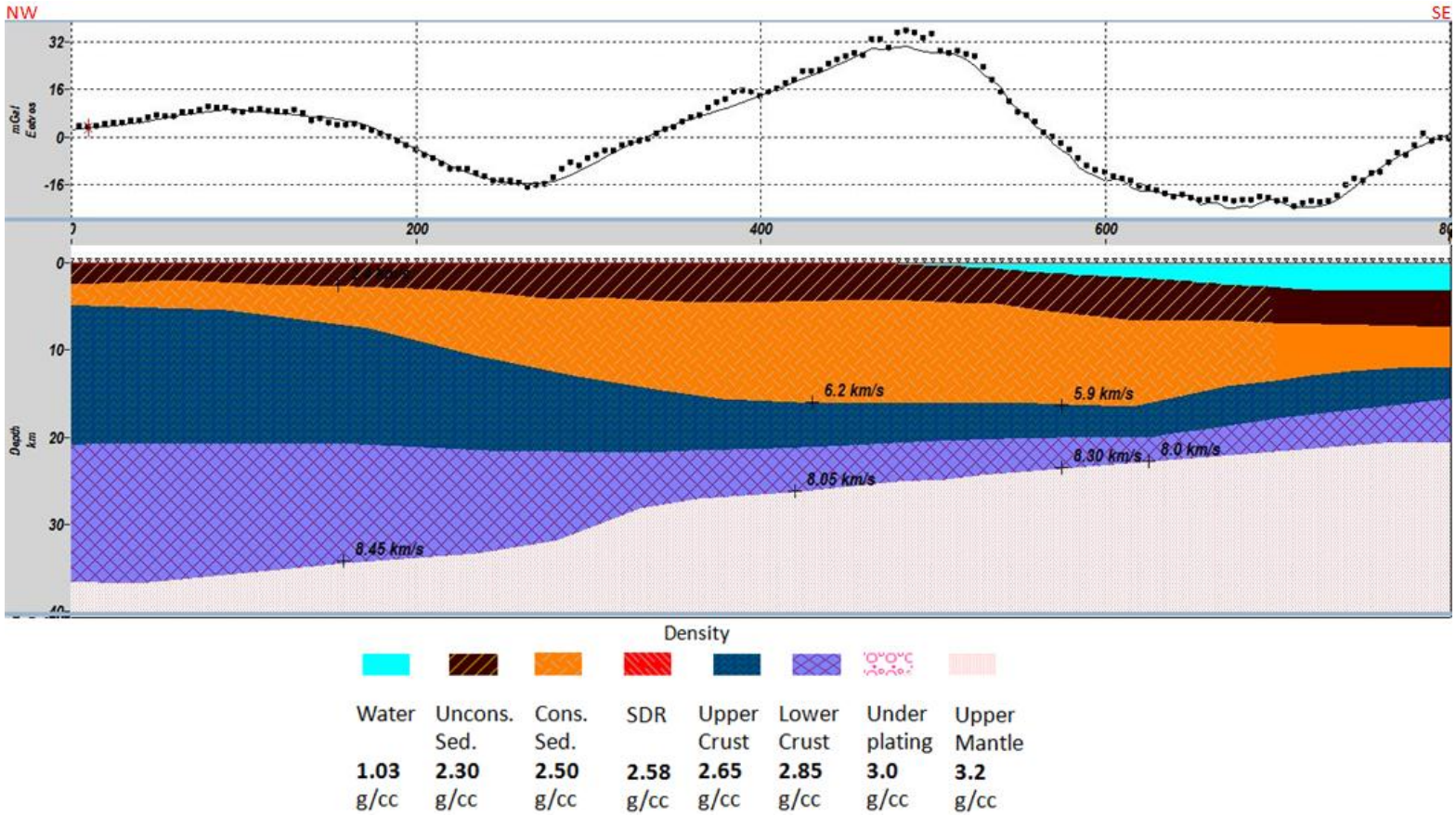

Figure 5.9 Initial model (without magmatic underplating) for profile 4 (v.e. 5)

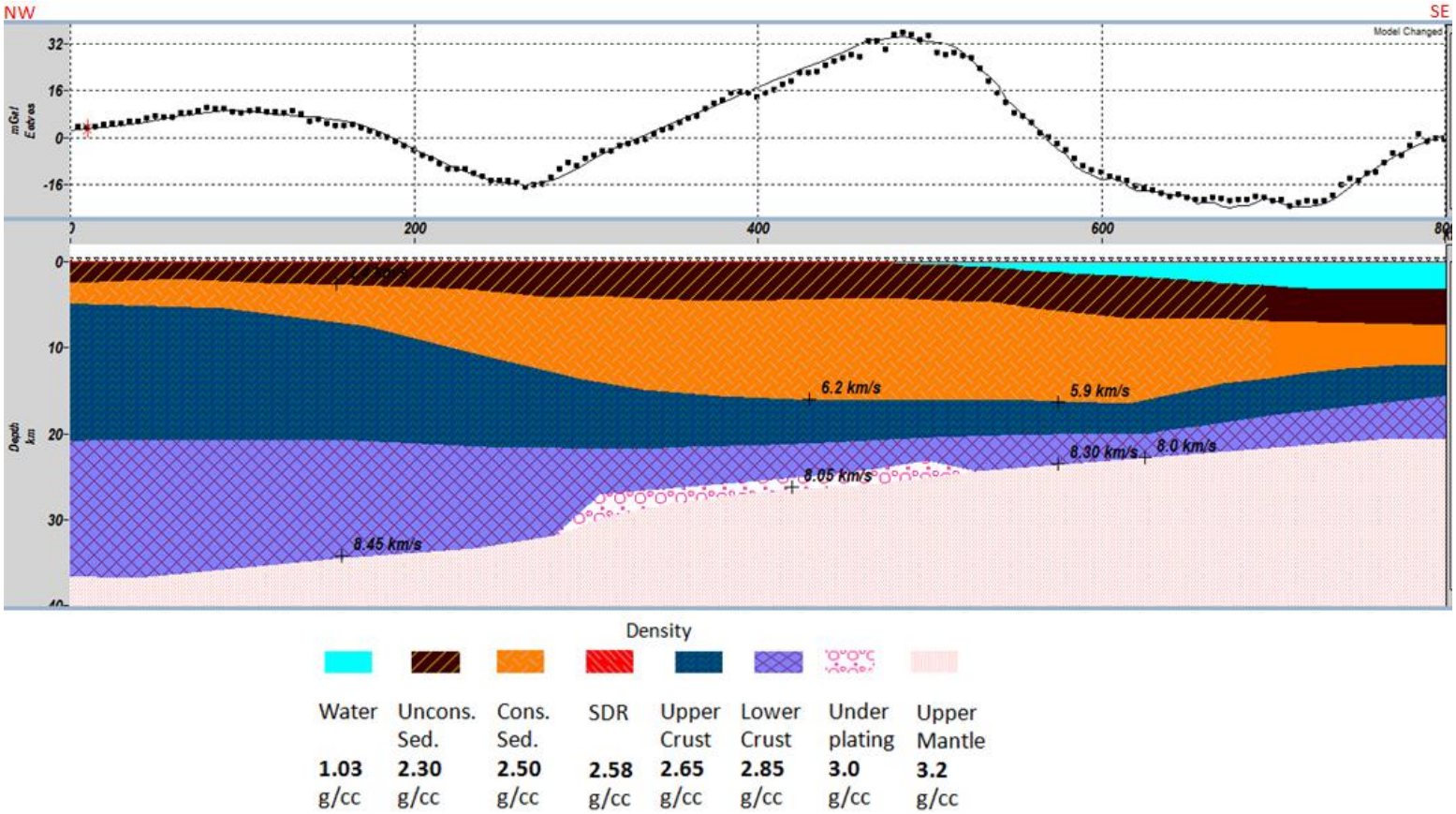

Figure 5.10 Final model for profile 4 (v.e. 5)

5.2.5. Profile 5

The easternmost profile is also 800 km long and oriented NE-SW, approximately orthogonal to the proposed ocean-continent boundaries *(Schouten and Klitgord, 1994; Marton and Buffler, 1994; Salvador, 1991; Buffler and Sawyer, 1985)*. The northern end of the profile starts from (32.0° N 92.5° W) onshore Louisiana extends southeastward into the northern Gulf of Mexico (25.5° N 89.15° W). Almost 350 km (71 stations with 5km spacing) of Profile 5 are located on shore Louisiana and 450 km of the remaining parts are offshore (91 stations with 5 km spacing). Profile 5 crosses the Sigsbee Escarpment at 27.30°N 90.0° W and extends for 200 km to the southeast.

Similar to Profile 4, Profile 5 has limited seismic control. For the sedimentary layers, the constructed model mostly depends on the total sediment thickness data (NGDC), previously published maps *(Galloway, 2011; Marton, 1995; Harry et al., 2004),* digital sediment thickness 1°x1° dataset *(Laske and Masters, 1997),* and a few seismic control points (*Emery and Uchupi, 1984; Dunbar and Sawyer, 1987; Marton, 1995).*

Water depth values are obtained directly from bathymetry data from ship tracklines (NGDC).

Crustal boundaries and Moho depth values are extracted from available seismic studies and previous published crustal models *(Ibrahim et al., 1981; Ebeniro et al., 1988; Buffler et al., 1981; Marton, 1995)*

Model 5 was constructed using the constraints described above. Similar to Profile 4, typical continental crust thicknesses were observed at the northern section of the Profile 5 (i.e., $\geq$ 32 km) from the beginning of the profile to km 150. Typical thickness for oceanic crust (≤ 9km) was observed at the southern end of the line extending from km 550 to the end of the Profile. A transition zone observed between km 260 and km 550 with thicknesses between 25 km to 9 km. The thickness of the crust between km 150 and km 260 varies from 32 km to 25 km. An initial model provided 2.2 mGal rms value (Figure 5.11).

Although there are no digitized magnetic data captured for the model 5, previously published magnetic maps are used to correlate features between profiles.

With the assumption of having underplated layer within the transition zone, *(Kelemen and Holbrook, 1995; Menzies et al., 2002)* magmatic underplating was introduced to the model (between km 280 and km 510). The gravity response between km 280 and km 510 is increased by 4.5 mGal due to density change on the new layer (2.85g/cc to 3.00 g/cc). In order to lower the calculated response, the model was modified in the following ways: (1) sediment layers were thickened, and (2) Moho depths were deepened between constraints (between km 280 and km 510). There are no control points available for the top of the magmatic underplating layer. The top part of the layer is shaped to provide improvement on the observed and calculated gravity response. The final model (Figure 5.12) generated with the underplating showed a 2.39 mGal rms value.

Altough there is no direct seismic control, by keeping the physical properties of such a feature similar to other examples around the world, magmatic underplatying was added to the Model 5 (total width of 230 km and 5 km average thickness).

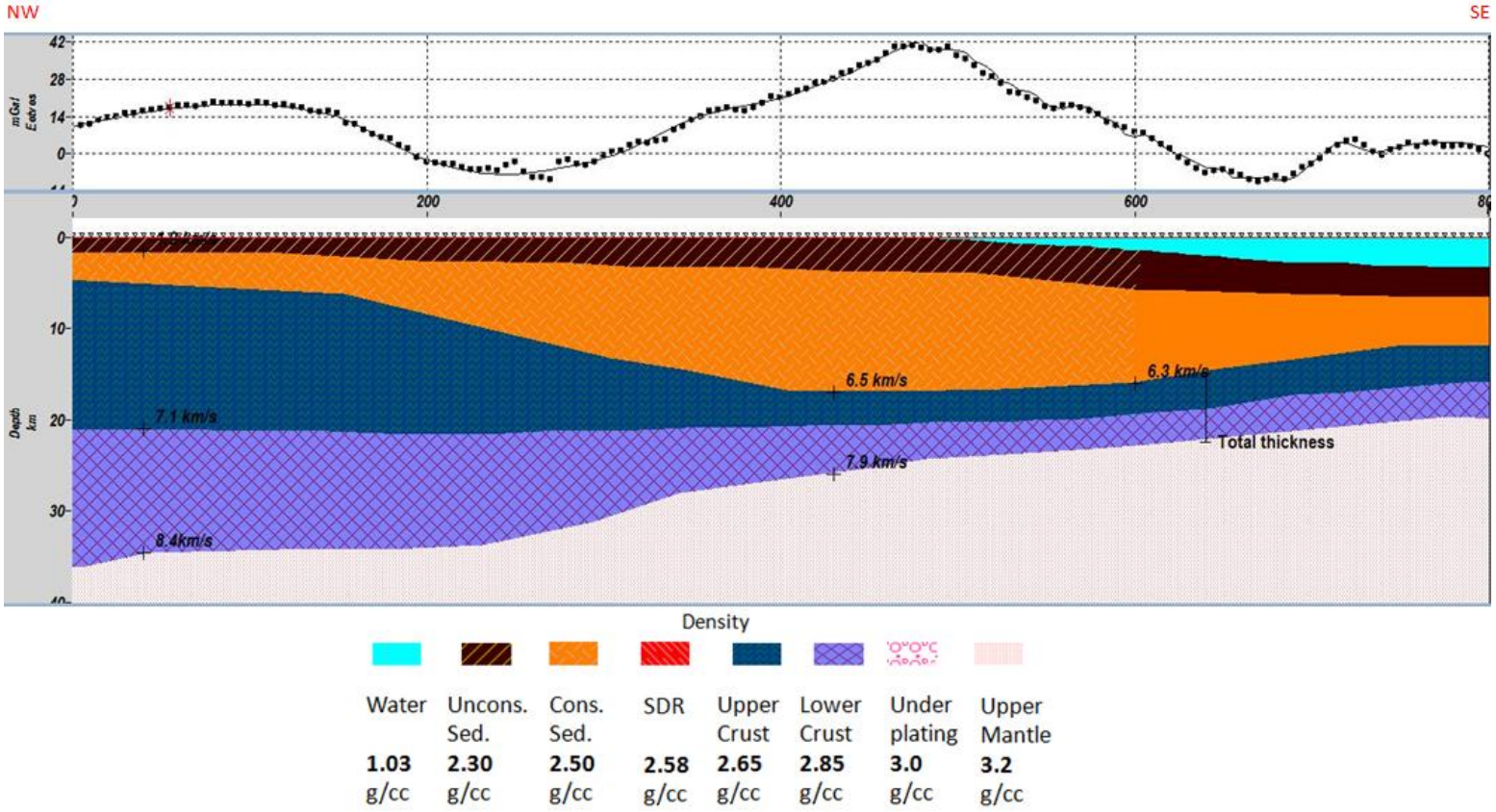

Figure 5.11 Initial model (without magmatic underplating) for profile 5 (v.e. 5)

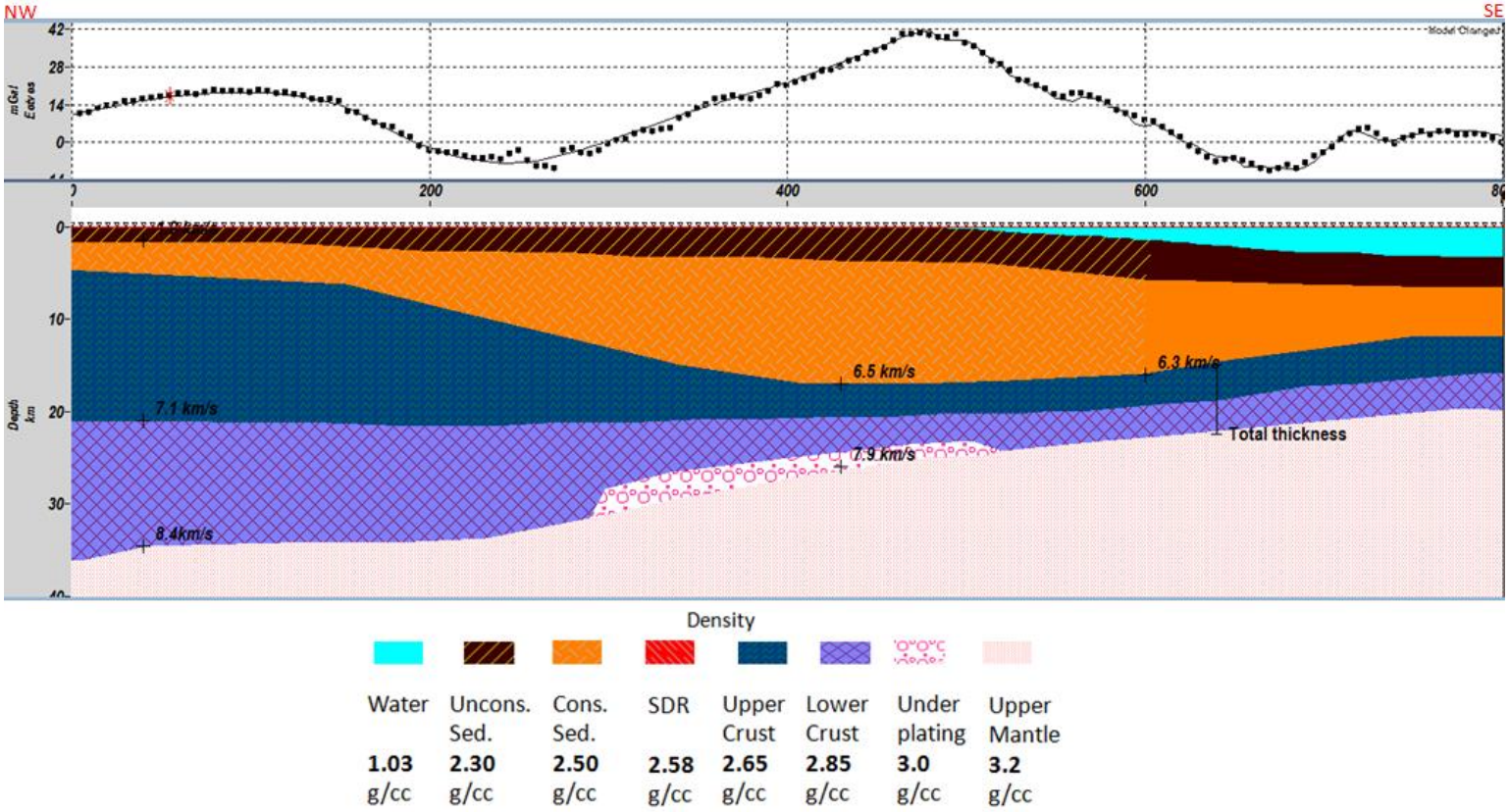

Figure 5.12 Final model for profile 5 (v.e. 5)

5.2.6. Profile 6

Due to limited seismic coverage over Profiles 4 and 5, Profile 6 was generated to provide additional details on the easternmost part of the study area. Profile 6 is 800 km long and oriented N-S. The northern end of the profile starts from onshore Mississippi (32.0 °N 89.9° W), extends south through Louisiana, and ends in the northern Gulf of Mexico at 25.5 °N 89.45°W. Only 300 km (21 gravity stations at 15 km spacing, 61 magnetic stations with 5 km separation) of Profile 6 are located onshore and the remaining 500 km (31 stations for gravity, 101 stations for magnetic) are offshore. Due to limited gravity data coverage over the offshore area, a gravity station spacing of 15 km was used. Profile 6 crosses Sigsbee Escarpment at 27.44°N 89.6° W and extends for 280 km to the south.

Seismic constraints are available at several points along Profile 6. Sediment boundaries are well constrained by previous studies and maps *(Galloway, 2011)* as well as seismic reflection/refraction studies and available well data *(Worzel and Watkins, 1973).* The boundary between the consolidated-unconsolidated sediments is obtained from previously published models *(Galloway, 2011),* and digital sediment thickness 1°x1° (*Laske and Masters, 1997)* dataset. Profile 6 crosses the Sigsbee Escarpment at km 520, beyond which the amount of salt is reduced significantly.

Water depth values are directly obtained from the bathymetry data collected along each ship trackline. The boundaries between crustal layers and Moho depth

values were extracted from available refraction studies (*Worzel and Watkins, 1973; Dunbar and Sawyer, 1987)*. Average P-wave velocities of 8.0-8.1 km/s for the upper mantle and 7.3km/s for lower crustal layer were observed. Due to the limited coverage of the upper-lower crustal boundary, the thickness of the crustal layers is mainly controlled by the effort of keeping their thickness ratio similar. For the areas where refraction studies are limited, Crust 2.0 was used to obtain the Moho depth.

An initial model was constructed using the constraints described above. Normal crustal thickness for the continental crust (i.e., $\geq$ 32 km) was modeled from the northern end of the profile to the km 90. Typical thickness for oceanic crust ($\leq$ 9 km) was used at the southern end of profile extending from km 520 to the end of the line. As a result, transition zone assigned for the area between km 240 and km 520 (280 km in width). Crustal thickness for the area between km 90 and km 240 varies between 32 km to 25 km. This initial model showed 2.2 mGal rms error value (Figure 5.13).

Magnetic data were acquired for Profile 6. Unlike the gravity data, magnetic station interval was kept at 5 km spacing. It has been shown by many authors that heavily intruded transitional crust ‘’covered with flood-basalts and tuffs’’ (SDRs) can generate distinct anomalies which can be tracked on magnetic data *(Geoffroy, 2005).* Three distinctive anomalies with roughly 100 nT to 150 nT total variation are observed on the magnetic data near km 260, km 380, and km 470.

An Initial model was generated with the assumption of uniform susceptibility within each individual layers (magnetic susceptibility values for individual layers were

described at the beginning of this chapter) (Figure 5.13). This model failed to explain the variation on the magnetic response. Another model was generated with the assumption that the anomalies are produced by SDR bodies (Figure 5.14). When the susceptibility values are assigned for SDR bodies (0.0045 cgs), model response was similar to the observed data. When the SDRs are introduced to the model, the calculated gravity response at corresponding areas have increased due to density variation (Surrounding sedimentary layers with 2.50 g/cc density values whereas the SDR bodies with 2.58 g/cc). In order to fit the data, the thickness of sedimentary layers as well as the Moho depth between available constraints (for the areas between km 250 and km 520) were increased by approximately 0.3 km. The final model with the SDR bodies has a 2.49 mGal error value (Figure 5.14).

Seismic data to determine the presence of magmatic underplating are not available along Profile 6 or any of the other modeled profiles. With the assumption of having underplated layer within the transition zone, (*Kelemen and Holbrook, 1995; Menzies et al., 2002)* a magmatic underplating layer was introduced into the model (between km 280 and km 515). The gravity response between km 280 and km 515 is increased by 6.5 mGal due to density change on the new layer (from 2.85g/cc to 3.00 g/cc). In order to lower the calculated response of the model (1) sediment layers were thickened by 0.4 km, (2) the boundary between crustal layers was lowered slightly (0.3 km), and (3) Moho depths were deepened between constraints (between km 280 and km 510). There are no control points available for the top of the magmatic underplating

layer. The top part of the layer is shaped to provide improvement in the fit of the calculated gravity response to the observed data. The final model (Figure 5.15) generated with the underplating showed a 2.68 mGal rms value.

Although there is no direct seismic control, by keeping physical properties of such a feature similar as the other examples around the world, magmatic underplating was added to the Model 6. The underplating had a total width of 235 km and an average thickness of 5 km.

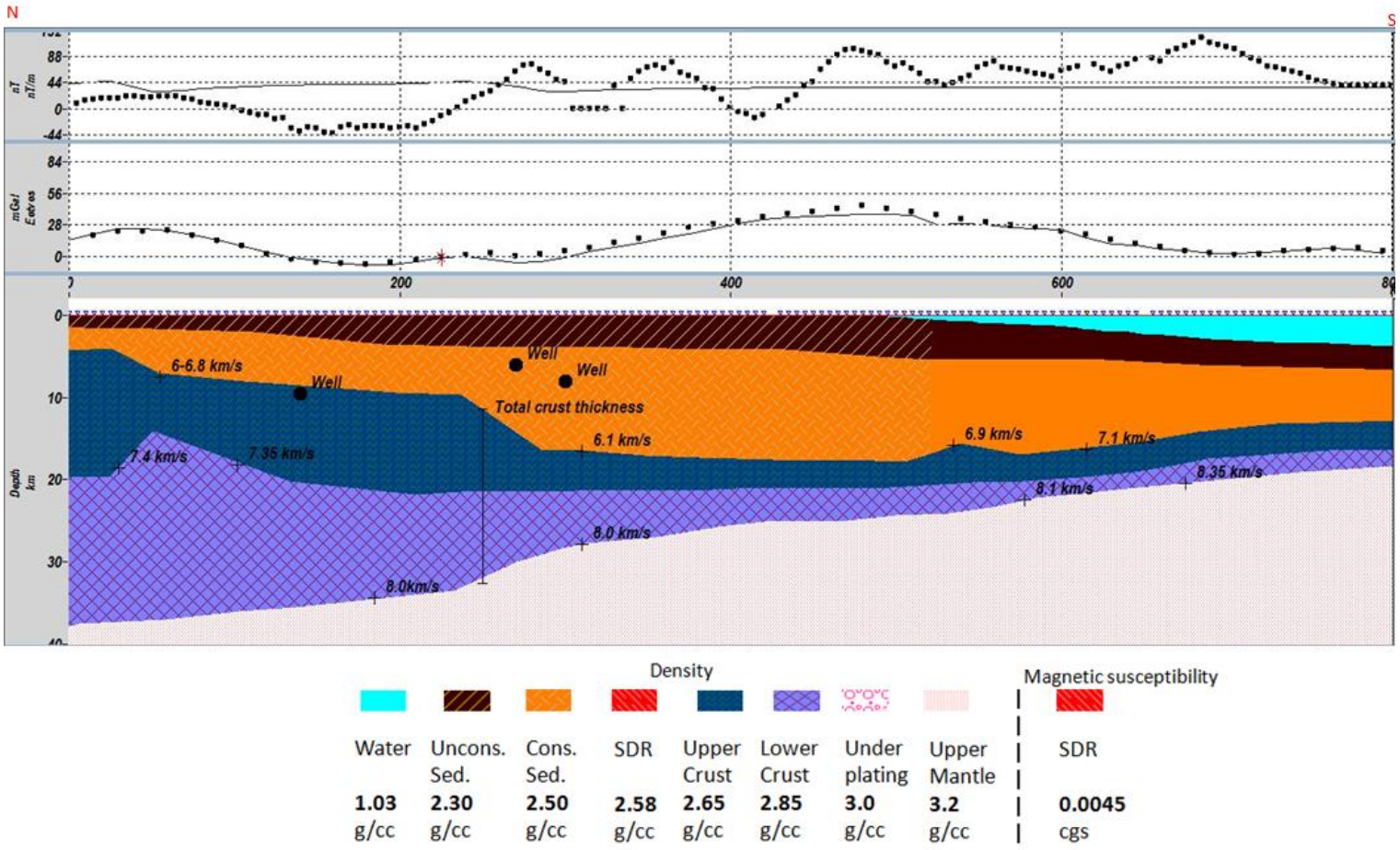

Figure 5.13 Initial model (without SDRs) for profile 6 (v.e. 5)

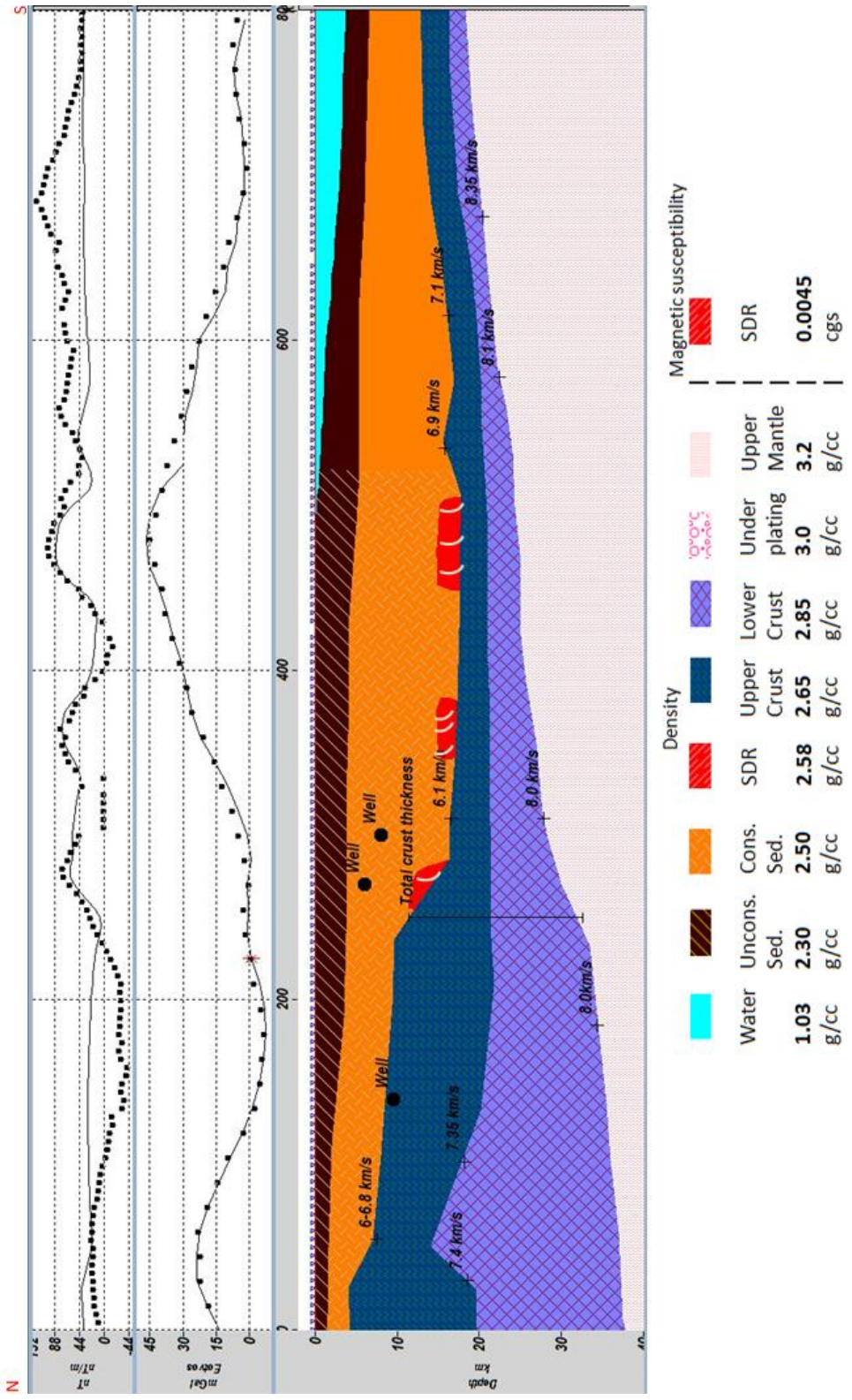

Figure 5.14 Initial model (with SDRs) for profile 6 (v.e. 5)

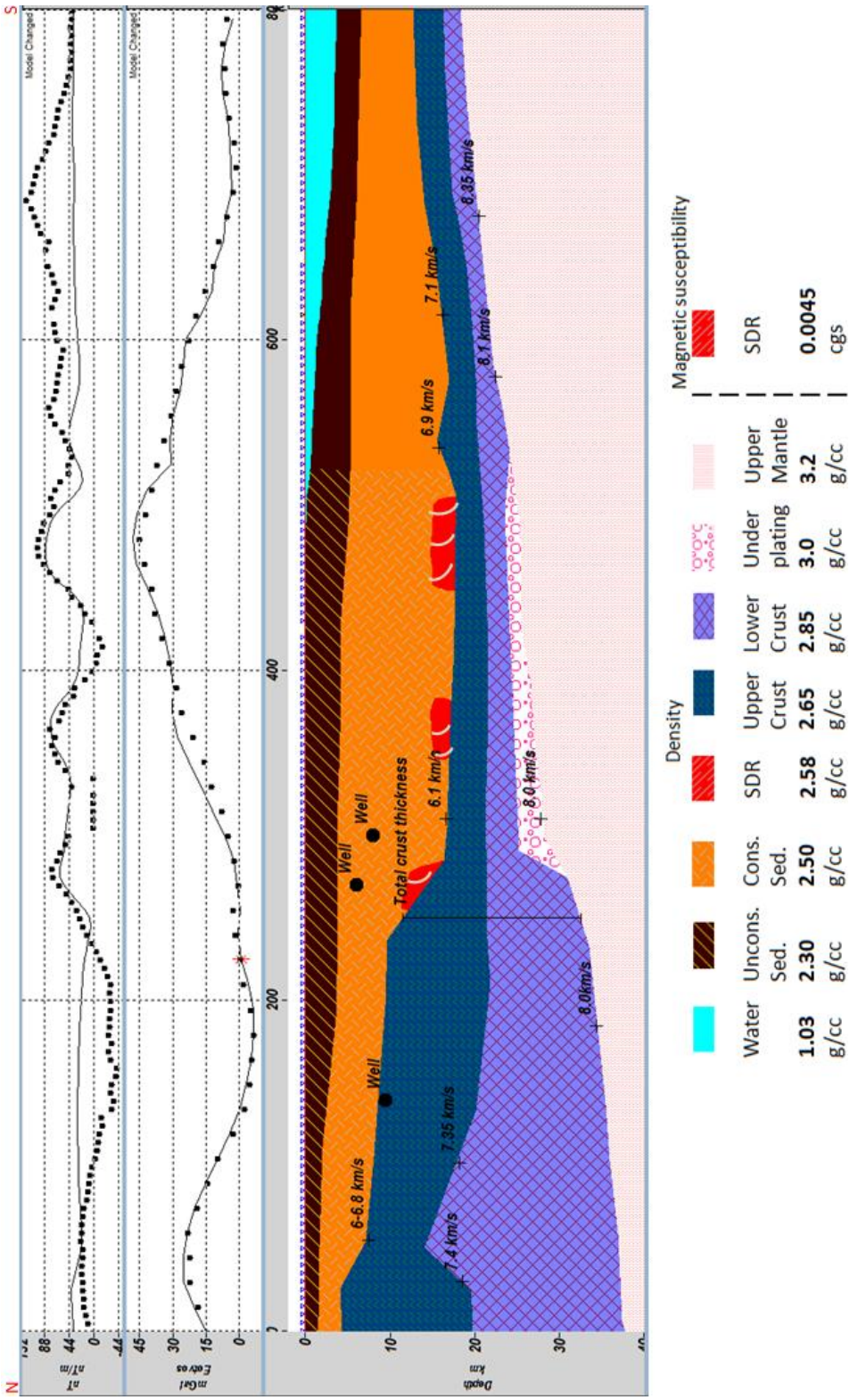

Figure 5.15 Final model for profile 6 (v.e. 5)

CHAPTER 6. ANALYSIS AND INTERPRETATION

I have identified and mapped different crustal types and their physical properties over part of the northern Gulf of Mexico and surrounding areas using 2D forward gravity modeling. I have generated crustal models along 6 profiles which are constrained by gravity and, where available, seismic (both reflection and refraction) and magnetic data.

Figures 5.1 through 5.16 show the derived crustal models. The descriptions for the crustal models were discussed in Chapter 5. I have interpreted the anomalous response of the transitional crust and surrounding area to provide an approach for the overall nature of the margin.

6.1. Magnetic Anomalies

Alternative models were constructed for each profile to test the existence of key geological elements of the margin.

High amplitude, well correlated magnetic anomalies have been proposed as the effects of SDRs on many passive margins around the world. Schreckenberger et al. (1987) explained that the positive magnetic anomalies can be defined as the

superposition of an upper normally polarized series of flood basalts on the Voring margin.

SDRs as a source for higher marine magnetic anomalies are indicated from many studies on volcanic passive margins (e.g. U.S. East coast margin, *Talwani et al., 1995; Talwani and Abreu, 2000;* Norwegian margin, *Schreckenberger et al., 1997*). Generation of SDRs related to subaerial to shallow marine volcanism which ended up as sheet-like body of flood basalt and intercalated sediments *(Schreckenberger et al., 1997).* In case of multiple wedge of SDRs (i.e. Namibian margin), the inner SDRs are assumed to have formed during rifting, whereas the outer SDRs formed in a deep sea environment by marine flood basalts. Some other proposed process for the generation of SDRs include (1) decompression melting controlled by rising plume *(Duncan and Richards, 1991)*, and (2) convective melting due to temperature difference controlled by rifting process *(Mutter et al., 1988).*

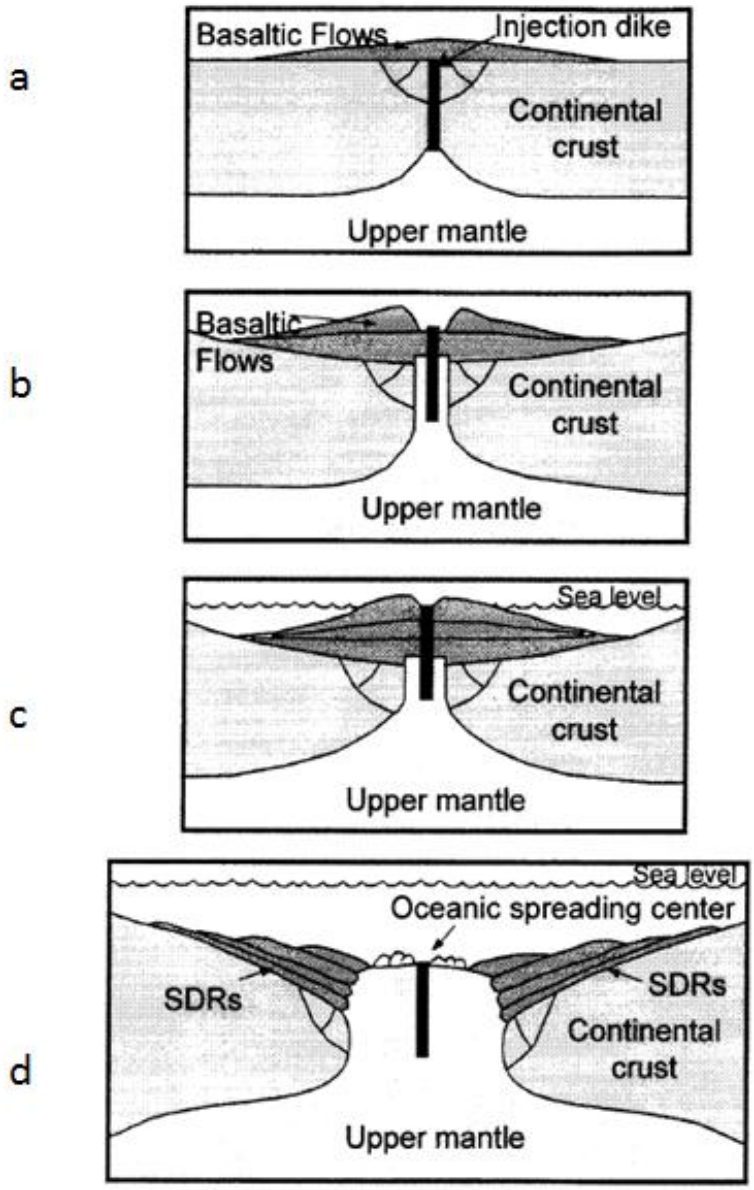

Figure 6.1 Emplacement of SDRs wedges proposed by Hinz (1981) (a) dike injection, (b) lava flows, (c) emplacement of lava flows, (d) cooling and loading with additional flows subside as well as dip in seaward direction

Profiles 1, 3, and 6 are selected for further investigation of SDRs. These profiles show three distinct magnetic anomalies with similar amplitudes (≥100 nT). Distinct magnetic anomalies on passive margins has been imaged and interpreted in various ways. Although Rabinowitz and LaBrecque (1979) interpreted the magnetic anomalies on Namibia margin as an edge effect, there are many studies that show these distinct anomalies are caused by extrusive basalt that can be identified as SDRs *(Gladczenko et al., 1997; Menzies et al., 2002; Talwani and Abreu, 2000).*

Imbert et al., (2001) and Imbert (2005), imaged SDRs in the eastern Gulf of Mexico. This implies that the origin of the margin can be characterized as a volcanic passive margin and some of the high magnetization anomalies might be explained by SDRs.

The distinct anomalies on observed magnetic data could not be explained with the assumption of uniform magnetic susceptibility throughout the models (Figure 5.1, 5.6, 5.13). Talwani et al., (1995) used a range of susceptibility between 0.003 and 0.005cgs for the U.S. East Coast SDRs, an average value of 0.0045 cgs for the magnetic susceptibility of the SDRs was chosen for basic igneous rocks. When this susceptibility value were assigned to proposed magnetic bodies an approximate match between observed and calculated magnetic data was obtained (Figures 5.2, 5.7, 5.14).

One can argue that these bodies could be random intrusions. If the magnetic anomalies are generated by random intrusions, the structures should be considered as

localized features, therefore they should not be correlated between models. Another dataset is introduced to test if the magnetic anomalies can be correlated between models. Aeromagnetic data from Hall and Najmuddin (1994) filled the area between Profile 3 and Profile 6. Figures 6.2 and 6.3 shows that these anomalous structures are not localized on certain profile and they can be tracked between profiles at the northern Gulf of Mexico. The magnetic anomalies on Profiles 3 and 6 were successfully correlated for Profiles 4 and 5 (Figures 6.2 and 6.3).

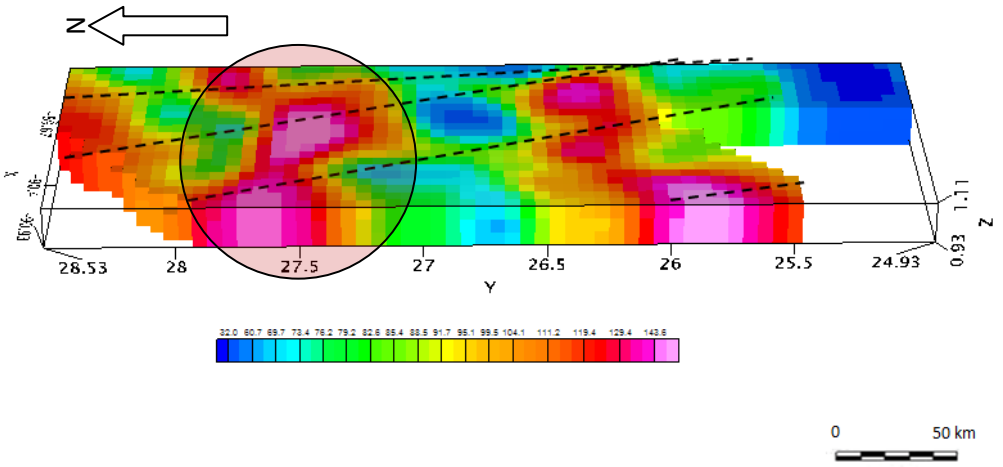

Figure 6.2 Gridded (3D) view of aeromagnetic data from Hall and Najmuddin 1994, anomalies in circled area proposed as the effects of SDRs.

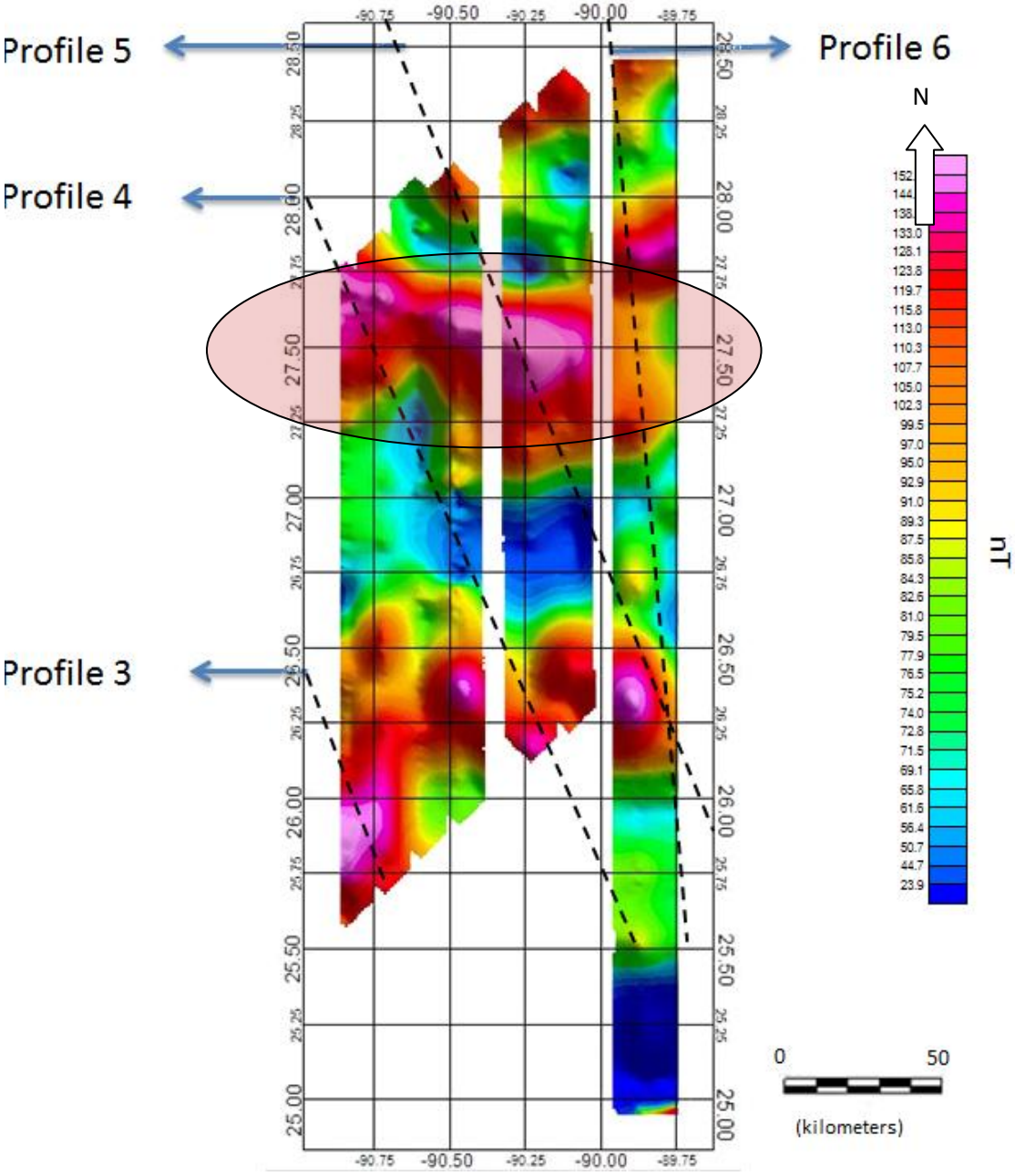

Figure 6.3 Gridded aeromagnetic data from Hall and Najmuddin, 1994, anomalies in circled area are proposed as the effects of SDRs .

A magnetic map from a recent potential fields study *(Mickus et al., 2009)* for the crustal structures at the northern Gulf of Mexico shows similar (Figure 6.4) continuous anomalies over the proposed SDR locations (at the northern Gulf of Mexico).

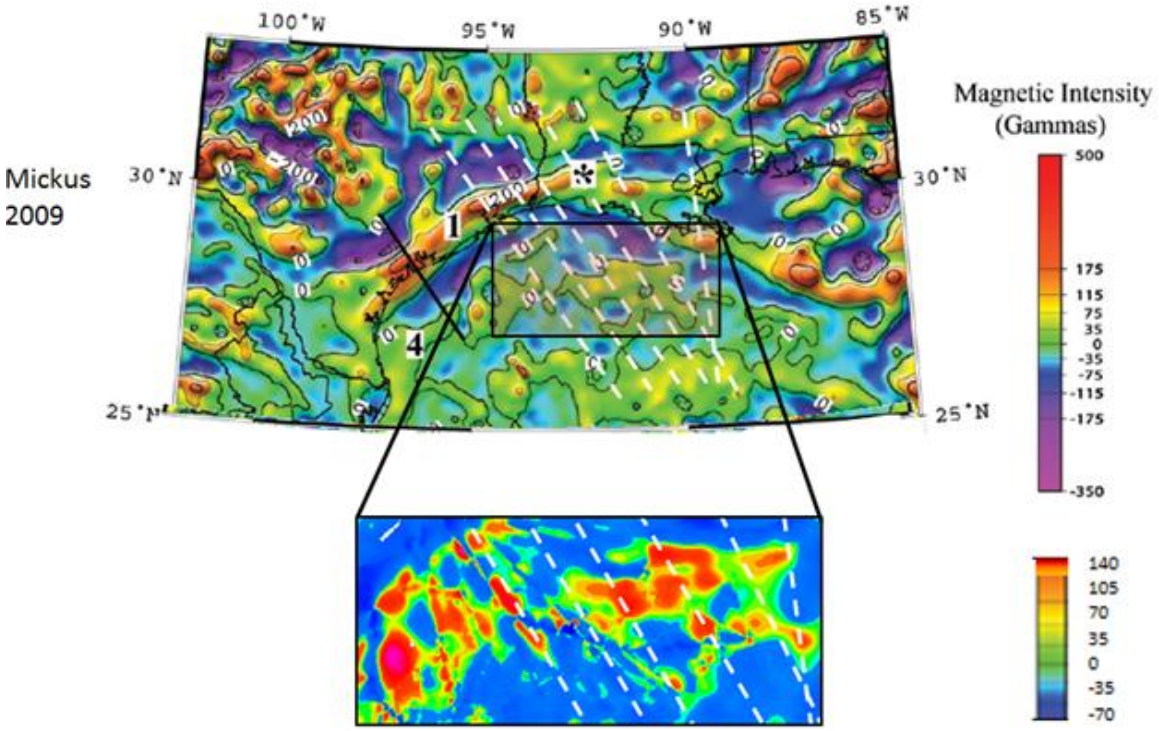

Figure 6.4 Magnetic intensity maps, profile locations highlighted with white color (Mickus et al., 2009)

6.2. Magmatic Underplating

Magmatic margins around the world are usually identified by SDRs and magmatic underplating *(White and McKenzie, 1989).* As the hypothesis for the existence of SDRs was shown to be plausible, another typical property (magmatic underplating) of volcanic passive margins was investigated.

Interpretation for lower crustal body (magmatic underplating) will directly affect the nature of the margin as it is often used as an indicator of volcanic margins *(White and Mckenzie, 1989).* Seismic data to determine the presence of magmatic underplating are not available along any of the profiles. The extent (e.g. location, dimension) of the magmatic underplating will be delineated by magnetic studies:

1. Existence of SDRs, properties of transition zone (i.e. width) indicates that the margin can be classified as a volcanic margin and therefore the existence of underplating is expected

2. SDRs often used as an indication of the extent of the ocean-continent transition *(White and McKenzie, 1989)*

3. There is a general agreement that lower crustal bodies are limited within the ocean-continent transition *(Menzies et al., 2002)*

Magmatic underplating (average 5 km thick) appears to underlie extended continental crust on many volcanic margins *(Wilson, 2002)*. Although there are some different models for the extent of the lower crustal body extension, there is a general agreement that the LCB is located in the ocean-continent transition (*Kelemen and Holbrook, 1995; Menzies et al., 2002*). In this study the properties of such a feature are kept similar to other examples around the world (e.g. SW Africa).

P-wave velocity structure that was obtained from available constraints suggests that the P-wave velocity of underplating layer lies between 7.5 km/s and 7.8 km/s. A value of 7.6 km/s was observed for the Namibia volcanic margin *(Bauer et al., 2000).*

6.3. Distribution of Crustal Types

Properties and interpretation for the different crustal types and their boundaries for each model were described in previous chapters. Correlation of the proposed crustal boundaries between models is also a concern of this study. Good correlation of the structures between models can provide support for the interpretation.

The initial interpretation for the crustal distribution is shown in Figure 6.5. According to the initial interpretation an average width of 280 km for the transition zone with the thickness values ranging between 25 km to 9 km is observed. The

distribution of crustal types is based on the assumption that the 3 distinct magnetic anomalies are all due to SDR bodies.

Previous studies on volcanic margins *(Bauer et al., 2000* and many more) have revealed a maximum width of the transition zone to be approximately 200 km. These studies are usually based on seismic studies in which researchers identified and characterized the crustal distribution. As the width of the magmatic underplating (230 km) and transition zone (270 km) of initial interpretation is found to be larger than that at other magmatic margins, it is possible that the outer SDR magnetic anomaly is related with sea-floor spreading (Figure 6.6). Discussion for the SDRs will be presented in the following chapter.

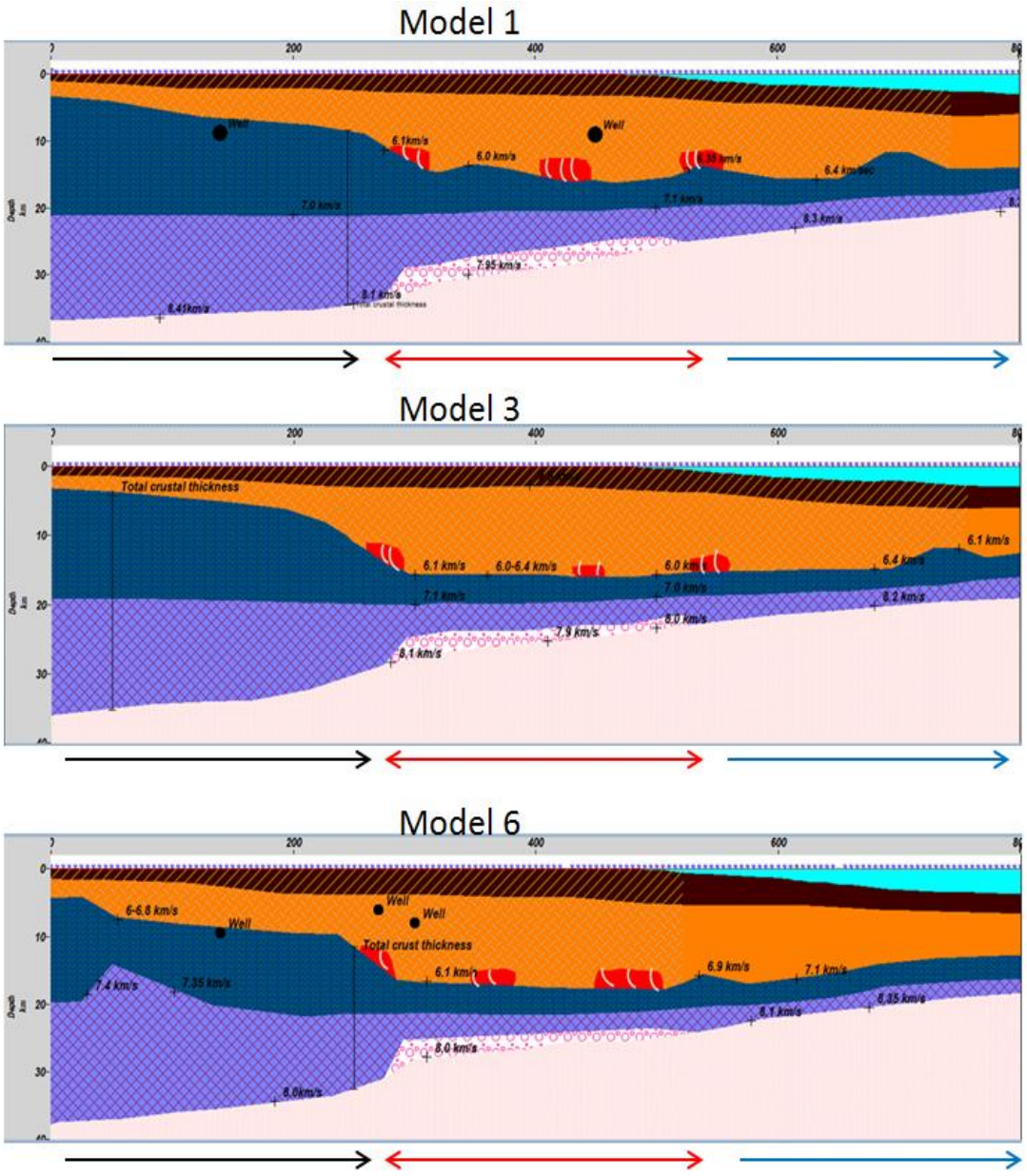

Figure 6.5 Initial interpretation for the crustal distiribution (Black line: continental crust, red line: transition zone, blue line: oceanic crust)

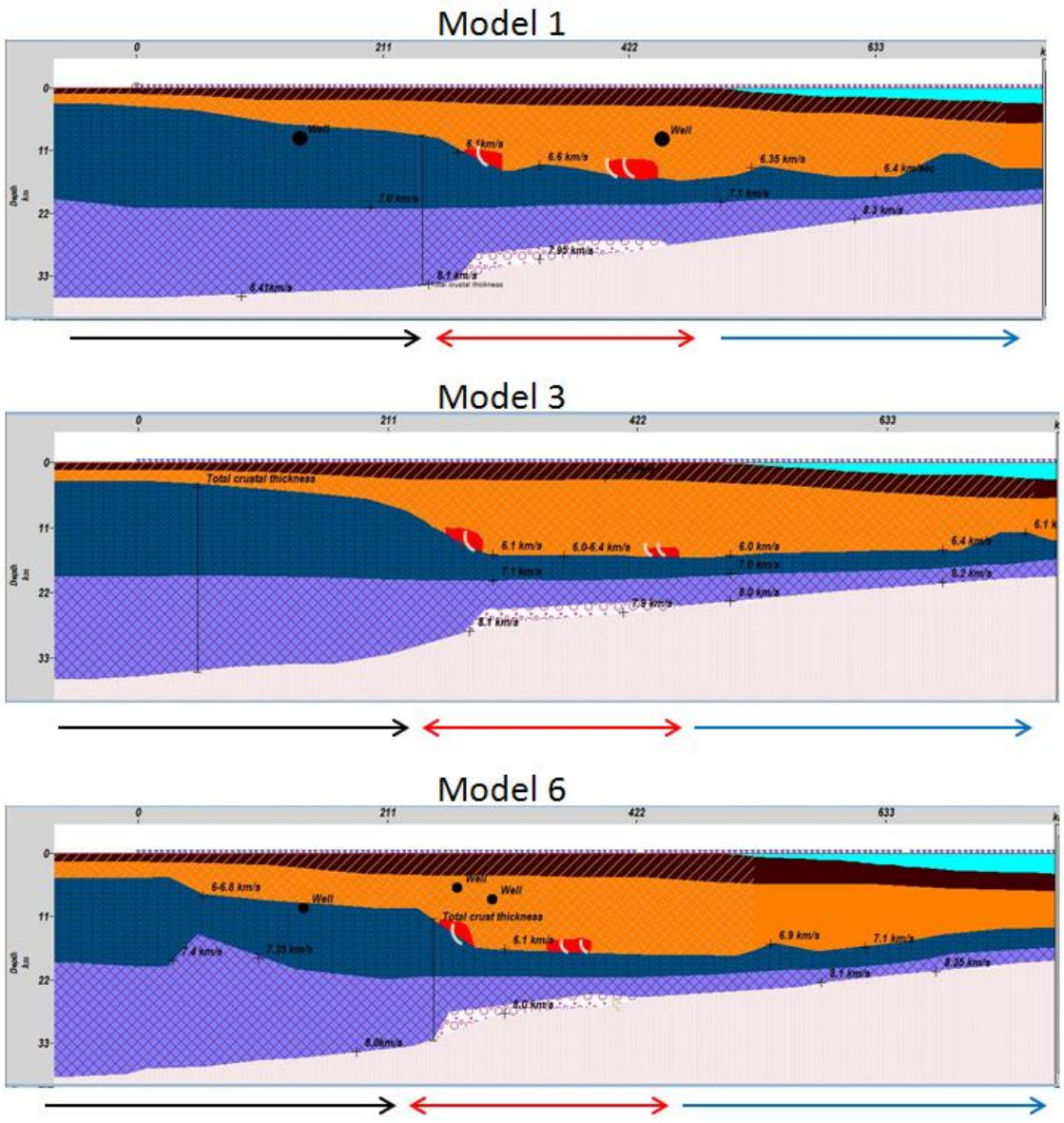

Figure 6.6 Final interpretation for crustal distribution (Black line: continental crust, red line: transition zone, blue line: oceanic crust)

6.3.1. Normal Oceanic Crust

Oceanic crust produced by sea-floor spreading is identified at the southern end of all profiles. The total thickness of oceanic basement is approximately 9 km, which is greater than average and could point to slightly higher melting rates during initial sea-floor spreading. The Moho depth beneath oceanic crust is about 18 km to 20 km for all profiles, whereas it is generally observed to be 15 km for normal oceanic crust around the world (e.g. Namibia, *Bauer et al., 2000*). Considering that the sediment thickness is approximately 11 km over oceanic crust on all profiles, an average Moho depth of 18 km to 20 km is found plausible.

6.3.2. Normal Continental Crust

Crust at the northern end of all profiles is identified as continental crust. The areas with crustal thickness ≥ 32 km are interpreted as typical continental crust.

6.3.3. Transition Zone

The crust beneath the zone of SDR wedges can be identified as extended, rifted continental crust which is heavily intruded and underplated by mafic magmas. Crustal

thickness of this zone varies between 25 kms to 9 kms. An average width of the zone is 200 kms.

The crust that is located between normal continental crust and transition zone is interpreted as stretched and minimally intruded crust. Some researchers preferred to name this portion as ''thick transitional crust'' (Buffler and Sawyer, 1985 and others).

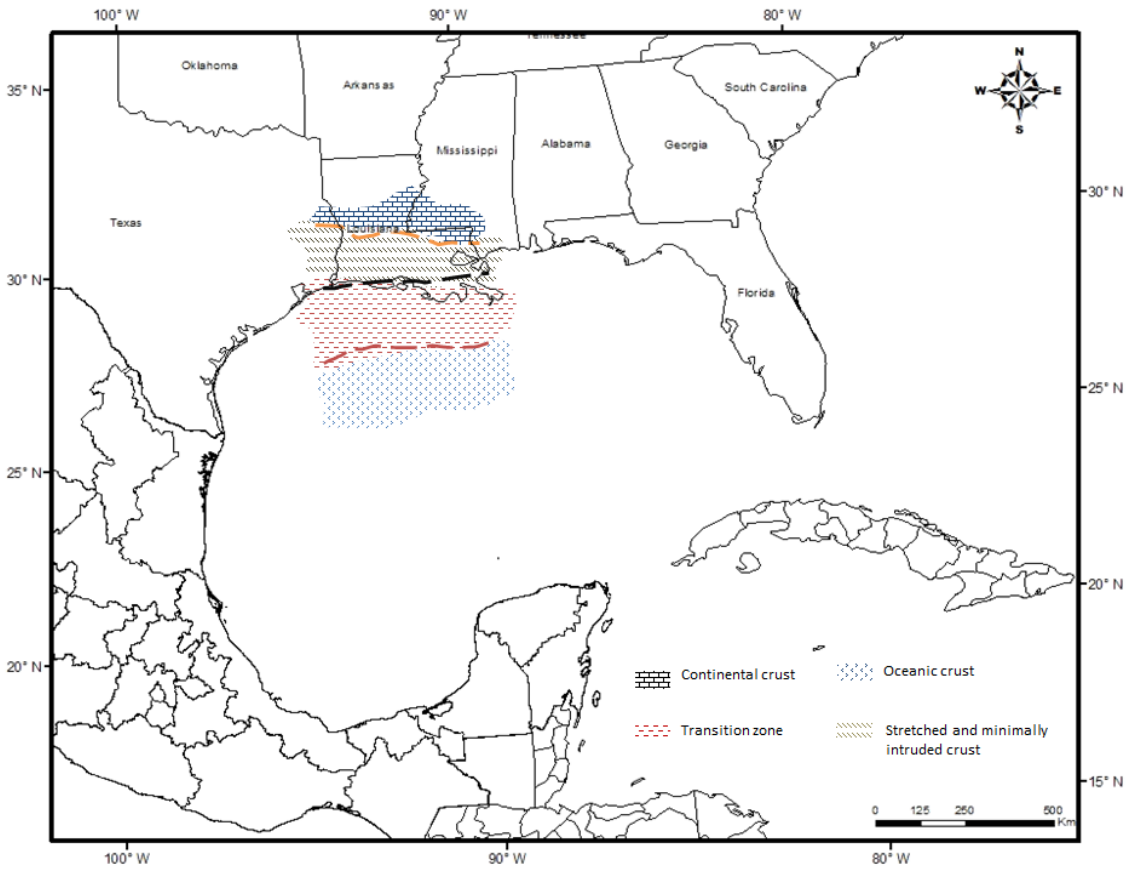

Figure 6.7 Interpretation for the boundaries of the different crustal types

The interpretations for the crustal boundaries (Figure 6.7) are based on the thickness of the crust gravity response of the margin, and the extent of the SDR wedges.

Properties of individual crustal types were described in previous chapters. Three main types of crust are generally recognized in the northern Gulf of Mexico. Although some researchers characterizes transitional crust as two pieces (thick and thin), I have defined transitional crust as a single body. On the other hand due to variation of the crustal thickness and the gravity response, I have defined the continental crust with the thickness values greater than 32 km.

6.4. Plate Tectonic Model and Reconstructions

The boundaries of the different crustal types are derived from the data within the study area. Therefore the reconstructions presented here are only the preferred reconstruction, alternatives to this model can also be generated.

Opening of the Gulf of Mexico by the counter clockwise rotation of the Yucatan block has been suggested by many authors. Some authors based this rotation on paleomagnetic *data (Molina Gorza et al., 1992)* and others explained it by the reconstruction of the ocean-continent transform boundary *(Hall and Najmuddin, 1994; Marton and Buffler, 1994; Pindell and Kennan, 2009)*. Gulf of Mexico evolutionary models by *Winker and Buffler (1988*) explain the Yucatan block rotation either by sub-parallel ocean-continent transform boundaries or single ocean-continent transform boundary. Although there are many proposed ideas for the rotation of the Yucatan,

most researchers consider this counterclockwise rotation to be between 40° to 60° (*Hall and Najmuddin, 1994; Marton and Buffler, 1994; Schouten and Klitgord, 1994; Bird et al., 2005)*

The development of the Gulf of Mexico occurred with continental crust extension followed by sea-floor spreading *(Dunbar and Sawyer, 1987; Hall and Najmuddin, 1994; Pindell, 1985; Marton and Buffler, 1994; Bird et al., 2005).*

There are many proposed ideas for the details of the rotation. Proposed studies differ from each other mainly by the rotation amount, rotation pole location, and geometry and orientation of sea-floor spreading. Figure 6.8 and Table 1 shows some of the proposed location for the rotation pole.

	Latitude	Longitude	Rotation
Dunbar and Sawyer, 1987	25.00	-79.00	45°
Hall and Najmuddin,1994	24.00	-81.5	55°
Shepherd,1983	24.00	-84.0	41°
Bird et al..,2005	24.00	-81.5	42°
Pindell, 1985	29.5	-81.4	43°

Table 1 Poles and amount of counter clockwise rotation for the Yucatan block (modified from Bird et al., 2005)

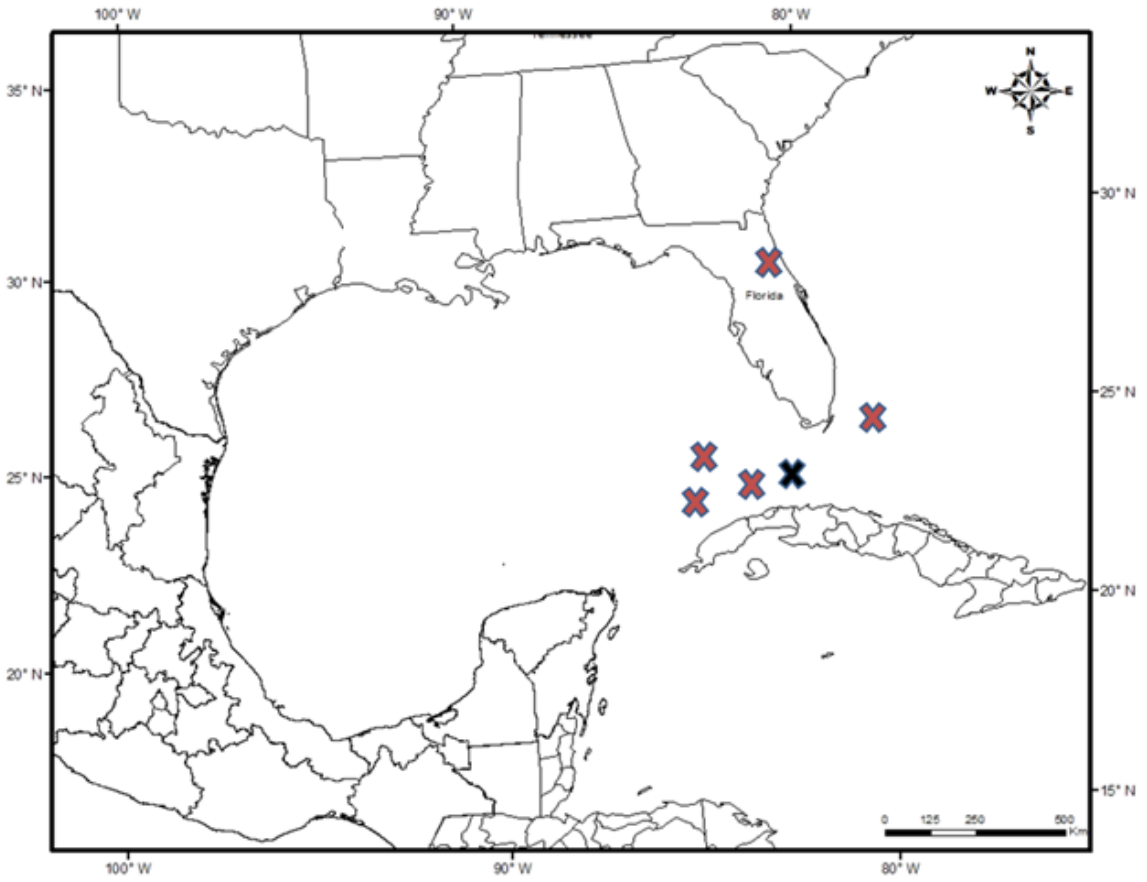

Figure 6.8 Proposed locations for rotation pole (pole used for this study colored in black)

Hall and Najmuddin (1994) explained the discontinuities in linear magnetic anomaly at the eastern Gulf of Mexico to be associated with fracture zones. Many authors *(Buffler and Sawyer, 1985; Hall et al., 1982; Pindell, 1985)* observed an east-west anomaly patterns on magnetic data, which strengthens the assumption of counterclockwise rotation.

The remaining discussion for reconstruction models is based on the rotation pole of Hall and Najmuddin, (1994).

The crust surrounding North America including the present Gulf of Mexico region is assumed to be continental crust with an average thickness ≥ 32km. Yucatan occupied the present Gulf of Mexico region approximately 190 Ma ago *(Pindell and Kennan, 2009).* It was proposed by Burke (1988) that there was no gap between Yucatan and western Florida (initially Yucatan was longer).

''Intra-continental rifting between the Yucatan and North America began with the collapse of the Appalachians and Ouachitas in the Middle to Late Triassic (230 Ma*)* and assumed to continue until 160 Ma'' *(Bird et al., 2005)*. At approximately at 160 Ma *(Bird et al., 2005)* rotations due to the continental extension had started.

The current crustal configuration of the northern Gulf of Mexico is shown in Figure 6.9. The average width for the transition zone and lower crustal body is obtained from models (200 kms and 170 kms). None of the profiles are perpendicular to the margin so the amount of underplating and transition zone is exaggerated by the obliqueness of the profiles. Extended measures of the profiles are multiplied with 0.905 to overcome this problem (155 km width for underplating, 181 km width for transition zone).

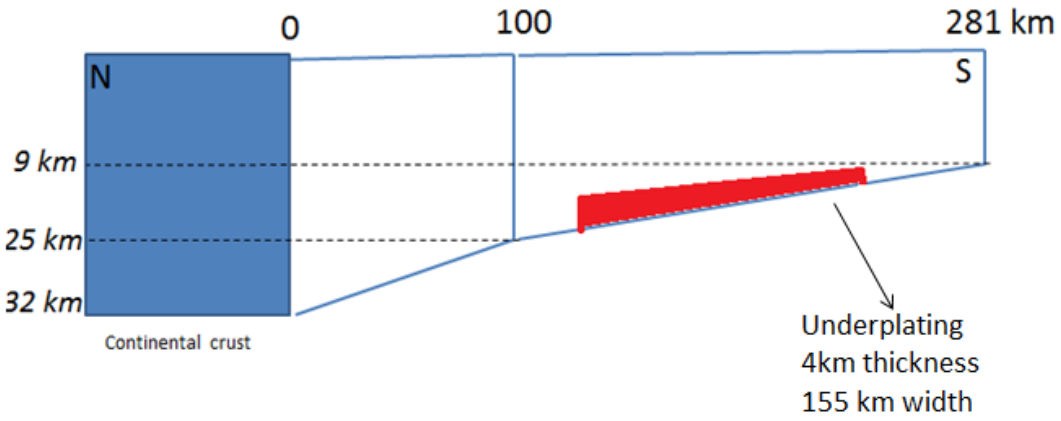

Figure 6.9 Simplified crustal configuration of the northern Gulf of Mexico

The first step of the plate reconstruction study is to restore the stretched continental crust (~100 km width). In order to do so, an assumption was made that this portion of the crust does not have intrusions of igneous material (or negligible amount). An updated model with original (32 km) crustal thickness has been created with 89 km width (Figure 6.10).

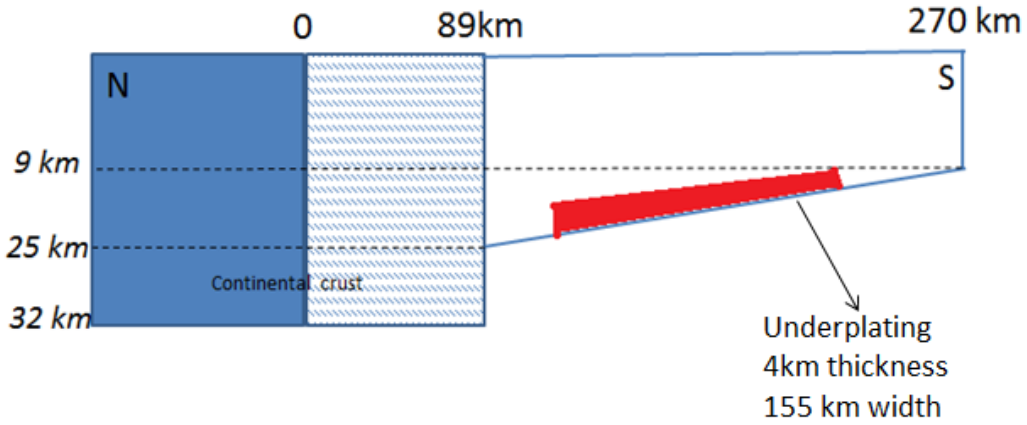

Figure 6.10 Restoration of minimally intruded, stretched continental crust

The next step of the plate reconstruction studies requires the restoration of the transition zone. Although prefect restoration of the transition zone is impossible because of the unknown amount of intruded and extruded material, an approximation can be made. The initial model (Figure 6.11) was generated with the assumption that there is no intruded material throughout the transition zone.

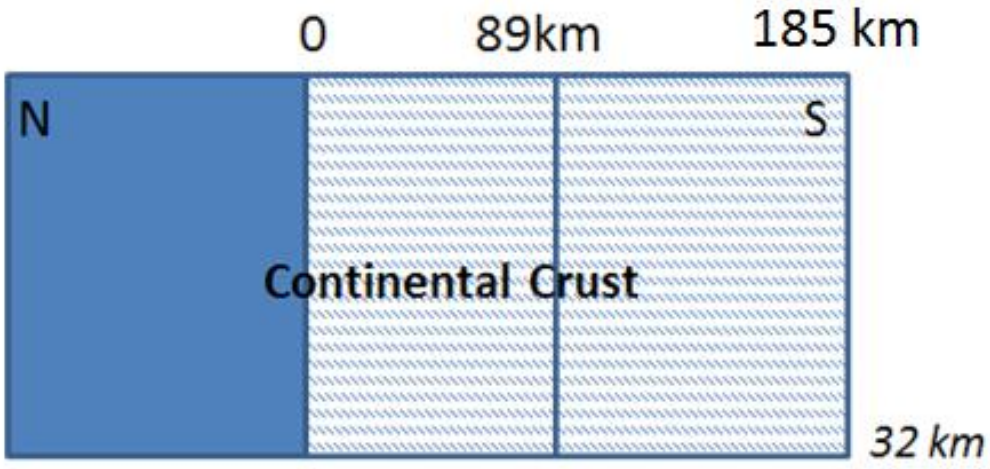

Figure 6.11 Maximum width of the restored crust, with the Transition zone restored back to the original thickness (32km) with an assumption of no intruded material

With no intrusion throughout the transition zone, the maximum width of the initial continental crust was calculated as 185 km. Another model was generated by taking out the contributions from the lower crustal body (Figure 6.12). Geoffroy (2005) explained that for the volcanic margins, a significant amount of intruded material in the transition zone attaches to the base of the crust and forms the lower crustal body.

Removing the lower crustal body from the transition zone resulted in a maximum width of the initial continental crust of 175 km. Since the contributions from intruded material should be less than the contributions from magmatic underplating an assumption was made (previous studies showed that the contribution from lower crustal body is usually twice the contribution other intrusions) and initial width of the continental crust interpreted as 170 km.

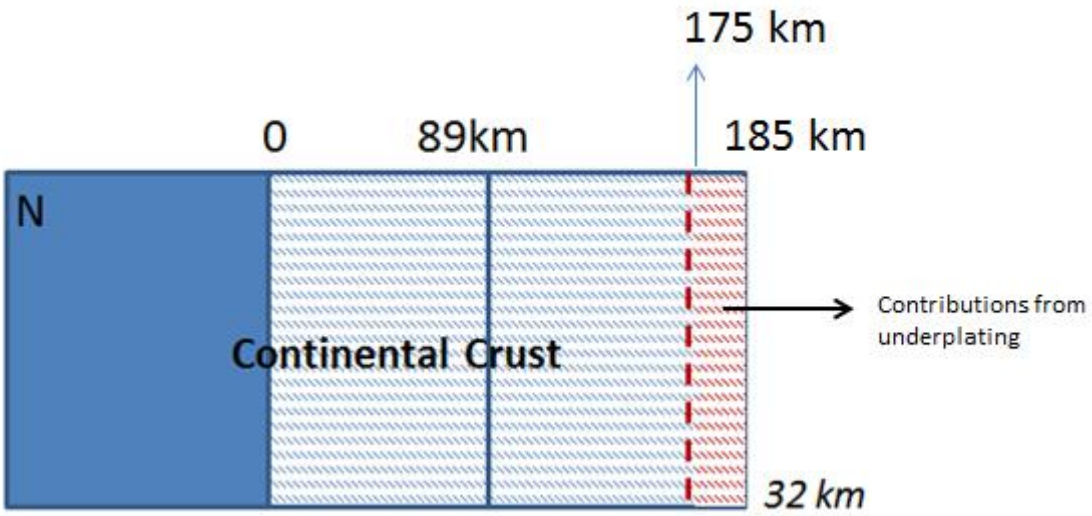

Figure 6.12 Initial Interpretation for the width of the continental crust (185 km with LCB, 175 km when contribution from LCB is removed)

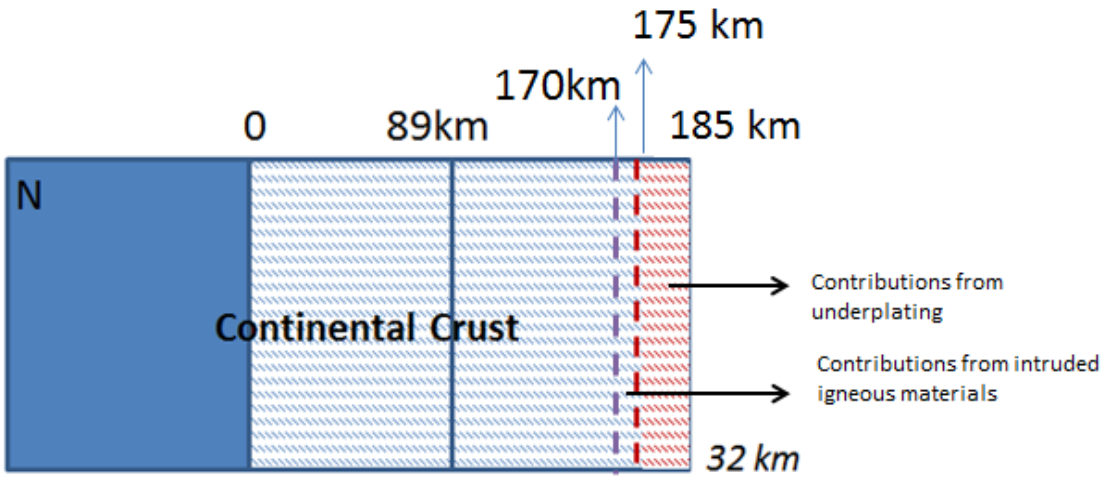

Figure 6.13 Final interpretation for continental crust

The finite rotation technique *(Cox and Brian, 1986)* was used in order to calculate the amount of rotation needed for the restoration.

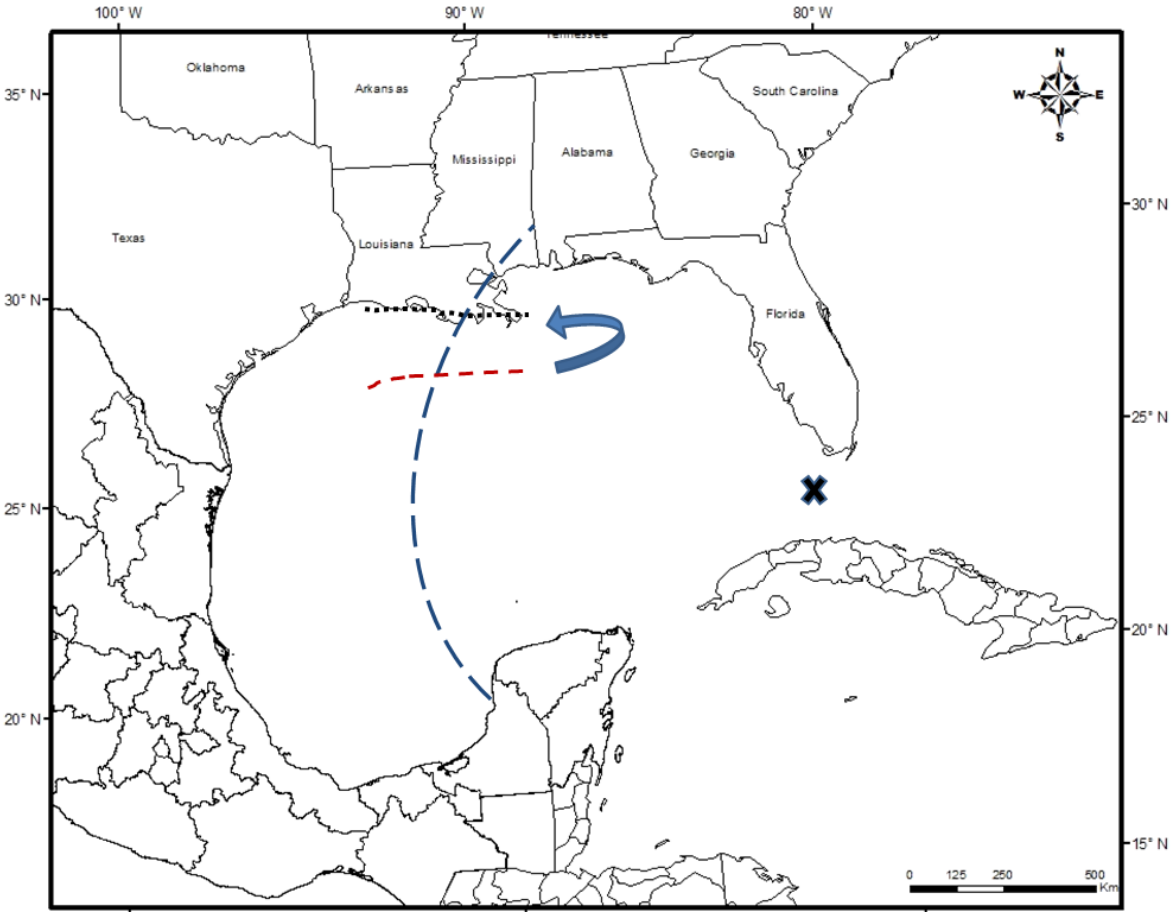

Figure 6.14 Location of interpreted boundaries and restoration arc, Initial continental crust (black dotted line) and current transition (red dashed lined) zone-oceanic crust boundary, rotation pole marked with X and restoration arc drawn with blue dashed line

The restoration arc that was generated by using the pole located just south of Florida is highlighted with black color on Figure 6.14. Restoring the transition zone back to its original crustal thickness required 15° of rotation along the restoration arc.

At about 150 Ma *(Bird et al., 2005*), sea-floor spreading started. With the sea-floor spreading, an oceanic crust was formed in the central Gulf of Mexico. Previous

studies *(e.g. Bird et al., 2005)* suggest that the Yucatan Block underwent a rotation of 20° (counter clockwise) due to the sea-floor spreading.

In the northern Gulf the width of the transitional crust is interpreted to be around 200 km (more than 300 km if ''partially thinned continental crust'' is assumed as thick transitional crust). Whereas, it was shown to be 150-200 km wide for the southern Gulf in previous studies (*Sawyer et al., 1991; Marton and Buffler, 1993*). As a result, the oceanic crust occupies an asymmetrical position relative to the northern and southern part of the Gulf area. It can be concluded that more crustal extension was accommodated in the northern Gulf of Mexico by the rifting process.

When the restoration calculation were done for the southern Gulf of Mexico by using the crustal thickness from TTS analyses (Figure 6.15, *Sawyer et al., 1991*), it has been concluded that 9° additional rotation is needed in order to restore the crust back to its original thickness (32 km). As the approximate boundary of oceanic crust is determined from the β values for the southern Gulf of Mexico, a rough calculation was made for the width of the oceanic crust along the restoration arc to check whether similar result can be obtained as the previous studies. It is found out that this rough estimation is within the range of previous studies results. An average width between 200 kms and 220 kms for the oceanic crust is found, and the amount of rotation needed to close the oceanic crust varies between 19° to 21° (average value of 20° was chosen). Thus, a total amount of 44° counterclockwise motion is needed to completely close the Gulf and restore the crust its pre-rifting thickness.

The asymmetric distribution of the transitional crust from this study suggests that the thinning of the lithosphere in the Gulf of Mexico during the continental extension period *(Marton and Buffler, 1993)* may best be explained by simple shearing.

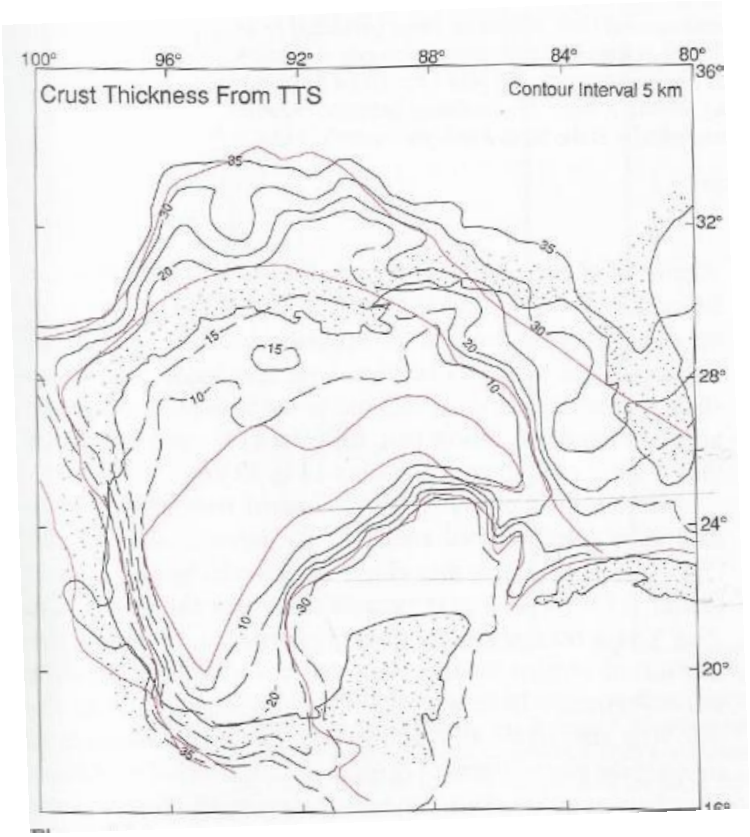

Figure 6.15 Map of estimated crustal thickness from TTS analyses (Sawyer et al., 1991)

The interpretation described here is based on the available gravity, magnetic, seismic data and previously published maps and models. The reconstruction from this study is compatible with some other studies. Although the amount of rotation varies between studies, the idea of a counter clockwise rotation of the Yucatan block and the

continental crust extension which was followed by sea-floor spreading is compatible with many previous studies *(Pindell, 1985; Buffler and Sawyer, 1985; Hall and Najmuddin, 1994; Bird et al., 2005)*

Passive margins can be classified as being volcanic and non-volcanic margin depending on the amount of volcanism occurred during rifting. The average width for the transitional crust of 200 km, well correlated magnetic data that shows anomalous response over the proposed boundary of transitional crust are the main similarities with the volcanic passive margin studies around the world (*Bauer et al., 2000; Stavar, 2007; Berndt et al., 2000; Geoffroy, 2005)*. As all these properties gathered (i.e. properties of Transitional crust, existence of SDRs, high possibility of magmatic underplating) it is interpreted that the northern Gulf of Mexico region corresponds as a volcanic passive margin.

CHAPTER 7.DISCUSSION

Regional gravity data are often used to extend the interpretation beyond where there is seismic control. Where deep seismic data are either not available or poor, potential field data (gravity and magnetics for this study) may be used to provide possible logical explanation of the subsurface. For the areas where seismic data are available, the gravity method can also be used to support seismically built models to provide an independent check. Although this integrated study has proven to be successful there are still some concerns for the interpretations and assumptions made for this study, as discussed below.

7.1. Seaward Dipping Reflectors

SDRs as a source for high amplitude magnetic anomalies are indicated on many volcanic continental margins *(Talwani et al., 1995);* however not everywhere that SDRs have been identified on seismic sections has a distinct magnetic anomaly been observed *(Schreckenberger et al., 1997).*

Although seaward dipping reflectors have been seismically imaged in the eastern Gulf of Mexico by Imbert et al., (2001), there is no other published direct evidence available for SDRs on the northern Gulf of Mexico. The authors discuss the age of the SDRs and interpret them as '' it is unlikely to consist of Triassic siliciclastics''. The authors support their interpretation for the age of the SDRs in terms of their relation to the Louann Salt which is located right on top of the SDR wedge '' therefore it postdates the beginning of the volcanic spreading along the eastern Gulf of Mexico'' and finalize discussion by proposing that the ''volcanic/oceanic spreading in the eastern Gulf of Mexico started before salt was deposited, continued during salt deposition, and ceased in the Early Cretaceous''.

Imbert (2005) did not include the amplitude scale for SDR-related positive magnetic anomalies on his paper, but it can be seen that the SDRs are characterized by positive anomalies which are surrounded by negative anomalies. The proposed SDR locations (from *Imbert, 2005)* were tracked on DNAG Database to test whether the similar amplitudes can be seen. The amplitudes for the proposed magnetic bodies (SDR) from both studies are similar with each other. The values are in the order of 80-120 nT for this study whereas they are around 100 nT to 150 nT for Imbert's study.

Mickus (2009) preferred to attribute the magnetic anomalies over the northern Gulf of Mexico as those produced by deeply buried mafic igneous complex (a single large body).

Another explanation for the magnetic anomalies over the northern Gulf of Mexico is that these anomalies (especially the outer SDRs) might be due to sea-floor spreading. Sea-floor spreading occurred in the central Gulf of Mexico province between 160 and 140 Ma and continued for approximately 20 m.y. *(Bird et al., 2005).*

There are some examples where the outer SDR bodies coincide with regions where magnetic anomalies are attributed to sea-floor spreading *(*Figure 7.1*, Bauer et al., 2000).*

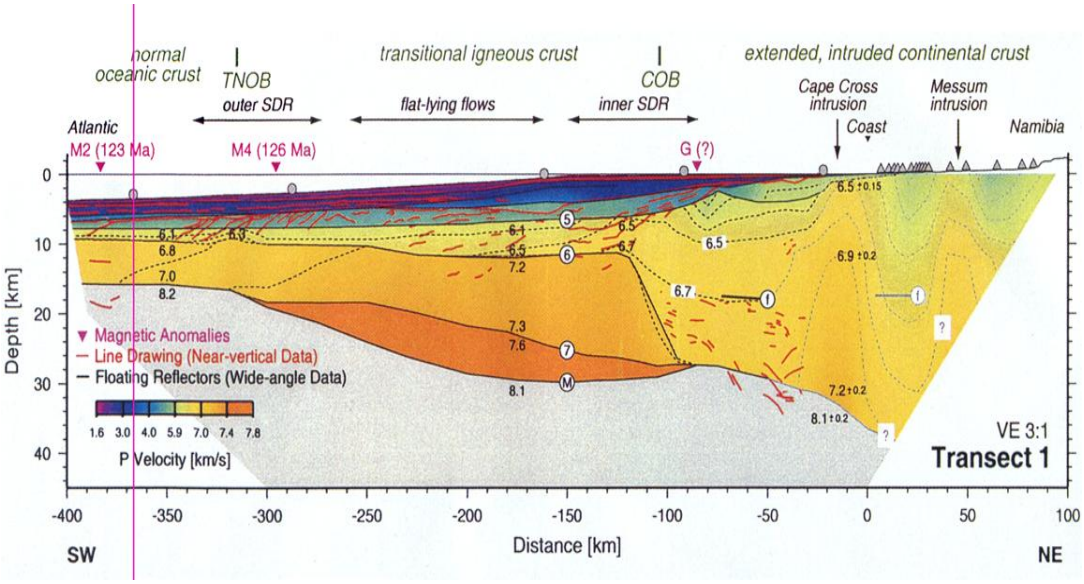

Figure 7.1 Interpreted crustal depth section on Namibia margin (*Bauer et al., 2000)*

The outer SDRs in this model coincide with one of the sea-floor spreading anomalies – M4 (~ 126 Ma)

As I lack detailed seismic data to image SDRs, alternative interpretations can be made. The positive anomalous magnetic signals might be explained by sedimentary concentrated infill zone (''deep graben'' *Imbert, 2005*). This alternative model fails to explain the amplitude of the anomalies, as the contrast and susceptibility of compacted sediments can only generate weak signals when compared with the SDR associated anomalies. This also fails to explain the spatial continuity across the northern part of the margin. These anomalous structures can be tracked across the profiles, and are unlikely to be caused by compacted sedimentary layers. Another explanation is that the responses might be due to intrusions. It is very difficult to separate the magnetic signal of dike type intrusions from the SDRs, as their response, size, and depths are very similar. Studies on Namibia margin *(Gladczenko et al, 1998)* showed intrusions with ~20 km width and densities higher than the sedimentary layer. Any type of these intrusions will also cause a significant (sharp, high amplitude) positive gravity response across the margin which was not observed in any of the selected profiles.

Another concern for the SDRs includes the density of magnetically anomalous bodies. Published densities for these bodies vary for different margins. Studies on the Norwegian margin have revealed the density range of 2.5 g/cc to 2.65 g/cc (*Mjelde et al., 2005)* whereas a value of 2.6 g/cc has been used for the Namibian margin *(Gladczenko et al., 1998).*

SDRs are a type of flood basalts which were extruded on the sea floor *(Hinz, 1981)*. One of the widely accepted idea is that SDR sequences are the mixture of

volcanic rocks and non-volcanic sedimentary rocks *(Menzies et al., 2002).* During the modeling stage the densities of the SDR bodies were chosen as 2.58 g/cc. Alternative models with slightly different densities can be constructed (between 2.50 g/cc and 2.65 g/cc). These alternative models should not cause any noticeable difference during the modeling (other than small, very local differences).

7.2. Magmatic Underplating

Models 1, 2, 3, and 6 were built based on various available seismic studies. Although there might be a variation in both the properties and the geometry of the subsurface layers associated with localized features, these do not affect the regional fit of the models to the data. On the other hand, there are only few seismic constraints available for Models 4 and 5. Two models were constructed based upon the few available constraints and a match was obtained between observed and calculated gravity data.

The gravity method is also known for its non-uniqueness. Certain gravity response can be generated by several different models. In order to control this problem, magnetic data were introduced into the models. Magnetic data provided a better constraint for the key elements of the model (SDRs location, extent of transitional

crust). As a result, integrated geophysical data provided a better approach for the non-uniqueness problem.

Although the integration of different geophysical data showed an improvement for the constraints over models, one can argue that the interpretations are based on indirect constraints.

As the magmatic underplating at this region has not been drilled or seismically imaged, there is no direct information available for the existence and properties of such a layer. Although the alternative models that test the existence of magmatic underplating showed that the similar results can be obtained with or without the magmatic underplating.

7.3. Width of Lower Crustal Body and Ocean-Continent Transition

The transition between extended continental crust and normal oceanic crust on rifted margins is described as transitional crust (*Eldholm et al., 2000).* Depending on the nature of the transition crust, there might be magmatic rocks within the zone that were linked to the breakup process *(Eldholm et al., 2000).*

In their research, Odegard and Dickson (2001) discuss proto oceanic crust that is not the same as oceanic crust due to its structure and composition. They also proposed

that distinctive gravity and magnetic signatures can be associated with proto oceanic crust *(Odegard, 2003; Odegard, 2010)*.

At many passive margins the ocean-continent transition is approximately 150 km wide *(Burke, 1988).*It has been shown from the studies at North Atlantic margins that the width of the lower crustal body usually varies between 50 km and 200 km (*Eldholm and Grue, 1994)*. The width of the ocean-continent transition was interpreted to be narrower at several volcanic margins *(Menzies et al., 2002).*

Some studies have investigated the role of magmatic underplating in terms of basin dynamics. These studies indicated that the extensional deformation is significantly concentrated at the region of underplating and that the width of underplating directly controls the width of the rift *(Yamasaki and Gernigon, 2006).*

The variation in thickness of the lower crustal body indicated higher magmatic underplating thickness on the SW African profiles, The average thickness of 6-7 km for magmatic underplating were generally assumed based on the available seismic data for the SW African margin *(Stavar, 2007).*

It was observed from the crustal studies on volcanic passive margins that the width of lower crustal body may vary. Interpretations on Norway and Greenland conjugate volcanic margins suggest 200 km for the width for the lower crustal body

(Voring Escarpment), and 100 km for the width of lower crustal boundary for Lofoten Basin *(Tsikalas et al., 2005).* Studies at the SW Africa revealed approximately 180 km width for the lower crustal body *(Bauer et al., 2000).*

Constructed models in this study suggest an average width of 230 km for the lower crustal body and 260 km for the ocean-continent transition zone. The extensions of the magmatic underplating and the ocean – continental transition zone are controlled by the proposed SDR location. As there are concerns whether the magnetic anomalies associated with the outer SDRs can be related with sea-floor spreading anomalies *(Bauer et al., 2000),* an alternative model is constructed for Profile 3. This model assumes that the magnetic anomalies after km 470 are associated with sea-floor spreading (Figure 7.2). An overall width of 180 km for the lower crustal body and 200 km for ocean-continent transition was observed from the alternative model.

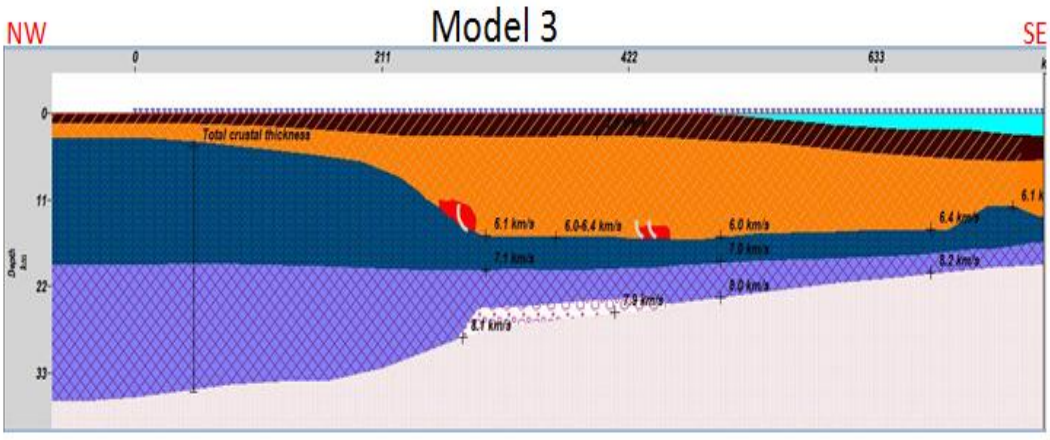

Figure 7.2 Updated model for Profile 3 with magmatic underplating width less than 200 km

7.4. Ocean-Continent Boundary

The boundary between oceanic and continental crust in the Gulf of Mexico has been interpreted in several ways by using gravity, magnetic data, seismic reflection, and refraction data.

The interpretation from Schouten and Klitgord (1994) is based on the magnetic response of the margin (Figure 7.3). They also proposed two possible mechanistic models for the opening of the Gulf of Mexico based on the magnetic response of the margin. According to the authors, low amplitude (long wavelength) magnetic anomalies associated with oceanic crust are surrounded by high amplitude (short wavelength) anomalies of continental crust. Hall and Najmuddin (1994) also interpreted the ocean-continent boundary by using magnetic response of the margin. Although their aeromagnetic study area is limited compared to the Schouten and Klitgord study, the proposed location for the OCB at the northern Gulf of Mexico is very similar.

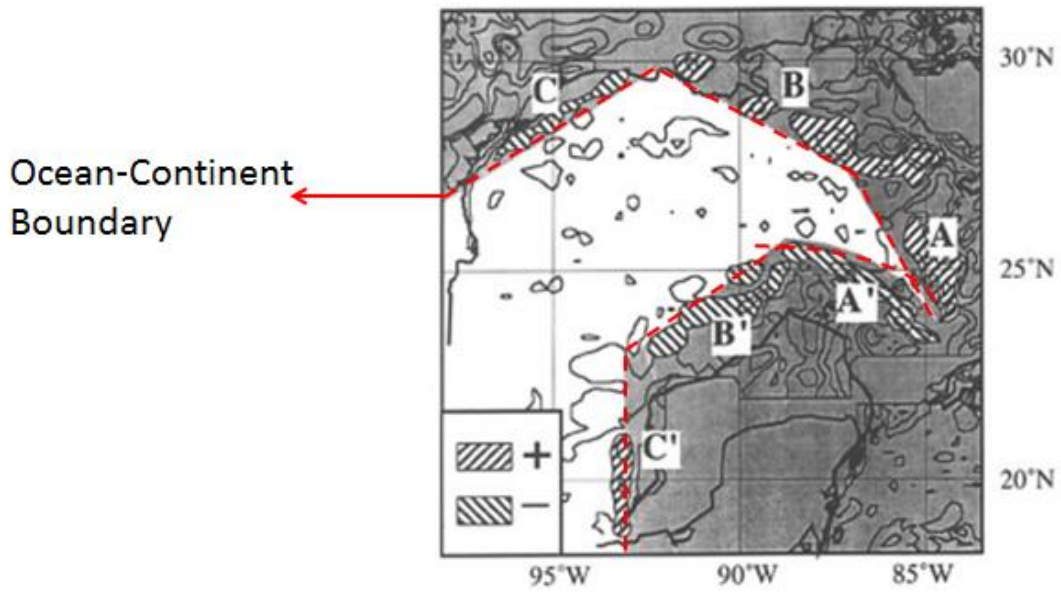

Figure 7.3 Magnetic anomaly field of Gulf of Mexico region (Schouten and Klitgord, 1994)

The existence and the properties of transitional crust were suggested by many authors. Buffler and Sawyer (1985) preferred to identify the transitional crust in two parts as being thick and thin. Authors used different methods to define the geometry and properties for the types of transitional crust. Dunbar and Sawyer (1987) used the relation between total tectonic subsidence (TTS) and crustal extension to provide an approach for the interpretations of the boundary. ''The total subsidence is the water depth plus the sediment thickness at a point, the TTS is the total subsidence less the loading effect of the sediments'' *(Sawyer et al., 1991).* Zero TTS is equivalent to the zero

extension which is described by β= 1, It was indicated that β=4.5 represents the OCB and when β ≥ 4.5 it corresponds to the oceanic crust *(Sawyer et al., 1991).* The results of TTS related studies are shown in the Figure 7.4. Total crustal thickness and Moho depth maps that were produced from TTS analyses were used during this study.

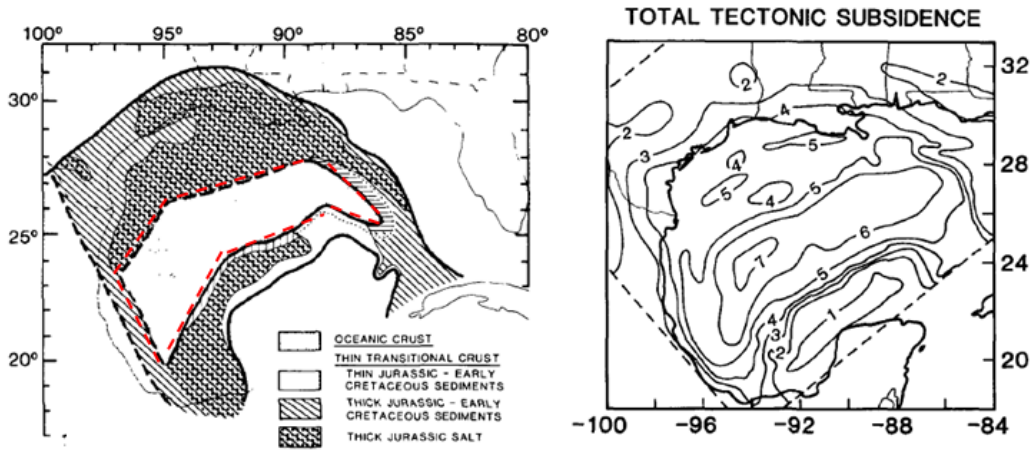

Figure 7.4 Analysis of different crustal types at Gulf of Mexico from TTS analyses, contours in kms (Buffler and Sawyer, 1985)

Unlike some of the previous studies, I have defined 3 different types of crust (continental, transitional zone, and oceanic crust). Interpretations for the boundary between thick and thin transitional crust vary from study to study. Variation on the boundary interpretation is mainly due to the lack of deep seismic images and deep well information at this margin. It can be seen from the models that the sediment thickness can reach up to 17 km depth. Most of the available seismic and well data provide a

detailed image for the sedimentary layers, but data to image deeper portions of the crust are very limited. Although the transitional crust is not subdivided for this study, depending on the gravity signature of the margin, an area between continental crust and transition zone where the thickness values are 25 km to 32 km was observed.

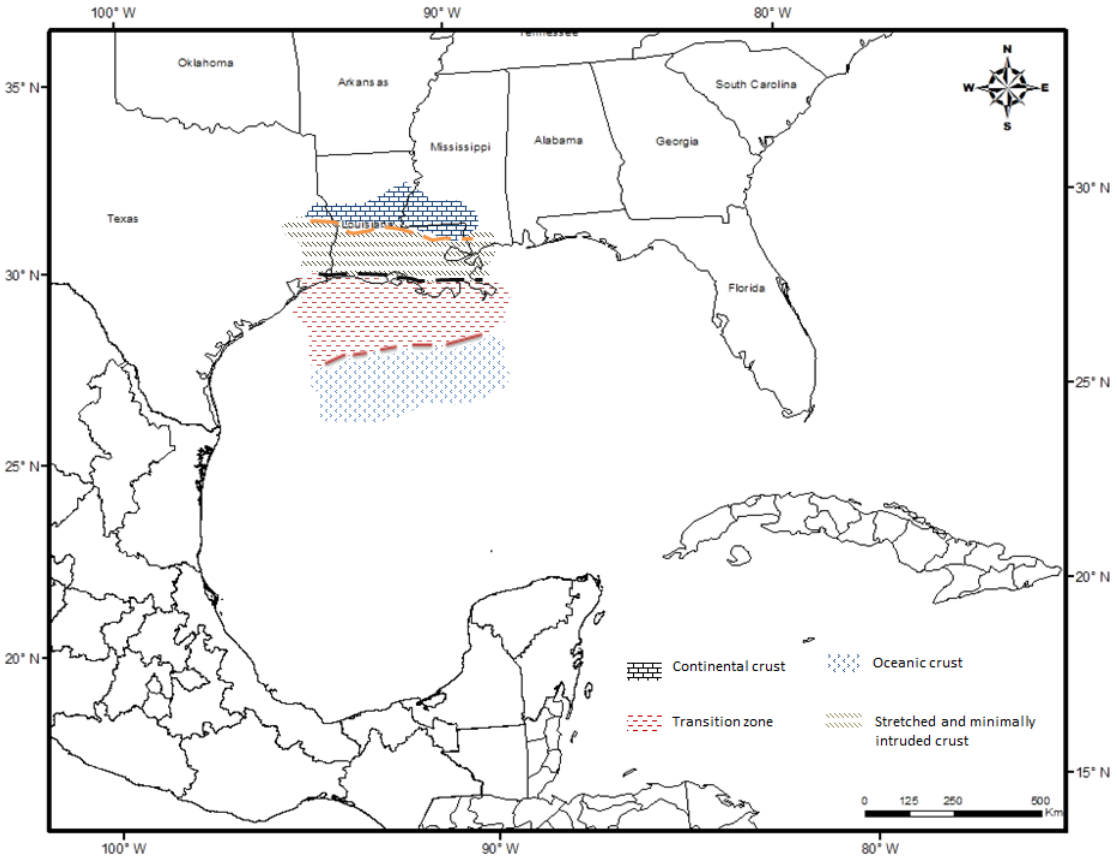

Figure 7.5 Proposed boundaries for different crustal types from this study

This portion of the crust has been referred to as partially thinned continental crust (Figure 7.5). The extension of the ‘’partially thinned continental crust’’ matches well with the interpretation from Buffler and Sawyer (1985) where the authors names this portion as thick transitional crust.

Another reason for the difference in the interpretations (Figure 7.6) is due to the availability of the data; as the time progresses more and more data become available with better quality. On the other hand, neither magmatic underplating nor oceanic crust has been drilled at the Gulf of Mexico. The existence of such a feature (underplating) or the exact location for the boundaries of crust types will remain as hypothesis until deep seismic images becomes available.

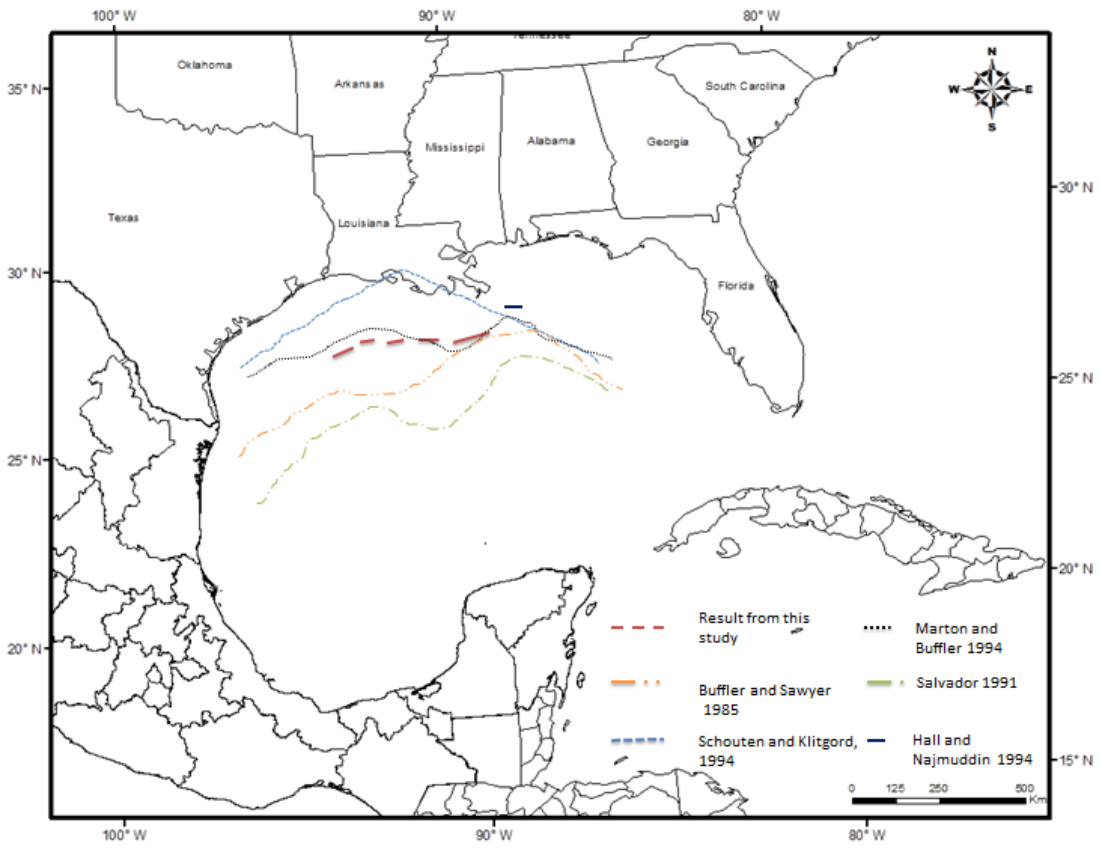

Figure 7.6 Interpreted oceanic crust-transition zone boundaries from previous studies

7.5. Gravity Response of the Margin

Models from this study display similarities with some of the previous suggested models *(*see chapter 2, *Watts and Marr, 1995; Watts, 2001a).*

In terms of the gravity signature, all models across the margin show similar properties. A single peak (single edge effect) with long wavelength (~200 km) gravity

response over the transition zone that suggests that the margin is strong (in terms of lithosphere structure) but the amplitudes (~50 mGal) of this long wavelength signal are less than those predicted and assumed to be related with the extreme sediment thickness for the case of Gulf of Mexico.

7.6. Sigsbee Escarpment

This geological feature is explained as "The bathymetric expression of salt flows that have overridden the abyssal plain of the Gulf of Mexico tens of kilometers since the Paleogene*" (Diegel et al., 1995).* Figure 7.7 shows the seismic illustration of the Sigsbee Escarpment.

As the profiles cross the Escarpment, their densities are increased due to lack of low density salt. Although the increase in the density was chosen to be .05 g/cc, alternative models can be constructed with different density variation values, as there are no observed data available for the density variation.

Alternative models were constructed to test the effects of density variations between .01 g/cc and .15 g/cc. It was concluded that .05 g/cc can represent an approximate approach for the density variation; any other density value provided similar results with slight variation which are assumed as negligible for this study.

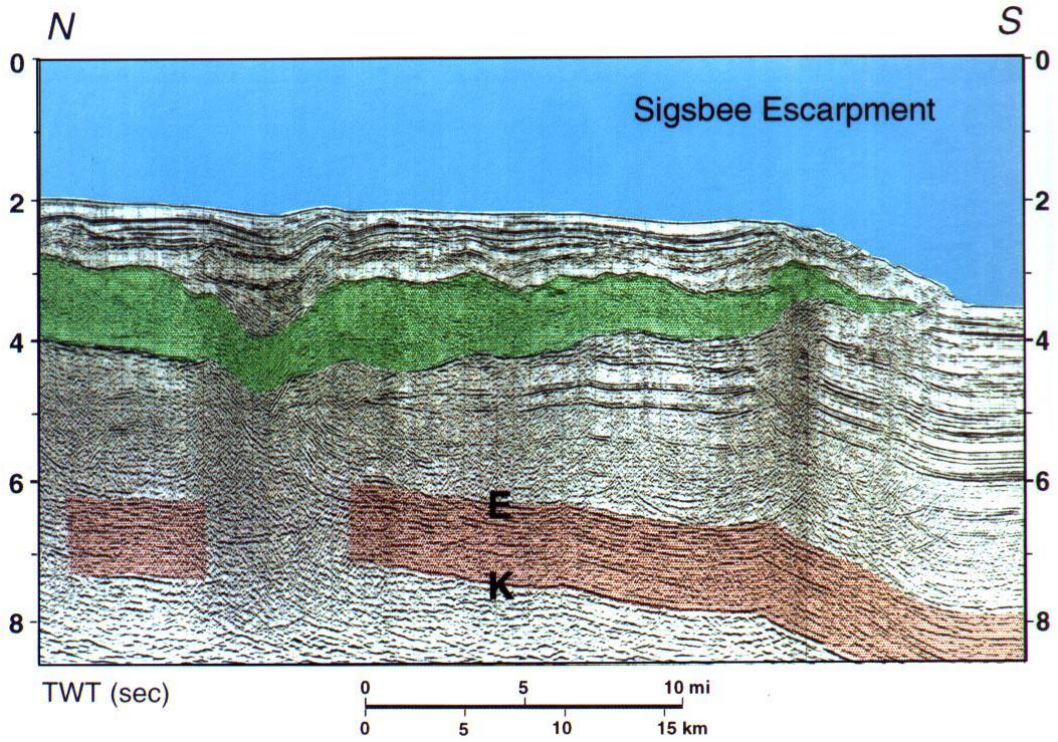

Figure 7.7 - Seismic expression of the Sigsbee Escarpment *(*corresponds to an area between Profile 2 and Profile 5*,* Eocene (E) and middle Cretaceous (K) (Diegel et al., 1995)

CHAPTER 8. CONCLUSION

Integrated geophysical data (free-air gravity, magnetic, and seismic reflection and refraction) have been used to investigate the crustal structure of the northern Gulf of Mexico. In spite of the significant amount of previous study, there is still no consensus for the overall structure of crustal types or the evolution of the basin.

Two-dimensional forward gravity models of free-air gravity data constrained by available seismic and magnetic data were used to investigate the major crustal structure and the nature of the transition zone.

Six 800 km-long forward gravity models, 5 oriented NW-SE and one oriented N-S, show a consistent response throughout the margin. On all the models, negative gradients are observed where the continental crust started to stretch. Distinct gravity lows (approximate value of -20 mGal) were observed where the intrusions increased to the point that the crust is considered as transitional crust. A steep positive gravity gradient is interpreted as an effect Moho depth decrease. Digital magnetic data were captured for Profiles 1, 3, and 6. These profiles show distinct anomalous response on these magnetic data. The sources of these magnetic anomalies are proposed as SDRs and this interpretation is supported by alternative models as well as the correlation of the responses between the models. Results from these two-dimensional gravity models, the mapped distribution of SDRs (which are associated with magmatic underplating over

transition zone), and the properties of transition zone are indicated that this margin is likely a volcanic passive margin.

The proposed plate reconstruction model is consistent with the results obtained from crustal modeling. Restoring the stretched continental crust and transition zone across the northern margin required a 15° of rotation about a pole south of Florida. A further 9° rotation is associated with the extension of the Yucatan margin. Previous studies suggest that the 20° further counter clockwise rotation is associated with sea-floor spreading. Thus the Yucatan Block underwent a total rotation of 44°.

REFERENCES

Allen, P.A., and Allen, J.R., 2005, Basin Analysis, Principles and Applications, 2nd edition, Blackwell Publishing, 549 pages.

Anderson, T.H., and Schmidt, V.A., 1983, The evolution of middle America and the Gulf of Mexico-Caribbean Sea region during Mesozoic time, Geological Society of America Bulletin, v.94, 941-966.

Bally, A.W., and Snelson, S., 1980, Realms of subsidence in facts and principles of world petroleum occurrence, Canadian Society of Petroleum Geologists Memoir, v.6, 9-94

Bally, A.W., 1981, Atlantic type margins, In Bally, A.W. (ed.), Geology of Passive Continental Margins: History, Structure, and Sedimentologic Record, American Association of Petroleum Geologists Education Course Note Series, v.19, 1-48.

Barbier, F., Duverge J, Le Pichon, X., 1986, Structure profonde de la marge Nord-Gascogne Implications sur le mechanisme de rifting et de formation de la marge continentale, Bulletin du Comite de Recherche et de Production de Societe Nationale d'ELF Aquitaine , v.10, 105-121.

Bassin, C., Laske, G., and Masters, G., 2000, The current limits of resolution for surface wave tomography in North America, EOS Trans American Geophysical Union, v.81, F897.

Bauer, K., Neben, S., Schreckenberger, B., Emmermann, R., Hinz, K., Fechner, N., Gohl, K., Schulze, A., Trumbull, R., and Weber, K., 2000, Deep structure of the Namibia continental margin as derived from integrated geophysical studies, Journal of Geophysical Research, v.105, 829-853.

Berndt, C., Skogly, O.P., Planke, S., Eldholm, O., and Mjelde, R., 2000, High velocity break-up related sills in the Vøring Basin off Norway, Journal of Geophysical Research, v.105, 428-43.

Bird, D.E., Hall, S.A., Casey, J.F., and Burke, K. 2005, Gulf of Mexico tectonic history: Hotspot tracks, crustal boundaries, and early salt distribution, American Association of Petroleum Geologists Bulletin, v.89, no. 3, 312-328.

Bott, M.H.P., 1995, Mechanisms of rifting: Geodynamic modeling of continental rift systems, In K.H. Olsen, (ed.), Continental Rifts: Evolution, Structure, Tectonics, Developments in Geotectonics, v.25, 27-43.

Buffler, R.T., Watkins, J. S., Shaub, F. J., and Worzel, J. L., 1980, Structure and early geologic history of the deep central Gulf of Mexico basin, In Pilger, R. H. (ed.), The Origin of the Gulf of Mexico and the Early Opening of the Central North Atlantic Ocean: Baton Rouge (Louisiana State University), 3-16.

Buffler, R.T., and Sawyer, D.S., 1985, Distribution of crust and early history of Gulf of Mexico Basin, Gulf Coast Association of Geological Societies Transactions, v.35, 333-344.

Buffler, R.T., and Thomas, W.A., 1994, Crustal structure and evolution of the southwestern margin of North America and the Gulf of Mexico basin, In Speed, R.C., (ed.), Phanerozoic Evolution of North American Continent–Ocean Transitions, Geological Society of America, DNAG continent–ocean transect volume, 219-264.

Burke, K., 1988, Tectonic evolution of the Caribbean, Annual Rev. Earth Planet Science, v.16, 201-230.

Buschow, H.J., 2001, Handbook of Magnetic Materials, Elsevier, v.13, 103.

Christensen, N.I., 1989, Pore pressure, seismic velocities, and crustal structure, In Pakiser, L.C., and Mooney, W.D., (eds.), Geophysical framework of the continental United States: Geological Society of America Memoir, v.172, 783–798.

Christenson, G., 1990, The Florida lineament, Trans. Gulf Coast, Association Geological Society, v.40, 99-115.

Coffin, M.F., Sawyer D.S., Reston, T., and Stock, J.M., 2006 Continental breakup and sedimentary basin formation, EOS, American Geophysical Union, v.87, 527-529.

Cox, K.G., 1980, A model for flood basalt volcanism, Journal of Petrology, 21, 4, 629-650.

Cox, A., Brian R., 1986, Plate Tectonics: How it works?, Blackwell Publishing, 219-263.

Dickson, W.G., and Odegard, M.E., 2000, Proto-oceanic crust - Defining and naming a trend from Congo to Benin, Poster, Houston Geological Society International Explorations Meeting.

Diegel, F.A., Karlo, J.F., Schuster, D.C., Shoup, R.C., and Tauvers, P.R., 1995, Cenozoic structural evolution and tectono-stratigraphic framework of the northern Gulf coast continental margin, In M. P. A. Jackson, D. G. Roberts, and S. Snelson, (eds.), Salt Tectonics: a Global Perspective, American Association of Petroleum Geologists Memoir, v.65, 109–151.

Dunbar, J.A., and Sawyer D.S., 1987, Implications of continental crust extension for plate reconstruction; an example from the Gulf of Mexico, Tectonics, v.6, 739-755.

Ebeniro, J.O., Nakamura, Y., Sawyer, D.S., and O Brien , W.P. Jr., 1988, Sedimentary and crustal structure of the northwestern Gulf of Mexico, Journal of Geophysical Research , v.93, no. B8, 9075-9092.

Eldholm, O., and Grue, K., 1994, North Atlantic volcanic margins, dimensions and production rates, Journal of Geophysical Research, v.99, 2955-2968.

Eldholm, O., Skogseid, J., and Planke, S., and Gladczenko, T.P., 1995, Volcanic margin concepts, In Banda E., Torne, M., and Talwani, M., (eds.), Rifted ocean-continent boundaries, Kluwer Academic Publishers, Netherlands, 1-16.

Eldholm, O., Gladczenko, T.P., Skogseid, J., and Planke, S., 2000, Atlantic volcanic margins: A comparative study, Nottved, Dynamics of the Norwegian Margin, Geological Society of London Special Publication, v.167, 411–428.

Emery, K.O., and Uchupi E., 1984, The Geology of the Atlantic Ocean, Spring-Verlang, N.Y., 1050-1067.

Franke, D., Neben, S., Schreckenberger, B., Schulze, A., Stiller, M., and Krawczyk, C. M., 2006, Crustal structure across the Colorado Basin, offshore Argentina, Geophysical Journal International, v.165, 850–864.

Galloway, W.E., 2011, Pre-Holocene geological evolution of the northern Gulf of Mexico Basin , Gulf of Mexico origin, waters and biota, Geology, v.3, 33-45.

Geoffroy, L., 2005, Volcanic passive margins, Geoscience, v.337, 1395-1408.

Gladczenko, T.P., Hinz K., Eldholm O, Meyer H , Neben S. and Skogseid J., 1997, South Atlantic volcanic margins , Journal of the Geological Society, London, v.154, 465-475.

Gladczenko, T.P., Skogseid J. and Eldholm O., 1998, Namibia volcanic margin, Marine Geophysical Research, v.20, 313-341.

Gose, W.A., Blecher R.C., and Scott, G.R., 1982, Paleomagnetic results from northeastern Mexico, evidence for large Mesozoic rotations, Geology, v.10, 50-54.

Hales, A.L., Helsley C.E., and Nation, J.B., 1970, Crustal structure study of Gulf Coast of Texas, American Association of Petroleum Geologists Bulletin, v.54, no.11, 2040-2057.

Hales, A.L., 1973, The crust of the Gulf of Mexico: a discussion, In S. Mueller, (ed.), The Structure of the Earth's Crust, based on Seismic Data, Tectonophysics, v.20, 217-225.

Hall, D.J., Cavanaugh, T. D., Watkins, J. S., and McMillen, K. J., 1982, The rotational origin of the Gulf of Mexico based on regional free-air gravity data, In Watkins, J. S. and Drake, C. L. (eds.), Studies in Continental Margins: Tulsa, Oklahoma, American Association of Petroleum Geologists Memoirs, v.34, 115-176.

Hall, S.A., and Najmuddin, I.J., 1994, Constraints on the tectonic development of the eastern Gulf of Mexico provided by magnetic anomaly data, Journal of Geophysical Research, v.99, 7161–7175.

Harry, D.L., Londono J., and Huerta A., 2004, Early Paleozoic transform-margin structure beneath the Mississippi coastal plain, southeast United States, Geology, v.31, no.11, 969-972.

Hinz, K., 1981, A hypothesis on terrestrial catastrophes: wedges of very thick oceanward dipping layers beneath passive margins-thin origin and paleoenvironmental significance, Geologisches Jahrbuch, E22, 3-28.

Hinz, K., Neben S., Schreckenberger B., Roesser H.A., Block, M., Goncalves de Souza, K., and Meyer, H., 1999, The Argentine continental margin north of 48°S: sedimentary successions, volcanic activity during breakup, Marine and Petroleum Geology, v.16, 1-25.

Holbrook, W.S., and Kelemen P.B., 1993, Large Igneous Province on the U.S. Atlantic margin and implications for magmatism during continental break up, Nature, 364, 433-436.

Holbrook, W.S., Purdy, G.M., Sheridan, R., E., Glover, Talwani, M., Ewing, J., and Hutchinson, D., 1994, Seismic structure of the U.S. mid Atlantic continental margin, Journal of Geophysical Research, v.99, 17871-17891.

Hooton, C.R., 1992, Interpretation of regional gravity anomalies over the north central margin of the Gulf of Mexico, Master thesis, University of Houston, 340 pages.

Hudec, M.R., and Martin P.A.J., 2007, Understanding the salt tectonics, Earth Science, v.82, 1-28.

Ibrahim, A.K., Carye, J., Latham, G. and Buffler, R.T., 1981, Crustal structure in Gulf of Mexico from OBS refraction and multichannel reflection data, American Association of Petroleum Geologists Bulletin, v.65, 1207– 1229.

Ibrahim, A.K., and Uchupi, E., 1982, Continental/oceanic crustal transition in the Gulf Coast geosyncline: Field Investigations of Margin Structure and Stratigraphy, American Association of Petroleum Geologists Special Volume, v.34, 155-165.

Imbert, P., Cramez, C., Talwani, M., and Jackson, M., 2001, Seaward-dipping reflectors in the eastern Gulf of Mexico: Implications for basin opening: Geological Society of America Abstracts with Programs, v.33, no. 6, 157–158.

Imbert, P., 2005, The Mesozoic opening of the Gulf of Mexico: Part 1, Evidence for oceanic accretion during and after salt deposition, In Post, P. J., Rosen, N. C., Olson, D. L., Palmes, S. L., Lyons, K. T. and Newton, G. B. (eds.) Transactions of the 25th Annual GCSSEPM Research Conference: Petroleum systems of Divergent Continental Margins, 1119-1150.

Jackson, M.P.A., Cramez C., and Fonck J.M., 2000, Role of subaerial volcanic rocks and mantle plumes in creation of South Atlantic Margins: implications for salt tectonics and source rocks, Marine and Petroleum Geology, v.17, 477-498.

Kelemen, P.B., and Holbrook, W.S., 1995, Origin of thick, high velocity igneous crust along the U.S. East Coast margin, Journal of Geophysical Research, v.100, B6, 10077-10094.

King, P. B., 1969, Tectonic map of North America: U.S. Geological Survey, scale 1:5,000,000, 2 sheets.

Kingston, D.R., Dishroon, C.P., and Williams, P.A., 1983, Global basin classification system, American Association of Petroleum Geologists Bulletin, v.67, no.12, 2175-2193.

Klitgord, K.D., and Schouten, H., 1988, Plate kinematics of the central Atlantic, In K.D. Klitgord, and H. Schouten, (eds.), The Western North Atlantic Region: The Geology of North America, Geological Society of America, 351-378.

Kruger, J.M., and Keller, G.R., 1983, Interpretation of crustal structure from regional gravity anomalies, Ouachita Mountains and Gulf coastal plain, American Association of Petroleum Geologists Bulletin, v.70, no.76, 667-689.

Laske, G., and Masters, G., 1997, A Global Digital Map of Sediment Thickness, EOS Transactions American Geophysical Union, v.78, F483.

Latin, D., and White N., 1990, Generating melt during lithospheric extension pure shear vs simple shear, Geology, v.18, 327-331.

Lister, G.S., Etheridge M.A., and Symonds P.A., 1986, Detachment faulting and the evolution of passive continental margins, Geology, v.14, 246-250.

Manatschal, G., and Bernoulli, D., 1999, Architecture and tectonic evolution of non-volcanic margins: present-day Galicia and ancient Adria, Tectonics, v.18, 1099- 1199.

Mancini, E.A., Parcell, W.C., Puckett T.M. and Benson D.J., 2009, Upper Jurassic (Oxfordian) Smackover carbonate petroleum system characterization and modeling, Mississippi Interior Salt Basin area, northeastern Gulf of Mexico, Carbonates and Evaporites, v.18, 125-150.

Martin, H., 1975, Structural and paleogeography evidence for Upper Paleozoic Sea between South Africa and South America, Proceedings at the IUGS 3rd Gondwana Symposium, Canberra, 37-51.

Marton, G., and Buffler R.T., 1994, Jurassic reconstruction of the Gulf of Mexico Basin, International Geology Review, v.36, 545-586.

Marton, G.L., 1995, Jurassic Evolution of the Southern Gulf of Mexico, PhD thesis, University of Texas Austin, 275 pages.

McKenzie, D.P., 1978, Some remarks on the development of sedimentary basins, Earth and Planetary Science Letters, v.40, 25-32.

Menzies, M.A., Klemperer, S. A., Ebinger, C.J., and Baker, J. (eds), 2002, Volcanic Rifted Margins, Geological Society of America Special Paper, no. 362, 245-254

Minshull, T.A., 2009, Geophysical Characterization of the Ocean-Continent Transition at Magma-Poor Rifted Margins, Comptes Rendus Geoscience, v.341, i.5, 382–393

Mickus, K., Stern, R.J., Keller, G.R., and Anthony, E.Y., 2009, Potential field evidence for a volcanic rifted margin along the Texas Gulf Coast, Geology, v.37, 387–390.

Miller, J., 2007, The Midcontinent Rift in the Lake Superior Region: A 1.1 Ga Large Igneous Province, University of Minnesota Duluth, Unpublished http://www.largeigneousprovinces.org/07nov.

Mjelde, R., Raum, T., Myhren B., Shimamura H., Murai Y., Takanami T., Karpuz R. and Naess U., 2005, Continent ocean transition on the Voring Plateau, NE Atlantic, derived from densely sampled ocean bottom seismometer data, Journal of Geophysical Research, v.110, B05101, 19 pages.

Mjelde, R., Raum, T., Murai Y., and Takanami T., 2007, Continent ocean transitions: Review, and a new tectonomagmatic model of the Voring Plateau, NE Atlantic, Journal of Geodynamics , v.43, n.3, 374-392.

Mohriak, W.U., Rosendahl B.R., Tuner J.P. and Valante, S.C., 2002, Crustal architecture of South Atlantic volcanic margins, In Menzies M.A. Klemperer S.L. Ebinger, C.J. and Baker J., (eds.), Volcanic Rifted Margins, Colorado, Geological Society of America, Special paper, v.362, 159-202.

Molina-Garza, R.S., Vander V., R., and Urrutia Fucugauchi, J., 1992, Paleomagnetism of Chiapas Massif, southern Mexico, evidence for rotation of the Maya block and

implications for the opening of the Gulf of Mexico, Geological Society of America Bulletin v.104, 1156-1168.

Mutter, J.C., Buck W.R., and Zehnder C. M, 1988, Convective partial melting model for the formation of thick basaltic sequences during the initiation of spreading , Journal of Geophysical Research , v.93, 1031-1048.

NGDC, 1991, Geodas Marine Geophysical Data: Bathymetry, Magnetics, Gravity, 1-3, version 4.1., U.S. Department of Commerce, Colorado, U.S.

Odegard, M.E., and Dickson, W.G., 2001, Proto-oceanic crust: type, emplacement mechanisms, and relationships to hydrocarbon maturation, Geological Society of America Annual Meeting Abstract.

Odegard, M.E., 2003, Geodynamic evolution of Atlantic Ocean: Constraints from potential field data, Extended abstract, 8th International Congress of the Brazilian Geophysical Society, Rio de Janeiro Extended Abstract.

Odegard, M.E., 2010, Passive Margin Development in the Atlantic and Gulf of Mexico with a special emphasis on Proto Oceanic crust, 25thAnnual Bob F. Parkins Research Conference: Petroleum Systems of Divergent Continental Margin Basins.

Olsen, K.H., and Morgan, P., 1995, Introduction: Progress in understanding continental rifts, In: K.H. Olsen, (ed.), Continental Rifts: Evolution, Structure, Tectonics, Developments in Geotectonics, v.25, 3-26.

Pindell, J.L., 1985, Alleghanian reconstruction and subsequent evolution of the Gulf of Mexico, Bahamas and Proto-Caribbean, Tectonics, v.4, 1-39.

Pindell, J.L., and Kennan, L., 2009, Tectonic evolution of the Gulf of Mexico, Caribbean and northern South America in the mantle reference frame: an update, Geological Society of London Special Publication, v.328, 1-55.

Planke, S., Skogseid, J., and Eldholm, E., 1991, Crustal structure off Norway 62°N to 70°, Tectonophysics, v.189, 91-107.

Roberts, D.G., Backman, J., Morton, A.C., Murray, J. W., and Keene, J. B., 1984, Evolution of volcanic rifted margins: synthesis of Leg 81 results on the west margin of Rockall Plateau, 81: Washington (U.S. Govt. Printing Office), 883-912.

Rabinowitz, P.D., and LaBrecque, J., 1979, The Mesozoic South Atlantic Ocean and evolution of its continental margins, Journal of Geophysical Research, v.84, B11, 5973-6002.

Ross, M.I., and Scotese, C.R., 1988, A hierarchical tectonic model of the Gulf of Mexico and Caribbean region, Tectonophysics, v.155, 139-168.

Rudnick, R.L., and Fountain D. M., 1995, Nature and composition of the continental crust: a lower crustal perspective, Reviews of Geophysics, v.33, no.3, 267–309.

Salvador, A., 1987, Late Triassic Jurassic paleogeography and origin of Gulf of Mexico basin, American Association of Petroleum Geologists Bulletin, v.71, 419-451.

Salvador, A., 1991, Origin and development of the Gulf of Mexico basin: in, Salvador, A., (ed.), The Gulf of Mexico Basin: The Geology of North America, Volume J., 389-444.

Sawyer, D.S., Buffler, R.T., and Pilger, R.H., 1991, The crust under the Gulf of Mexico basin, In Salvador, A., (ed.), The Gulf of Mexico Basin: Boulder, Colorado, Geological Society of America, Geology of North America, v. J, 53–72.

Schreckenberger, B., Hinz, K. and Roesser, H.A., 1997, Magnetic modeling of seaward dipping reflector sequence: examples from Atlantic volcanic margins, Abstract, ILP Volcanic Margins Workshop, November 1997, Potsdam, Germany.

Schouten, H., and Klitgord, K.D., 1994, Mechanistic solutions to the opening of the Gulf of Mexico, Geology, v. 22, 507–510.

Scrutton, R.A., 1982, Dynamics of passive margins, Geodynamics series v.6, 5-13.

Sengor, A.M.C., and Burke K., 1978, Relative timing of rifting and volcanism on Earth and its tectonic implications, Geophysical Research letters, v.6, 419-421.

Shepherd, A.V., 1983, A Study of the Magnetic Anomalies in the Eastern Gulf of Mexico: Master's thesis, University of Houston, Houston, Texas, 197 pages.

Stavar, D.D., 2007, Integrated Geophysical Study of the Conjugate Passive Margins of South West Africa and South America, PHD Thesis University of Houston, 480 pages.

Stewart, J., Watts A.B., and Bagguley, J.G., 2000, Three dimensional subsidence analyses and gravity modeling of the continental margin offshore Namibia, Geophysical Journal International, v.141, 724-726.

Talwani, M., Ewing, J., Sheridan, R.E., Holbrook, W.S., and Glover, L., 1995, The EDGE experiment and the U.S. Coast Magnetic anomaly, in NATO/ARW Series book, Rifted Ocean–Continent Boundaries, 155–181.

Talwani, M., and Abreu, V., 2000, Inferences regarding initiation of oceanic crust formation from the U.S. East Coast margin and conjugate South Atlantic margins, In Mohriak, W., and Talwani, M., (eds.), Atlantic Rifts and Continental Margins: American Geophysical Union Geophysical Monograph, v.115, 211– 233.

Tarbuck, E.J., Lutgens, F.K, and Tasa, D., 2008, Earth Science, 9th edition, 19-20

Thomas, W.A. 1991, The Appalachian-Ouachita rifted margin of southeastern North America: Geological Society of America Bulletin, v.103, 415– 431.

Tsikalas, F., Eldholm O., and Faleide, J.I., 2005, Crustal structure of the Lofoten Vesteralen continental margin of Norway, Tectonophysics, v.404, 151-174.

Uchupi, E., and Emery K.O., 1968, Structure of continental margin off the Gulf Coast of the United States, American Association of Petroleum Geologists Bulletin, v.52, 1162-1193.

Warren, D., Healy, J., and Jackson, W., 1966, Crustal seismic measurements in southern Mississippi: Journal of Geophysical Research, v. 71, 3437–3458.

Watts, A.B., and Marr, C., 1995, Gravity anomalies and the thermal and mechanical structure of rifted continental margins, In E. Bande et al. (eds.), Rifted Ocean-Continent Boundaries, Kluwer Academic Publishers, the Netherlands, 65-95.

Watts, A.B., and Stewart J., 1998, Gravity anomalies and segmentation of the continental margin offshore West Africa, Earth and Planetary Science letters, v.156, 239-252.

Watts, A.B., and Fairhead, J.D., 1999, A process oriented approach to modeling the gravity signature of continental margins, The Leading Edge, v.18, no.2, 258-263.

Watts, A.B., 2001a, Isostasy and Flexure of the Lithosphere, Cambridge University Press, 458 pages.

Watts, A.B., 2001b, Gravity anomalies, flexure and crustal structure at the Mozambique rifted margin, Marine and Petroleum Geology, v.18, 445-455.

Wernicke, B., 1985, Uniform sense normal simple shear of the continental lithosphere, Canadian Journal of Earth Sciences, v.22, 108-125.

White, R.S., Westbrook, G.S., Spence, G.D., Fowler, S.R., Barton, P.J. , Jopen, M., Morgan J., Bowen A.N., Presscott C., and Bott, M.H.P., 1987, Hatton Bank continental margin structure, Geophysical Journal of the Royal Astronomical Society, v.89, 265-271.

White, R.S., and McKenzie, D., 1989, Magmatisim at rift zones: The generation of volcanic continental margins and flood basalts, Journal of Geophysical Research, v.94, no.B6, 7685-7729.

White, R.S., McKenzie D., and O Noins, R.K., 1992, Oceanic crustal thickness from seismic measurements and rare earth element inversions, Journal of Geophysical Research, v.97, no. B13, 19683-19715.

Wilson, M., 2002, Magma migration and the thermal evolution of volcanic rifted passive margins, American Association of Petroleum Geologists Hedberg Conference, Hydrocarbon Habitat of Volcanic Rifted Margins, Stavanger, Norway, 2 pages.

Winkler, C.D., and Buffler, R.T., 1988, Paleogeographic evolution of early deep-water Gulf of Mexico and margins, Jurassic to Middle Cretaceous (Comanchaean), American Association of Petroleum Geologists Bulletin, v.72, 318-346.

Worzel, J.L., and Watkins, J.S., 1973, Evolution of the northern Gulf Coast deduced from geophysical data: Gulf Coast Association of Geological Societies, Transactions, v.23, 84-91.

Yamasaki, T., and Gernigon L., 2006, Magmatic underplating as a possible origin of deformation localization during lithospheric extension, American Geophysical Union Meeting, CA, Abstract, abstract no. T53A-1582

Yegorova, T., and Gobarenko V., 2010, Structure of the Earth's crust and upper mantle of West- and East-Black SeaBasins revealed from geophysical data and its tectonic implications, In R.A., Stephenson, N. Kaymakci, M. Sosson, V. Starostenko, F. Bergerat, (eds.), Sedimentary Basin Tectonics from the Black Sea and Caucasus to the Arabian Platform, Geological Society London, Special Publication, no.340, 23—41.

Zietz, I., 1982, Composite magnetic anomaly map of the United States; Part A, Conterminous United States: U.S. Geological Survey Investigations Map GP-954-A, 59 pp., 2 sheets, scale 1:2,500,000.

APPENDIX

Mathematical Development and Software Listing

Finite rotation formulas were taken from study by Cox and Brian (1986). Matlab 2009-b software was used in order to complete the required calculations for this method. Matlab code that was used for this study:

```
a=
b=
c=
d=
x=input('insert degree   ')
T1=cosd(c)*cosd(d)
T2=sind(d)*cosd(c)
T3=sind(c)
R1=cosd(b)*cosd(a)
R2=sind(b)*cosd(a)
R3=sind(a)
R11=R1*R1*(1-cosd(x))+cosd(x)
R12=R1*R2*(1-cosd(x))-(R3*sind(x))
R13=R1*R3*(1-cosd(x))+(R2*sind(x))
R21=R2*R1*(1-cosd(x))+(R3*sind(x))
R22=R2*R2*(1-cosd(x))+cosd(x)
R23=R2*R3*(1-cosd(x))-(R1*sind(x))
R31=R3*R1*(1-cosd(x))-(R2*sind(x))
R32=R3*R2*(1-cosd(x))+(R1*sind(x))
R33=R3*R3*(1-cosd(x))+cosd(x)
F1=R11*T1+R12*T2+R13*T3
F2=R21*T1+R22*T2+R23*T3
F3=R31*T1+R32*T2+R33*T3
FLAT=asind(F3)
long= F1/cosd(FLAT)
FLONG= acosd(long)
```

```
a; pole latitude
b; pole longitude
c; point of interest latitude
d; point of interest longitude
```